University of Naples Federico II
Polytechnic and Basic Sciences School

Department of Chemical Sciences

Ph.D. in Chemical Sciences

Evaluation of the functional properties of phenolic compounds for food packaging applications

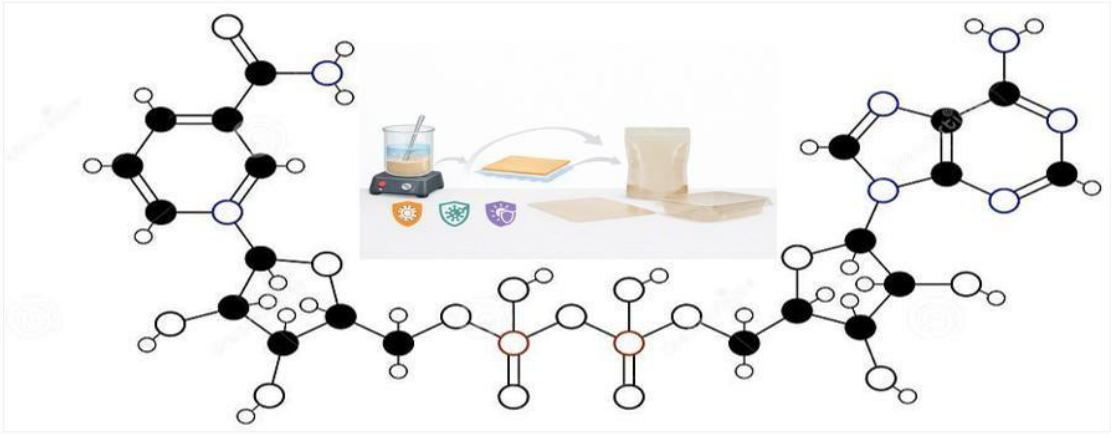

Tahir Zaman

Advisor
Prof. Lucia Panzella

Examiner
Prof. Alessio Cimmino

XXXVIII Cycle 2023-2025

Coordinator: Prof. Alessandra Napolitano

Table of contents

2.2 Physicochemical and Functional Characterization of PVA Films Embedded with Duckweed (*Lemna minor*) Leaf Extract and (Nano)chitosan Intended for Active Food Packaging

Chapter 3

Design of Chitosan-Based Bioactive Composite Films Containing Lignin and Lignin-Silver Nanocomposites

Chapter 4

Preliminary Insight into the Effects of Phenol-Rich Extracts Prepared from Agri-Food By-Products by in situ-Generated Deep Eutectic Solvents on Chitosan-Based Films

Acronyms and Abbreviations Table

Acronym/Abbreviation	Full term
ATR-FTIR	Attenuated Total Reflectance – Fourier Transform Infrared Spectroscopy
NCH	Nanochitosan
CS	Chitosan
CUPRAC	Cupric reducing antioxidant capacity
DPPH	2,2-Diphenyl-1-picrylhydrazyl
DTG	Derivative thermogravimetric
FRAP	Ferric Reducing/Antioxidant Power
HPLC	High-Performance Liquid Chromatography
LC- MS	Liquid Chromatography–Mass Spectrometry
LIG	Lignin
LNPs	Lignin Nanoparticles
MHB	Mueller–Hinton Broth
NMR	Nuclear Magnetic Resonance
PVA	Poly (vinyl alcohol)
SEM	Scanning Electron Microscopy
TEM	Transmission Electron Microscopy
TGA	Thermogravimetric Analysis
UV	Ultraviolet Spectroscopy
WVTR	Water Vapor Transmission Rate

Abstract

This PhD research project has been mainly focused on the exploitation of natural phenolic compounds, widely recognized for their antioxidant and antimicrobial properties, in food packaging, to enhance shelf life and ensure product safety. Recent advancements have also demonstrated that these compounds may significantly improve not only the functional but also the physicochemical (*e.g.*, thermal resistance and mechanical properties) of biopolymer-based films, contributing to the development of sustainable packaging solutions. More in detail, the main aim of this PhD work was an in-depth and systematic analysis of the effects of different additives on the performance of films intended for food packaging to provide data that could guide the selection of the specific combinations to obtain film with specific properties. As to the film polymeric matrix, the attention was focused mainly on poly (vinyl alcohol) (PVA) and chitosan, whereas the main phenolic compounds tested were (nano)lignin, phenols from *Lemna minor* leaves, and phenols recovered from agri-food wastes and by-products such as grape pomace, spent coffee grounds, and pomegranate peels. In addition, the possibility to exploit phenolic compounds also to produce silver nanoparticles endowed with antimicrobial properties was explored.

Key findings were the following:

a) Differential effects of the antimicrobial (nano)chitosan and of the antioxidant/UV-Vis radiation blocking agent (nano)lignin on the morphological, optical, mechanical, thermal, antioxidant, and antibacterial properties of poly (vinyl alcohol)-based films were observed. Indeed, films containing both nanolignin and nanochitosan exhibited the most homogeneous surface and the highest UV-Vis radiation blocking efficacy and water resistance, whereas mechanical and thermal testing showed reduced performance when nanoscale additives were incorporated. In addition, antioxidant and antimicrobial properties were higher for films

containing lignin alone. Similar results were obtained when a phenol-rich *Lemna minor* leaf extract was employed as additive in place of lignin.

b) Integrating chitosan with PVA, lignin and lignin-silver nanocomposites may significantly enhance the physicochemical and functional performance of films intended for food packaging applications. FTIR analysis revealed that lignin acted primarily as a filler, being physically embedded in the polymer matrix without altering its chemical structure. On the other hand, lignin and particularly the lignin-silver nanocomposite imparted UV-Vis radiation blocking ability to the films. Films with high PVA content exhibited superior flexibility compared to pure chitosan films. Antioxidant assays confirmed potent radical scavenging and reducing properties attributed to the phenolic groups of lignin, with PVA differentially affecting the efficacy of the films depending on the assay medium.

c) Incorporation of deep eutectic solvents (DES) improved film flexibility and mechanical strength of chitosan films, therefore DES can be easily exploited as both green solvents for the extraction of phenolic compounds from agri-food wastes and as film plasticizers.

Keywords

Phenolic compounds, lignin, chitosan, poly (vinyl alcohol), antioxidant, biodegradable films, agri-food wastes

Publications

T. Zaman, M. L. Alfieri, Y. Deng, E. Piccolo, R. Gaglione, M. Lefebvre, E. Y. Wardhono, A. Arciello, A. Napolitano, E. Guénin "A deeper insight into the effects of chitosan, lignin and their nanoforms on the morphological, mechanical and functional properties of poly(vinyl alcohol) films intended for food packaging", Submitted to Industrial Crops & Products (Manuscript number INDCRO-D-25-08238).

Communications

Poster presentation at 8th International Conference on Multifunctional, Hybrid, and Nanomaterials, 3-5 March 2025, Montpellier, France. Poster title: "Development and characterization of poly (vinyl alcohol) (PVA)/chitosan/lignin nanocomposite films for sustainable food packaging applications".

Poster presentation at 18th European Winter School on Physical Organic Chemistry (E-WISPOC 2025), 2-7 February 2025, Bressanone, Italy. Poster title: "Nanolignin and nanochitosan reinforced polymeric films: a sustainable paradigm for functional food packaging".

1. Introduction and Literature Review

1.1 Background and Motivation

The adoption of biopolymers derived from renewable resources such as agro-industrial wastes and by-products in the food packaging sector represents a promising solution to the environmental challenges posed by conventional petroleum-based plastics (Castro-Domínguez *et al.,* 2025). However, while biopolymers offer clear environmental benefits, such as renewability, biodegradability, and low carbon footprint, they often require reinforcement and functionalization to meet the performance demands of food packaging materials. Indeed, many biopolymers display limitations in their mechanical strength, barrier properties (e.g., to water or gases), and durability under real-world packaging conditions (Shaghaleh *et al.,* 2018; Agarwal *et al.,* 2022). To enhance their functionality and ensure they can substitute conventional plastics effectively, biopolymers are frequently modified through blending, composite formation, or incorporation of additives (González-López *et al*., 2023; Periyasamy *et al*., 2025). One particularly promising approach involves the use of phenolic compounds, which can act both as reinforcing and functionalizing agents: when embedded into biopolymer films, these compounds may indeed impart antioxidant and antimicrobial properties, improve barrier and mechanical performance, and stabilize the polymer matrix (Moeini *et al*., 2022; Periyasamy *et al*., 2025; Sani *et al*., 2025). Such functionalization strategy allow biopolymer-based films not only to approach or in some cases match the performance of traditional plastic-based packaging, but also to add value in terms of active preservation, food safety, and sustainable waste valorization, aligning with circular-economy goals (Castro-Domínguez *et al.,* 2025; Periyasamy *et al.,* 2025).

1.2 Phenolic Compounds: Chemical Diversity and Functional Roles

Phenolic compounds have garnered significant attention from the scientific community due to their widespread presence in plants and other natural sources, as well as their well-established antioxidant and antimicrobial properties, among others. These properties have spurred interest in phenolic compounds across a variety of sectors, including functional foods, pharmaceuticals, agriculture, and sustainable materials, particularly in the realm of food packaging. In this context, they are increasingly being incorporated into active packaging films, where their multifunctional properties are exploited to improve the shelf-life and quality of food products. The inclusion of phenolic compounds in food packaging may also contribute to the development of more sustainable and eco-friendly packaging solutions.

1.2.1. Chemical Diversity of Phenolic Compounds

Phenolic compounds are characterized by the presence of one or more hydroxylated aromatic rings and include a wide range of substances such as:

- Phenolic acids
- Flavonoids
- Stilbenes
- Lignans
- Phenolic polymers include lignin and tannins (hydrolyzable and condensed).

These diverse structures correspond to different sources and bioactivities, enabling broad applications in packaging systems with specific functional attributes (Table 1) (Singh *et al*., 2022).

Table 1.1 *Classification, basic skeleton and main sources of phenolic compounds.*

Phenolic Compounds	Basic Skeleton	Main Sources	References
Flavonoids	C6-C3-C6	Berries, herbs, cacao, grapes, green and black tea, citrus fruits, spinach, soybeans, olives, cherries, red wine	Durazzo *et al*., 2019; Albuquerque *et al*., 2021
Tannins	Not uniquely defined	Tea, coffee, chocolate, berries, apples, wine	Albuquerque *et al.,* 2021
Phenolic acids	C6-C-1 and C6-C-3	Berries, persimmon, apple juice, grape, mustard, orange, rye, coffee, mushrooms, propolis, tea, wine	Manessis *et al.*, 2020
Lignans	C6-C-3	Oilseeds such as flaxseed, sesame, legumes, whole grains, berries	Sangiorgio *et al*., 2023
Stilbenes	C6-C-2-C6	Grapes, pine, almond, peanuts, sorghum, berries, wine	Durazzo *et al*., 2019
Lignins	C-6-C3) n	Spruce, jute, cotton, hemp, pine, birch	Faustino *et al*., 2010; Bouzon *et al*., 2005

1.2.2. Functional Roles of Phenolic Compounds in Food Packaging

1.2.2.1. Antioxidant Properties

Phenolic compounds play a crucial role in active food packaging by preventing oxidation, a primary factor responsible for food nutrient loss, discoloration, and degradation of sensory attributes such as taste and aroma. Phenolic compounds exhibit antioxidant activity through several complementary mechanisms, enabling them to effectively protect food products and extend shelf life.

One of the primary mechanisms is radical scavenging through donation of hydrogen atoms or electrons to neutralize hydroxyl (·OH), superoxide ($O_2^{-\cdot}$), and peroxyl radicals, thereby interrupting chain reactions that lead to oxidative deterioration (Zhao *et al.,* 2019; Martillanes *et al.,* 2017). The marked antioxidant properties of phenolic compounds may be ascribed in part to their structural features. Most natural phenolic compounds possess multiple hydroxyl groups on aromatic rings contributing to stabilization of the radical intermediates formed

during electron or hydrogen donation (Ordoñez *et al.* (2022); Singh *et al.,* 2022). Additionally, phenolic compounds may react with lipid hydroperoxides converting them into stable, non-radical species, minimizing further oxidation (Singh *et al.,* 2022).

Another critical mechanism underlying the antioxidant properties of phenolic compounds is metal chelation. Transition metals, especially iron, catalyze radical-forming reactions such as the Fenton reaction, which generates reactive hydroxyl radicals. By forming stable complexes with these metals, phenolic compounds prevent them from participating in these reactive pathways (Feng *et al*., 2023). This chelating ability is particularly valuable in food systems where trace metals often accelerate spoilage.

Practical applications of these mechanisms have been confirmed in biodegradable films and coatings. Flavonoids and phenolic acids derived from natural sources such as green tea (catechins, epicatechin gallate) and rosemary (gallic acid) have been successfully incorporated into edible films to protect nuts, seeds, and meats against oxidative spoilage (Singh *et al.,*2022; Martillanes *et al.,* 2017). By maintaining nutritional integrity and sensory quality, phenolic compounds serve as highly effective natural antioxidants, supporting the development of sustainable and functional active food packaging materials.

1.2.2.2. Antimicrobial Activity

The antimicrobial activity of phenolic compounds involves multiple mechanisms targeting the structural and functional integrity of microbial cells. Phenolic compounds may disrupt bacterial cell walls and membranes through hydrogen bonding and hydrophobic interactions, leading to increased permeability and leakage of cellular contents (Bae *et al.,* 2022). They interfere with critical bacterial enzymes and proteins essential for replication, metabolism, and virulence, effectively inhibiting bacterial growth (Fig. 1) (Bae *et al.,* 2022). Additionally, phenolic compounds may chelate metal ions such as iron and copper, which are vital cofactors for microbial enzymatic activity and proliferation, thereby limiting microbial growth (Singh

et al., 2023; Sultana *et al.,* 2024). This multifaceted action restrains the proliferation of foodborne pathogens and spoilage microorganisms, making phenolic compounds potent antimicrobial agents in food preservation. For instance, chitosan-based coatings enriched with phenolic extracts from pomegranate peel and olives have effectively inhibited fungal growth and bacterial spoilage, successfully extending the shelf life and sensory quality of meat (Basumatary *et al.,* 2022). By disrupting biofilm formation, interfering with quorum sensing, and targeting microbial metabolism, phenolic compounds offer a natural, broad-spectrum antimicrobial strategy suitable for enhancing food safety and extending product shelf life (Bae *et al.,* 2022; Satchanska, G. 2022; Singh *et al., 2023).*

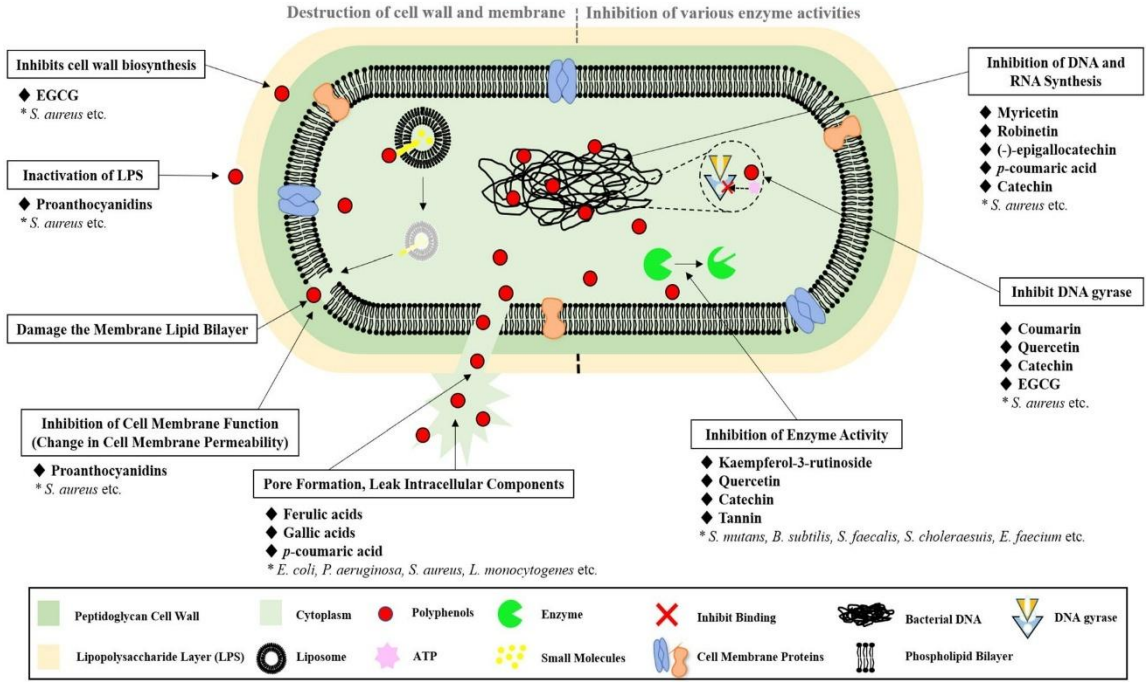

Fig. 1.1 *Schematic illustration of antibacterial mechanisms of polyphenols against foodborne pathogens (based on Bae et al., 2022).*

1.2.2.3. UV Protection

Phenolic compounds may act as effective natural UV radiation blockers in food packaging due to their conjugated aromatic structures, which enable them to absorb UV-A and UV-B light, thereby preventing photooxidation that can lead to degradation of color, texture, flavor, and nutrients in food (Fig.2) (Pan *et al.,* 2024). In addition to absorbing UV radiation, phenolic

compounds also act as antioxidants, scavenging radical species generated by UV-induced reactions and further protecting the food from oxidative damage (Hu *et al.* 2017; Farjadmand *et al.* (2021). Phenolic compounds have been therefore incorporated into biopolymer matrices, such as poly(vinyl alcohol) (PVA) and chitosan, to enhance UV protection while maintaining the film's transparency and structural integrity, making phenolic compounds-enriched packaging an eco-friendly alternative to synthetic UV blockers (Viscusi, 2024). This integration not only supports the protective role of the packaging but also contributes to the sustainability of the packaging industry by offering a natural, efficient solution without compromising on the aesthetics or performance of the packaging (Mushtaq *et al.,* 2025).

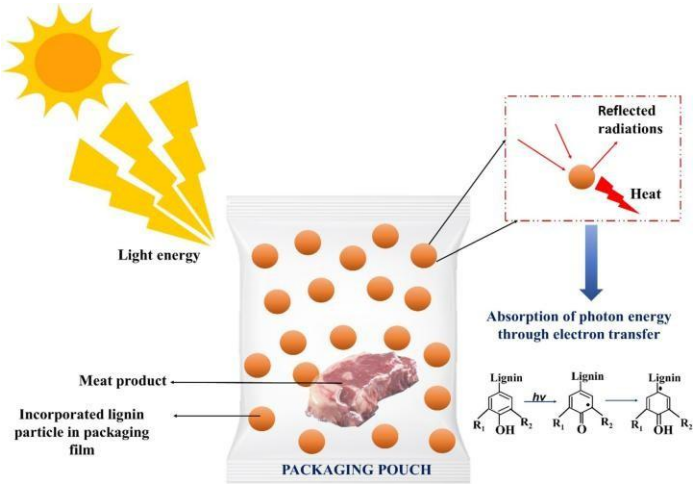

Fig. 1.2 *Mechanism for preventing photooxidation by lignin as a natural UV radiation blocking agent in food packaging applications.*

1.2.2.4. Enhancement of Film Mechanical Properties

Phenolic compounds may act as natural, multifunctional crosslinkers in biodegradable food packaging films. They may form covalent bonds, hydrogen bonds, and/or establish electrostatic interactions with polymer matrices, which increase the crosslink density and significantly enhance mechanical properties like tensile strength, stiffness/ductility, and thermal stability. These crosslinking interactions also reduce water vapor and oxygen permeability, improving film barrier properties, which are crucial for food shelf-life extension (Table 2).

Table 1.2 *Effects of Phenolic Compounds on Crosslinking and Mechanical Enhancement in Biopolymer Food Packaging Films*

Phenolic Compound / System	Crosslinking Mechanism	Mechanical Enhancement	Barrier & Morphology Effects	Additional Functionalities	Key References
Tannic acid	Hydrogen bonding and spontaneous oxidation under basic conditions, generating quinone groups that react with amino groups	Higher tensile strength and modulus; stiffer, more rigid films	Higher film density; lower water-vapor permeability; increased crystallinity	Antioxidant, antimicrobial and UV-protective functions	Choi *et al.,* 2018; Singh *et al.,* 2022; Hamzah *et al.,* 2024; Singh *et al.*, 2024
Caffeic acid and ferulic acid	Oxidative covalent bonding with amino and hydroxyl groups of biopolymers	Increased tensile strength and stiffness; improved rigidity	Improved water-vapor and oxygen-barrier performance	Antioxidant and antimicrobial functionalities	Choi *et al.,* 2018; Li *et al.,* 2019; Ozdemir *et al.,* 2022
Green tea polyphenols	Hydrogen bonding and covalent interactions involving quinone structures	Improved tensile strength with balanced elongation	Improved morphology and reduced crystallinity	Strong antioxidant and antimicrobial actions	Singh *et al.,* 2022; de Oliveira *et al.,* 2022
Gallic acid	Hydrogen bonding and covalent crosslinking through quinone-type intermediates	Enhanced mechanical strength and film stiffness	Reduced water permeability; more uniform film structure	Antioxidant enhancement and extended shelf-life of packaged products	Singh *et al.,* 2022; Ordóñez *et al.,* 2022

Phenolic compounds are thus positioned as multifunctional natural additives in the development of sustainable, active packaging materials that meet consumer demands for minimally processed, safer foods, with longer shelf stability. Their wide occurrence in easily available, low cost sources such as agri-food waste and by-products further contribute to their increasing exploitation in a circular economy perspective.

1.3 Phenolic Compounds Sources and Sustainable Extraction Techniques

Phenolic compounds have traditionally been sourced from fruit, but there is increasing interest in using agro-industrial by-products such as grape pomace, citrus and apple peels, and nutshells as low-cost, underutilized sources of these bioactive compounds (Zhou *et al.,* 2023; Sahu, 2025). These by-products are rich in flavonoids, tannins, and phenolic acids, which can be valorized for use in various industries. A prominent role in terms of sustainability is played by lignin, which is particularly abundant in lignocellulosic agri-food byproducts such as wheat straw, wheat bran and distiller's grain, spent coffee grounds from the industrial production of soluble coffee, sawdust and other wastes from the wood industry (Panzella *et al.*, 2020).

To optimize extraction while minimizing energy and solvent toxicity, green methods like Ultrasound-Assisted Extraction (UAE) and Microwave-Assisted Extraction (MAE) are commonly used (Table 3). UAE enhances solvent penetration by using acoustic cavitation, while MAE uses microwave-induced heating to rapidly release phenolics, reducing extraction time and solvent consumption (Martínez *et al*., 2019; Zhang *et al*., 2020).

Natural Deep Eutectic Solvents (NADES) have become a key green alternative for extracting phenols. These solvents are composed of a hydrogen-bond acceptor (e.g., choline chloride) and a hydrogen-bond donor (e.g., polyols, sugars, or organic acids), forming a eutectic mixture that enhances phenolic compound solubilization (Ferreira *et al.,* 2024; Bonacci, *et al.,* 2020). NADES may provide extracts with improved yields and antioxidant properties compared to traditional solvents. For example, NADES extraction from wild thyme increased polyphenol content and antioxidant capacity compared to conventional methods (Pavlić *et al*., 2022), and in the case of *Toona sinensis* seeds, NADES composed of choline chloride and oxalic acid extracted up to 32.58 mg gallic acid equivalents (GAE)/g dry weight, outperforming ethanol and water (Wang *et al.,* 2023).

NADES are particularly effective for extracting phenols from agri-food by-products, supporting sustainable practices and a circular economy approach (Jiang *et al*., 2024). However, challenges remain in scaling up the process, including solvent viscosity, recovery, and regulatory compliance (Table 3) (Sahu, 2025; Zhou *et al.,* 2023).

Table 1.3. *Some Examples of Sustainable Phenolic Compound Recovery Methods*

Waste Source	Extraction Method	Solvent Composition	Yield (mg GAE/g of dry weight)	Reference(s)
Pomegranate peel	UAE	50–70% ethanol in water	Up to 8923 mg /100g	Huang *et al.,* 2025
Almond shell, grape skin	MAE	Ethanol/water, DES	200–300 mg/100 g	Bernini *et al.,* 2024; Mir-Cerdà *et al*., 2024
Broccoli stem, onion leaves	DES	Choline chloride–urea, cholinne chloride-propylene glycol	5.1 mg/g	Huang *et al.,* 2025; Mir-Cerdà *et al*., 2024; Rodrigues *et al*., 2025
Spent coffee grounds	DES	Betaine:triethylene glycol, choline chloride:1,2-propanediol	30 mg/g	Rodrigues *et al.,* 2025; Mir-Cerdà *et al*., 2024

GAE: Gallic acid equivalents

1.4 Natural and biodegradable polymers for developing active food packaging

Food packaging has traditionally relied on petroleum-based polymers such as polyethylene (PE), polypropylene (PP), polyethylene terephthalate (PET), polystyrene (PS), and polyvinyl chloride (PVC). These materials exhibit excellent mechanical strength, barrier properties, and ease of processing (Mafe *et al.*, 2024). They effectively protect food products, ensuring extended shelf life and quality retention. However, the non-biodegradability of these materials,

their origin from finite fossil resources, and their contribution to plastic pollution have raised significant environmental concerns. This has prompted a global search for sustainable alternatives (Yin, 2024). Biopolymers derived from renewable sources, such as starch, cellulose, gelatin, and chitosan, have gained importance due to their biodegradability and biocompatibility (Ullah & Ahmed, 2025; Cazón, *et al*., 2025). Alongside these, biodegradable synthetic polymers like poly (lactic acid) (PLA), polyhydroxyalkanoates (PHAs), poly(vinyl alcohol) (PVA), poly(butylene succinate) (PBS), and polycaprolactone (PCL) have been widely exploited. These alternatives are designed to offer mechanical and barrier properties that are competitive with traditional plastics (Rahman Khan *et al.,* 2024; Ullah & Ahmed, 2025).

The convergence of natural polymers and/or biodegradable synthetic polymers, and active additives such as phenolic compounds has contributed to the design of sustainable active food packaging systems (Cazón *et al.,* 2025), able to interact with food or its environment to enhance shelf life and safety.

1.5 Aim of the PhD work

Within the context briefly described in the previous paragraphs, the main aim of this PhD work was an in-depth and systematic analysis of the effects of different additives, with a particular focus on phenolic compounds, on the performance of films intended for food packaging to provide data that could guide the selection of the specific combinations to obtain films with specific properties.

In particular, the following activities were performed:

a) Comparative study of the effects of (nano)lignin or lignin-silver nanocomposite on the functional and physicochemical properties of PVA-(nano)chitosan films

b) Functionalization of films of PVA blended with different biopolymers with phenolic-rich extracts from *Lemna minor* leaves
c) Evaluation of the effects of phenolic-rich extracts prepared by use of deep eutectic solvents on the properties of biopolymer-based films.

Part of the work described under the research lines a) and b) was carried out during a three-month stage at Université de Technologie de Compiègne in France, whereas part of the research activity c) was performed during a four-month stage at Yonsei University in South Korea. *Lemna minor* sample was provided by Prof. Ferranti from the Department of Agricultural Sciences of University of Naples Federico II in the frame of National Recovery and Resilience Plan (NRRP) project funded by the European Union - NextGenerationEU "ON Foods - Research and innovation network on food and nutrition Sustainability, Safety and Security – Working ON Foods".

1.6 References

Agarwal, A., Shaida, B., Rastogi, M., & Singh, N. B. (2023). Food packaging materials with special reference to biopolymers-properties and applications. *Chemistry Africa*, *6*(1), 117-144.

Albuquerque, B. R., Heleno, S. A., Oliveira, M. B. P., Barros, L., & Ferreira, I. C. (2021). Phenolic compounds: Current industrial applications, limitations and future challenges. *Food Function, 12*(1), 14–29.

Bae, J. Y., Seo, Y. H., & Oh, S. W. (2022). Antibacterial activities of polyphenols against foodborne pathogens and their application as antibacterial agents. *Food Science and Biotechnology*, *31*(8), 985-997.

Basumatary, I. B., Mukherjee, A., Katiyar, V., & Kumar, S. (2022). Biopolymer-based nanocomposite films and coatings: Recent advances in shelf-life improvement of fruits and vegetables. *Critical Reviews in Food Science and Nutrition*, *62*(7), 1912-1935.

Bernini, R., Campo, M., Cassiani, C., Fochetti, A., Ieri, F., Lombardi, A., ... & Vita, C. (2024). Polyphenol-rich extracts from agroindustrial waste and byproducts: Results and perspectives

according to the green chemistry and circular economy. *Journal of Agricultural and Food Chemistry*, *72*(23), 12871-12895.

Bonacci, S., Di Gioia, M. L., Costanzo, P., Maiuolo, L., Tallarico, S., & Nardi, M. (2020). Natural deep eutectic solvent as extraction media for the main phenolic compounds from olive oil processing wastes. *Antioxidants*, *9*(6), 513.

Castro-Dominguez, B., Gröls, J. R., Alkandari, S., Perge, L., Sierra-Avila, C., Ramirez, H. Z., ... & da Silva Barud, H. (2025). Biopolymers and biocomposites: a comprehensive review offeedstocks, functionalities, and advanced manufacturing techniques for sustainable applications. *Biotechnology for Sustainable Materials*, *2*(1), 8.

Cazón, P., Mateus, A. R., & Silva, A. S. (2025). Advances in active packaging using natural biopolymers and fruit by-products for enhanced food preservation. *Food Research International*, 116439.

Choi, I., Kim, Y., & Park, H. (2018). Effect of oxidized phenolic compounds on cross-linking and properties of biodegradable films. *International Journal of Biological Macromolecules, 114*, 1336–1343.

de Oliveira Silva, M., Macedo, B. E., & de Castro, R. J. S. (2025). Revealing the phenolic profile, and antioxidant and antidiabetic properties of enzymatically hydrolyzed seriguela: A strategic approach to enhance the value of an exotic fruit. *Journal of Future Foods*

Durazzo, A., Lucarini, M., Souto, E. B., Cicala, C., Caiazzo, E., Izzo, A. A., Novellino, E., & Santini, A. (2019). Polyphenols: A concise overview on the chemistry, occurrence, and human health. *Phytotherapy Research, 33*(9), 2221–2243.

Farjadmand, F., Karimpour-Razkenari, E., Nabavi, S. M., Ardekani, M. R., & Saeedi, M. (2021). Plant polyphenols: natural and potent UV-protective agents for the prevention and treatment of skin disorders. *Mini Reviews in Medicinal Chemistry*, *21*(5), 576-585

Faustino, H., Gil, N., Baptista, C., & Duarte, A. P. (2010). Antioxidant activity of lignin phenolic compounds extracted from kraft and sulphite black liquors. *Molecules*, *15*(12), 9308- 9322.

Feng, Y., Jin, C., Lv, S., Zhang, H., Ren, F., & Wang, J. (2023). Molecular mechanisms and applications of polyphenol-protein complexes with antioxidant properties: A review. *Antioxidants*, *12*(8), 1577.

Ferreira, C., & Sarraguça, M. (2024). A comprehensive review on deep eutectic solvents and its use to extract bioactive compounds of pharmaceutical interest. *Pharmaceuticals*, *17*(1), 124.

González-López, M. E., Calva-Estrada, S. D. J., Gradilla-Hernández, M. S., & Barajas- Álvarez, P. (2023). Current trends in biopolymers for food packaging: a review. *Frontiers in Sustainable Food Systems*, *7*, 1225371.

Hamzah, N., Ibrahim, S., & Tjahjono, D. H. (2024). Evaluation of phenolic compounds as cross-linkers to improve the qualities of halal gelatin from milkfish scales (Chanos chanos). *Narra J*, *4*(3), e907.

Hu, S., Zhang, X., Chen, F., & Wang, M. (2017). Dietary polyphenols as photoprotective agents against UV radiation. *Journal of Functional Foods*, *30*, 108-118.

Huang, Z., Foo, S. C., & Choo, W. S. (2025). A review on the extraction of polyphenols from pomegranate peel for punicalagin purification: techniques, applications, and future prospects. *Sustainable Food Technology*.

Jiang, J., Zhang, W., Yi, X., Lei, Q., Liao, Y., Tan, Y., & Yu, W. (2024). Recent progress in properties and application of antibacterial food packaging materials based on polyvinyl alcohol. *e-Polymers*, *24*(1), 20230097.

Mafe, A. N., Edo, G. I., Akpoghelie, P. O., Joshua, O. A., Isoje, E. F., Igbuku, U. A., & Essaghah, A. E. A. (2024). Comparative analysis of the environmental impact of biopolymer- based and conventional plastic packaging in food engineering applications. *Al-Mustaqbal Journal of Sustainability in Engineering Sciences*, *2*(2), 4.

Manessis, G., Kalogianni, A. I., Lazou, T., Moschovas, M., Bossis, I., & Gelasakis, A. I. (2020). Plant-derived natural antioxidants in meat and meat products. *Antioxidants*, *9*(12), 1215.

Martillanes, S., Rocha-Pimienta, J., Cabrera-Bañegil, M., Martín-Vertedor, D., & Delgado-Adámez, J. (2017). Application of phenolic compounds for food preservation: Food additive and active packaging. In *Phenolic compounds-biological activity*. IntechOpen.

Martínez-Patiño, J. C., Gómez-Cruz, I., Romero, I., Gullón, B., Ruiz, E., Brnčić, M., & Castro, E. (2019). Ultrasound-assisted extraction as a first step in a biorefinery strategy for valorisation of extracted olive pomace. *Energies*, *12*(14), 2679.

Mir-Cerda, A., Ramos-Calero, V., Beltran, J. L., Cortina, J. L., Saurina, J., Sentellas, S., & Granados, M. (2024). Towards a sustainable recovery of polyphenol from agrifood waste:

Performance of polymeric sorbents with natural deep eutectic solvent extracts. *LWT*, *207*, 116632.

Moeini, A., Pedram, P., Fattahi, E., Cerruti, P., & Santagata, G. (2022). Edible polymers and secondary bioactive compounds for food packaging applications: Antimicrobial, mechanical, and gas barrier properties. *Polymers*, *14*(12), 2395.

Mushtaq, H., Piccolella, S., Cimmino, G., Ferrara, E., Brahmi-Chendouh, N., Petriccione, M., & Pacifico, S. (2025). Polyphenols from Olea europaea L. cv. Caiazzana leaf pruning waste for antioxidant and UV-blocking starch-based plastic films. *Food Packaging and Shelf Life*, *47*, 101447.

Ordoñez, R., Atarés, L., & Chiralt, A. (2022). Biodegradable active materials containing phenolic acids for food packaging applications. *Comprehensive Reviews in Food Science and Food Safety*, *21*(5), 3910-3930.

Pan, J., Li, C., Liu, J., Jiao, Z., Zhang, Q., Lv, Z., ... & Liu, H. (2024). Polysaccharide-based packaging coatings and films with phenolic compounds in preservation of fruits and vegetables—A review. *Foods*, *13*(23), 3896.

Panzella, L., Moccia, F., Nasti, R., Marzorati, S., Verotta, L., & Napolitano, A. (2020). Bioactive phenolic compounds from agri-food wastes: An update on green and sustainable extraction methodologies. *Frontiers in nutrition*, *7*, 60.

Pavlić, B., Mrkonjić, Ž., Teslić, N., Kljakić, A. C., Pojić, M., Mandić, A., ... & Mišan, A. (2022). Natural deep eutectic solvent (NADES) extraction improves polyphenol yield and antioxidant activity of wild thyme (Thymus serpyllum L.) extracts. *Molecules*, *27*(5), 1508.

Periyasamy, T., Asrafali, S. P., & Lee, J. (2025). Recent Advances in Functional Biopolymer Films with Antimicrobial and Antioxidant Properties for Enhanced Food Packaging. *Polymers*, *17*(9), 1257.

Pouteau, C., Cathala, B., Dole, P., Kurek, B., & Monties, B. (2005). Structural modification of Kraft lignin after acid treatment: characterisation of the apolar extracts and influence on the antioxidant properties in polypropylene. *Industrial Crops and Products*, *21*(1), 101-108.

Rahman Khan, M. M., Rumon, M. M. H., & Islam, M. (2024). Synthesis, Rheology, Morphology, and Mechanical Properties of Biodegradable PVA-Based Composite Films: A Review on Recent Progress. *Processes*, *12*(12).

Rodrigues, F., Cuffaro, D., & Digiacomo, M. (2025). Exploring bioactive polyphenols in agri-food wastes: from extraction to biological impact. *Frontiers in Nutrition*, *12*, 1638180.

Sahu, S., Kumari, D., Kuila, A., Gurjar, R. S., Sharma, K., & Verma, R. (2025). Deep eutectic solvent extraction of polyphenol from plant materials: Current status and future prospects in food applications. *Food Chemistry*, *482*, 144125.

Sangiorgio, P., Errico, S., Verardi, A., Moliterni, S., Tamasi, G., Rossi, C., & Balducchi, R. (2023). Bioactive lignans from flaxseed: Biological properties and patented recovery technologies. *Nutraceuticals*, *3*(1), 58-74.

Sani, M. A., Velayati, N., Alighadri, T., Abedini, A., Khezerlou, A., Khan, A., & Rhim, J. W. (2025). Phenolic/carboxylic acid-functionalized films: a promising and innovative strategy in next-generation packaging materials. *Colloids and Surfaces B: Biointerfaces*, 115081.

Satchanska, G. (2022). Antibacterial activity of plant polyphenols. *Secondary metabolites—trends and reviews*, 1-14.

Shaghaleh, H., Xu, X., & Wang, S. (2018). Current progress in production of biopolymeric materials based on cellulose, cellulose nanofibers, and cellulose derivatives. *RSC advances*, *8*(2), 825-842.

Singh, A. K., Kim, J. Y., & Lee, Y. S. (2022). Phenolic compounds in active packaging and edible films/coatings: Natural bioactive molecules and novel packaging ingredients. *Foods, 11*(22), 3636.

Singh, A., Mittal, A., & Benjakul, S. (2023). Chitosan, chitooligosaccharides and their polyphenol conjugates: preparation, bioactivities, functionalities and applications in food systems. *Food reviews international*, *39*(4), 2297-2319.

Sultana, S., Imran, S., Naveed, A., Hussain, S., Khattak, R., Shah, L. A., ... & Haider, F. (2024). Fabrication of nano filler doped PVA/starch biodegradable composites with enhanced thermal conduction, water barrier and antimicrobial performance for food industry. *Heliyon*, *10*(7).

Ullah, A., & Ahmed, S. (Eds.). (2025). *Green biopolymers for packaging applications* (1st ed.). CRC Press.

Viscusi, G., & Gorrasi, G. (2024). Polyphenols for Packaging Application. *Science and Engineering of Polyphenols: Fundamentals and Industrial Scale Applications*, 211-252.

Wang, J., Zhou, L., Wang, Z., Tao, Y., Chen, L., & Zhang, W. (2023). Effects of natural deep eutectic solvent on the extraction efficiency and antioxidant activities of Toona sinensis seed polyphenols: Composition and mechanism. *Food Bioscience*, *56*, 103151.

Yin, Y., & Woo, M. W. (2024). Transitioning of petroleum-based plastic food packaging to sustainable bio-based alternatives. *Sustainable Food Technology*, *2*(3), 548-566.

Zhang, Y., Zhang, W., Yuan, J., Tian, H., Qin, X., Wang, K., ... & Zhu, Q. Metal–Polyphenol Network Nanocomposites Loaded Edible Films With Enhanced Performance and Controllable Antibacterial Capability. *Available at SSRN 4946787*.

Zhao, X., Zhang, M., & Zhou, L. (2019). Antioxidant activities of plant polyphenols and their roles in food preservation. *Food Research International, 116*, 734–742.

Zhou, M., Fakayode, O. A., & Li, H. (2023). Green extraction of polyphenols via deep eutectic solvents and assisted technologies from agri-food by-products. *Molecules*, *28*(19), 6

Chapter 2

Functionalization of PVA-Based Films for Active Food Packaging: Impact of Bulk and Nano-Additives on the Physicochemical and Functional Properties

General Introduction

The ongoing transition towards sustainable and multifunctional food packaging materials has catalyzed significant research into advanced, possibly biodegradable, polymer films, with poly (vinyl alcohol) (PVA)-based systems at the forefront due to their favorable physicochem- ical and processability profiles. Actually, modern packaging not only requires biodegradability but also the integration of active functions, such as antioxidant and antimicrobial properties, water barrier performance, and enhanced optical properties, all attributes crucial for prolonging food shelf life and ensuring food safety. Within this paradigm, the blending of PVA with nat- ural polymers and plant-derived extracts, as well as their nanoscale counterparts, has emerged as an effective strategy to impart multifunctionality and optimize material properties.

This chapter explores two complementary lines of investigation focused on PVA-based films: one centered on the comparative roles of bulk and nanosized chitosan and lignin additives, and the other examining composite films embedded with duckweed (*Lemna minor*) leaf extract alongside bulk and nano-chitosan. These approaches fall into a broader scientific effort to rationalize the effects of functional components, whether natural extracts, polymers, or their nanoparticles, on morphology, barrier effects, and functionality of biopolymer-based films intended for food packaging. By systematically evaluating films for their morphological, optical, mechanical, thermal, antioxidant, and antibacterial characteristics, the studies described herein aim to clarify the additive, synergistic, or detrimental effects achieved through bio-based and nanocomposite formulations.

Part of this study was performed during a three month- stay at Université de Technologie de Compiègne in France under the supervision of Prof. Erwann Guénin.

2.1 Effects of (nano)chitosan and (nano)lignin on the morphological, mechanical and functional properties of poly (vinyl alcohol) films intended for food packaging

2.1.1. Introduction

The need to replace traditional, non-degradable plastics derived from fossil fuels with environmentally friendly alternatives is becoming increasingly urgent. This global concern has intensified research into biodegradable biopolymers for various applications, especially in food packaging (Tammina *et al*., 2025; Debeaufort *et al*., 2025; Prasad *et al*., 2025). However, many biopolymers present some drawbacks such as low mechanical strength and high sensitivity to environmental conditions. Efforts have therefore focused on the development of films based on blends of different biopolymers (Choi *et al*., 2024; Deng *et al*., 2024; Pesaranhajiabbas *et al*., 2023), nature-based plasticizers (Vieira *et al*., 2011; Mehrabi Mazidi *et al*., 2024), and/or nanoreinforcements (Rhim & Ng, 2007; Hoyos-Merlano *et al*., 2022; Rhim *et al*., 2013), which can improve specific properties for packaging purposes.

Poly(vinyl alcohol) (PVA) is widely recognized for its outstanding film-forming capability, mechanical performance, gas barrier properties, solvent resistance, and biocompatibility, making it highly suitable for applications not only in food packaging, but also in biomedical devices, household products, and construction materials (Suganthi *et al*., 2020; Panda *et al*., 2022; Sobhiga *et al*., 2024). However, the high moisture sensitivity and relatively slow biodegradation rate limit its independent application, prompting the development of PVA-based composites, involving the use of *e.g.*, starch, (nano)cellulose, gelatin (Deng *et al*., 2024; Sobhiga *et al*., 2024; Fortunati *et al*., 2013; Zhuang *et al*., 2025; Abdullah *et al*., 2019), and particularly

chitosan (Haghighi *et al*., 2020; Mathew *et al*., 2025), and (micro/nano)lignin (Chen *et al*., 2025; Han *et al*., 2024; Sun *et al*., 2026; Odili *et al*., 2025; Wang *et al*., 2018).

Chitosan, a biopolymer derived from the deacetylation of chitin from crustacean shells, is well known for its film-forming ability, biodegradability, biocompatibility, and intrinsic antimicrobial properties (Gomes *et al*., 2021; Olunusi *et al*., 2025; Stachowiak *et al*., 2020). When blended with PVA, chitosan may contribute to form a more compact polymer network *via* hydrogen bonding, leading to improved tensile strength, reduced permeability, and enhanced moisture resistance—essential characteristics for preserving *e.g,* food quality. Furthermore, chitosan may contribute antimicrobial activity, providing active protection in food packaging systems (Haghighi *et al*., 2020; Mathew *et al*., 2025; Stachowiak *et al*., 2020; Irmukhametova *et al*., 2025; Abraham & Soloman, 2016; de Souza Costa-Júnior *et al*., 2009).

Lignin, a naturally occurring phenolic polymer, has emerged as another promising additive for conferring antioxidants, UV-Vis blocking, and antimicrobial properties to biopolymer-based films for active food packaging applications (Boarino & Klok, 2023; Las-Casas *et al*., 2025; Marcoaldi *et al*., 2025; Monteiro *et al*., 2021). In addition, it has been reported to acts as a nucleating agent in PVA-based films, improving mechanical properties, thermal stability, and crystallinity, particularly when used at the nanoscale, enabling stronger interaction with the PVA matrix (Chen *et al*., 2025; Han *et al*., 2024; Sun *et al*., 2026; Odili *et al*., 2025; Wang *et al*., 2018; Priyadarshi *et al*., 2024; Yang *et al*., 2018; Yang *et al*., 2016; Zhang *et al*., 2025).

Recent studies have specifically explored the use of (nano)lignin in PVA–(nano)chitosan films. The interaction between the phenol groups in lignin and amino groups in chitosan have been reported to foster the development of cohesive networks, enhancing both structural integrity and functional performance. In addition, the combined antimicrobial effects of chitosan and lignin, especially against Gram-negative bacteria such as *E. coli*, have been reported to enhance food safety (Yaneva *et al*., 2022; Li *et al*., 2024; Wu & Zhao, 2025).

Nanochitosan and lignin nanoparticles, in particular, may offer notable advantages over their bulk counterparts when integrated into PVA films, allowing better dispersion and stronger interactions, resulting in elevated barrier and functional properties (Zhang *et al*., 2019; Zhang *et al*., 2025). However, a systematic approach aimed to investigate and rationalize the effects of chitosan and lignin nanoparticulation on PVA film properties is apparently lacking in the literature. Starting from this scenario, this study was directed to the preparation and characterization of multifunctional PVA-based films by incorporating chitosan and lignin or their nanoforms to investigate the effects of nanoparticulation and synergism of the additives on the film physicochemical and functional properties for the development of biocompatible active food packaging material.

2.1.2 Experimental

2.1.2.1. Materials

Poly(vinyl alcohol) (PVA; MW 124–146 kg/mol, 99% hydrolyzed), glycerol (≥99%), chitosan (CH) from crab shells (low molecular weight, 75–85% deacetylation), alkali lignin (LIG), sodium acetate (≥99%), 2,4,6-tris(2-pyridyl)-*s*-triazine (TPTZ, ≥98%), iron(III) chloride hexahydrate ($FeCl_3 \cdot 6H_2O$, ≥97%), copper(II) chloride ($CuCl_2$, ≥97%), neocuproine (≥98%), hydrogen peroxide solution (30% w/w), (HCl, ≥37%), sodium hydroxide (NaOH, ≥98%), sodium metabisulfite ($Na_2S_2O_5$, ≥97%), dimethyl sulfoxide (DMSO, ≥99.5%), sodium acetate trihydrate (≥99.0%), glacial acetic acid (CH_3COOH, ≥99.5%), and ammonium acetate (≥98.0%) were purchased from Sigma-Aldrich (Milan, Italy).. Ethylene glycol (≥99%), ethanol (96% v/v), nitric acid (HNO_3, 67–69%), glacial acetic acid (100%), and sodium tripolyphosphate (TPP, ≥98%) were sourced from Thermo Fisher Scientific (Waltham, MA, USA). All chemicals were used as received without further purification.

2.1.2.2. Preparation of lignin nanoparticles (LNPs)

A 2.5% w/w lignin solution was prepared by dissolving 1 g of LIG in 40 g of ethylene glycol with the aid of a rotor-stator homogenizer at 5000 rpm for 30 min. Then, 12 mL of 0.05 M nitric acid were added dropwise, and the solution was sonicated for 1 h at 20 kHz while taking an ice bath. The solution was dialyzed in deionized water for 4 days, changing the water 4 times a day for the first 3 days. Finally, the LNPs solution was freeze-dried at −80°C for 4 days to obtain solid nanoparticles (Zhang *et al*., 2022).

2.1.2.3. Preparation of nanochitosan (NCH)

0.6 g of acetic acid were added to 100 mL of water and the mixture was stirred for 10 min at 2000 rpm at room temperature. Then, 0.5 g of CH were added, and the mixture was stirred at 8000 rpm for 5 h, until CH was completely dissolved. Next, 10 mL of a 0.05 g/mL TPP solution in distilled water were added dropwise to the solution, and stirring continued for 30 min. The solution was then ultrasonicated at 20 kHz for 1 h and maintained at 4 °C (Pinem *et al*., 2020).

2.1.2.4. Preparation of PVA-based films

6 g of PVA were added to 50 mL of distilled water, and the mixture was taken under stirring at 80°C for 6 h until a clear solution was obtained. To remove air bubbles, the solution underwent sonication at 20 kHz for 30 min. Control films were prepared without the addition of lignin, chitosan, or their nanoparticle counterparts. For film casting, 3 mL of the solution were poured into a 9 cm Petri dish and dried at 45 °C for 24 h. For blended films, the same process was followed, with the addition of 2.5 mL of glycerol and other additives after PVA dissolution (Table 2.1), followed by an extra 30 min of stirring. Two different batches were formulated: batch B (bulk form) contained PVA, glycerol, CH, and LIG, and batch N (nanoform), in which CH was replaced with NCH and lignin was replaced with LNPs.

Table 2.1. *PVA-based film formulations adopted in the present study.*

Code	Formulation	PVA (%w/w)	Glycerol (%w/w)	CH/NCH (%w/w)	LIG/LNPs (%w/w)
A	PVA	100	-	-	-
A1	PVA/Glycerol	98	2	-	-
B1	PVA/Glycerol/LIG	92	2	-	6
B2	PVA/Glycerol/CH/LIG	88	2	4	6
N1	PVA/Glycerol/NLPs	92	2	-	6
N2	PVA/Glycerol/NCH/NLPs	88	2	4	6

2.1.2.5. Nanoparticles characterization

The hydrodynamic diameter and zeta potential of the nanoparticles were characterized by DLS using a Malvern Panalytical Zetasizer Ultra. The morphology of the nanoparticles was characterized by TEM (JEOL, JEM-2100F) at an acceleration voltage of 200 kV, by dispersing the samples in ultra-pure water and depositing them on carbon-coated copper grids. NMR spectra of LIG and LNPs were recorded in DMSO-d_6 at 400 MHz on a Bruker 400 MHz spectrometer. UV-Vis spectra of DMSO solutions of LIG and LNPs after dilution in methanol were recorded on a Jasco V-730 spectrophotometer.

Chemical degradation of LIG and LNPs was performed as previously described (Venezia et al., 2024; Grappa et al., 2024; Gómez-Cruz et al., 2025). Briefly, 10 mg of each sample were treated under stirring for 24 h with 1 mL of 1 M NaOH and 50 µL of 30 % hydrogen peroxide. Then, 200 µL of a 5 % w/v aqueous solution of $Na_2S_2O_5$ were added, and the solution was taken to pH 3 with 6 M HCl and filtered on a 0.45 µm polyvinylidene fluoride (PVDF) filter. Finally, the mixture was analyzed by LC-UV- MS in positive ion mode on an Agilent LC-MS ESI-TOF 1260/6230DA instrument equipped with a UV detector set at 254 nm under the fol- lowing conditions: capillary voltage 3500 V; drying gas (nitrogen) 5 L/min, 325 °C; fragmentor voltage 175 V; nebulizer pressure 35 psig.

An Agilent Eclipse Plus ODS column (150 × 4.6 mm, 5 μm) was used, and a gradient elution at a flow rate of 0.4 mL/min was performed using 0.1 % formic acid (solvent A)/methanol (solvent B): 5 % B, 0–10 min; from 5 to 80 % B, 10–47.5 min.

2.1.2.6. Characterization of the physicochemical properties of the films

The morphology and thickness of the composite films were characterized by SEM using a JEOL JEM-2100F at an acceleration voltage of 200 kV. To enhance conductivity, all film samples were gold-coated prior to observation and analysis.

IR analysis was performed using a ThermoScientific Nicolet iS5 FTIR equipped with a horizontal reflection ATR accessory including a germanium crystal. The background was recorded under ambient conditions without the sample. IR spectra were recorded in the wavenumber range 600-4000 cm^{-1}, with 16 scans collected at a nominal resolution of 4 cm^{-1}. The spectra were recorded in triplicates, and the resulting curves were averaged.

Moisture content, swelling degree, and total soluble matter were determined gravimetrically using a three-step method. Briefly, square-shaped film samples (1 cm^2) were weighed on an analytical balance with a precision of 0.0001 g to obtain the initial mass (M_1). In the first step, the samples were dried at 105 °C for 24 h to determine the initial dry mass (M_2). In the second step, the oven-dried samples with a known M_2 value were separately immersed in water (30 mL) and left at room temperature for 24 h, after that any excess water not absorbed by the film specimens was removed using paper wipes, and the samples were weighed again to obtain the wet mass of the film (M_3). In the final third step, the samples were dried once more at 105 °C for 24 h to determine the final dry mass (M_4).

All experiments were performed in triplicates. Moisture content, that is the percentage of mass loss due to water evaporation after drying the samples at 105 °C for 24 h, was calculated using Eq. (1). Swelling degree, that is the percentage of mass gain resulting from water absorption after immersing the dry samples in water for 24 h, was determined using Eq. (2). Total soluble

matter, defined as the percentage of the film dry matter solubilized after 24 h of immersion in water, was calculated using Eq. (3) (Apriliyani *et al*., 2020; Kowalczyk *et al*., 2015).

$$\textit{Moisture content}\ (\%) = (M_1 - M_2)/M_1 * 100 \quad (1)$$

$$\textit{Swelling degree}\ (\%) = (M_3 - M_2)/M_2 * 100 \quad (2)$$

$$\textit{Total soluble matter}\ (\%) = (M_2 - M_4)/M_2 * 100 \quad (3)$$

The color of the films was determined using a CR-400 colorimeter (Konica Minolta). A white plate was used as the standard (L = 93.25, a = 0.19, b = 3.95), against which the color difference (ΔE) was calculated according to Eq. (4), where L*, a*, b* represent the tendency towards whiteness, from green to red and from blue to yellow, in that order.

$$\Delta E = \sqrt{(L^*|L)^2 + (a^*|a)^2 + (b^*|b)^2} \quad (4)$$

The transmittance and opacity of the prepared films were determined with a Jasco V-730 spectrophotometer. Film samples were cut into 1 cm × 4 cm dimensions and transmittance was measured. Absorbance values at 600 nm (Abs_{600}) were recorded, and opacity was calculated using Eq. (5) (Riaz *et al*., 2018).

$$\textit{Opacity} = Abs_{600}/\textit{film thickness} \quad (5)$$

The mechanical properties of the prepared films, including tensile strength and elongation at break were determined by Prof. Endarto Wardhono (University of Sultan Ageng Tirtayasa, Indonesia) using a Zwick/Roell universal testing machine according to the ASTM D 638 standard method. The films were cut into appropriate specimen dimensions with a consistent width of 2.4 cm and positioned between the grips of the testing machine with an initial grip-to-grip separation of 30.00 mm. The test was conducted at a constant speed of 200 mm/min under ambient conditions, and a pre-load of 0.1 MPa was applied to ensure proper gripping and alignment of the specimens. Tensile strength and elongation at break were calculated based on the recorded stress-strain data. The stress (MPa) was measured as the force per unit area, and

the elongation (%) was calculated as the percentage increase in length of the specimen at the point of fracture relative to the original length. The results from three specimens were averaged to obtain the mean values for tensile strength and elongation at break.

The thermal properties of the prepared films were tested by Dr. Michaël Lefebvre (Université de Technologie de Compiègne, France) using DSC 2500 TA Instruments. The analysis were carried out between 0°C and 400°C with a ramp of 5K/min with a nitrogen flow rate of 50 mL/min.

2.1.2.7. Antioxidant property characterization

A 1 cm² film sample was added to the ferric reducing/antioxidant power (FRAP) or cupric reducing antioxidant capacity (CUPRAC) assay solution at a 2.8 mg/mL dose, and the absorbance of the solution was periodically monitored over time. The FRAP assay solution was prepared using 0.3 M acetate buffer (pH 3.6), 1.7 mM $FeCl_3 . 6H_2O$ in distilled water, and 0.83 mM TPTZ in 40 mM HCl solution in a 10:1:1 v/v/v ratio. The reducing power was evaluated by measuring the absorbance at 593 nm (Benzie & Strain, 1996). The CUPRAC assay solution was prepared by mixing 1 M ammonium acetate buffer (pH 7.0), 10 mM $CuCl_2$ in distilled water, 7.5 mM neocuproine in ethanol, and distilled water in a 1:1:1:1 v/v ratio, and the reducing power was evaluated by measuring the absorbance at 450 nm (Apak *et al*., 2004). Control experiments were carried out under the same conditions but without the films.

In separate experiments the FRAP and the CUPRAC assay were performed on LIG and LNPs. Briefly, 2-15 μL of a 10 mg/mL DMSO solution of each sample were added to 2 mL of the FRAP or CUPRAC assay solution and after 10 min under stirring the absorbance at 593 (FRAP) or 450 (CUPRAC) nm was measured. Results were expressed as Trolox eqs.

2.1.2.8. Antibacterial activity characterization

The characterization of the antibacterial activity of the films was run by Prof. Angela Arciello and her staff at the Department of Chemical Sciences of University of Naples Federico II.

2.1.2.8.1. Bacterial strains and culture conditions

Bacterial strains *Salmonella enterica* serovar Typhimurium ATCC® 14028, *Salmonella enterica* serovar Enteritidis 706 RIVM, and *Enterococcus faecalis* ATCC® 29212 were cultured in Muller-Hinton Broth (MHB, Becton Dickinson Difco, Franklin Lakes, NJ, USA) and on Luria-Bertani Agar (LBA; tryptone 10 g/L, yeast extract 10 g/L, sodium chloride 5 g/L). For all experiments assessing the antimicrobial activity of air-dried PVA-based film, bacterial cells were inoculated into MHB and incubated overnight at 37 °C. The following day, cultures were transferred to fresh MHB and grown to the mid-logarithmic phase.

2.1.2.8.2. Evaluation of bacterial growth inhibition

To assess cell viability, bacterial cells were diluted into 0.5× MHB to approximately 2×10^6 CFU/mL. A 500 µL aliquot of the bacterial culture was placed onto a 1 cm^2 square of each tested film and incubated at 37 °C overnight. The following day, the cultures were diluted in 0.5× MHB medium and plated on LBA to perform the colony counting.

2.2.2.9. Statistical analysis

Statistical analysis was performed by using a student's t-Test. Significant differences were indicated as *($P < 0.05$), **($P < 0.01$) or ***($P < 0.001$).

2.1.3 Results and discussion

2.1.3.1. Lignin nanoparticle (LNPs) and nanochitosan (NCH) preparation and characterization

LNPs were prepared starting from commercially available alkali lignin by the ultrasonic dialysis freeze drying method (Zhang *et al*., 2022). NMR, UV-Vis, and chemical degradation analysis indicated the lack of significant chemical modifications induced on lignin by the approach adopted for nanoparticle formation. The alkaline hydrogen peroxide degradation adopted in this study is commonly used for the analysis of insoluble and structurally complex phenolic polymers such as melanin pigments and lignins, and is based on the identification of highly

structure-specific chromatographable markers resulting from the oxidative breakdown of the polymer (Venezia *et al*., 2024; Grappa *et al*., 2024; Gómez-Cruz *et al*., 2025; Panzella *et al*., 2012). LC–UV–MS profiles of the alkaline hydrogen peroxide degradation mixture of LIG and LNPs (Fig. 1a) were quite completely superimposable and were characterized by the presence of a main peak eluted at approximately 32 min identified as vanillic acid, a typical marker of non-cross-linked guaiacyl units in lignin samples (Grappa *et al*., 2024). Similarly, no significant differences between LIG and LNPs were observed by ^{1}H NMR analysis. Indeed, both samples exhibited a complex set of signals in the ranges 5.5–7.8 ppm (Fig. 1b), consistent with the chemically heterogeneous and polymeric structure of lignin, although in the case of LNPs these signals appeared less defined and broader, likely as a consequence of the aggregation process underlying LNPs formation. On the contrary, the broad signal in the region 8.5–9.5 ppm attributed to the phenolic −OH groups were slightly more resolved in the case of LNPs than in the LIG sample, possibly due to the higher specific surface area resulting in a greater exposure of lignin functional groups, including phenolic hydroxyls.

Finally, UV-Vis analysis (Fig. 2.1c) confirmed the similarity in terms of chemical features of LIG and LNPs, although the spectrum appeared more intense and lower scattering was observed in the case of LNPs due to their higher solubility.

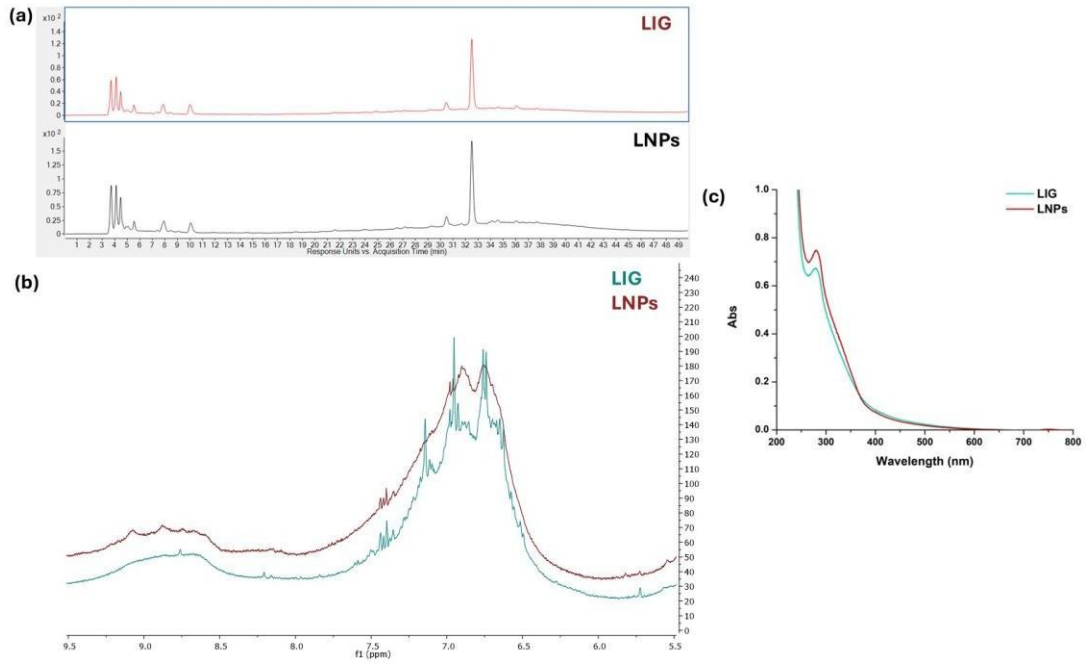

Fig. 2.1 *(a) HPLC profile of the alkaline hydrogen peroxide degradation mixtures, (b) ^{1}H NMR spectra, and (c) UV-Vis spectra of LIG and LNPs.*

DLS analysis of LNPs revealed a Z-average hydrodynamic diameter of 114 ± 11 nm with a relatively high polydispersity index (PDI) of 0.62 ± 0.07, indicating a broad size distribution and suggesting the coexistence of both well-formed nanoparticles and aggregates, possibly due to the inherent structural heterogeneity of lignin and different possibly occurring intermolecular interactions between lignin functional groups. The zeta potential of –37 ± 1 mV confirmed in any case good colloidal stability through electrostatic repulsion. In contrast, NCH synthesized by a modified ionic gelation method (Pinem *et al*., 2020), exhibited a larger hydrodynamic diameter of 246 ± 22 nm but a lower PDI of 0.43 ± 0.08, indicating a more uniform size distribution. As expected, NCH carried a high positive surface charge with a zeta potential of +40 ± 1 mV, attributed to protonated amino groups, ensuring strong electrostatic stabilization in aqueous medium.

TEM analysis (Fig. 2.2) provided visual confirmation of the DLS results for both nanoparticle types. LNPs appeared predominantly spherical with core sizes ranging from 30 to 80 nm, which were smaller than the DLS-reported sizes due to the absence of hydration layers in dry-state

imaging, and were interspaced with irregular aggregates, particularly visible in lower-magnification images. In contrast, NCH displayed more uniform spherical morphologies with estimated core sizes between 50 and 150 nm.

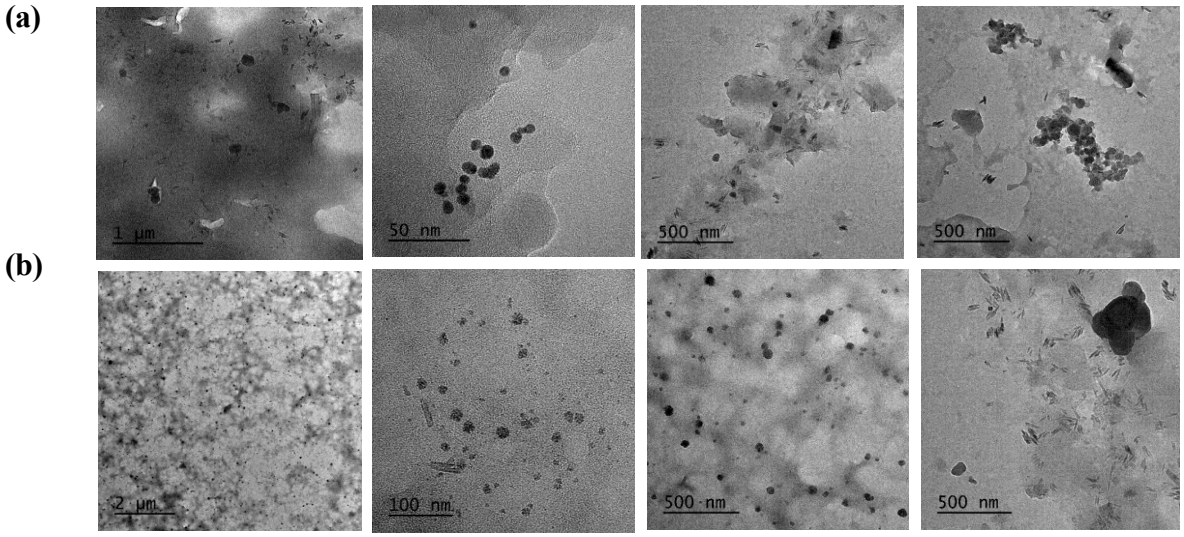

Fig. 2.2 *TEM images of (a) LNPs and (b) chitosan nanoparticles at various magnifications.*

2.1.3.2. Poly (vinyl alcohol)(PVA)-based films preparation and physicochemical characterization

The PVA-based films were prepared by the solvent casting method using glycerol as a plasticizer and lignin (LIG) or lignin nanoparticles (LNPs), and chitosan (CH) or nanochitosan(NCH) as active/reinforcing agents (Table 2.1). The ATR-FTIR spectra revealed key insights into molecular interactions among these components. The pure PVA film exhibited a broad O–H stretching band between 3200–3600 cm^{-1}, characteristic of strong intra-chain hydrogen bonding, with sharp C–O peaks at 1077 cm^{-1} and 1412 cm^{-1} reflecting ordered crystalline domains. Upon adding glycerol, the O–H band broadened significantly, indicating intermolecular hydrogen bonding between PVA chains and glycerol hydroxyl groups. However, no significant changes were observed with the addition of lignin, LNPs, chitosan, or NCH. The FTIR spectra of the lignin/LNP-containing films showed a shift in the O–H stretching band from ~3397 cm^{-1} for pure PVA to ~3298–3307 cm^{-1}, suggesting an increase in hydrogen-bonded hydroxyl groups due to interfacial association between PVA–OH and lignin/LNP oxygenated functionalities. This is

consistent with prior reports of strong intermolecular hydrogen bonding in PVA–lignin systems (Kubo & Kadla, 2003). The aliphatic C–H stretching bands near 2965–2954 cm^{-1} persisted across all samples, indicating retention of the aliphatic framework in PVA, with minor variations attributed to conformational changes caused by blending and filler addition. For chitosan-containing films, shifts in the ~1670–1550 cm^{-1} region were observed, indicating contributions from bound water and chitosan amide/amine vibrations. These shifts are typical indicators of interaction and complexation in PVA–chitosan systems (Kadir *et al*., 2011; Vicentini *et al*., 2010). Overall, the FTIR data confirm that the PVA backbone remains intact after incorporating lignin and chitosan, with the observed spectral changes indicating hydrogen bonding and intermolecular interactions, which play a crucial role in the films physical and chemical properties.

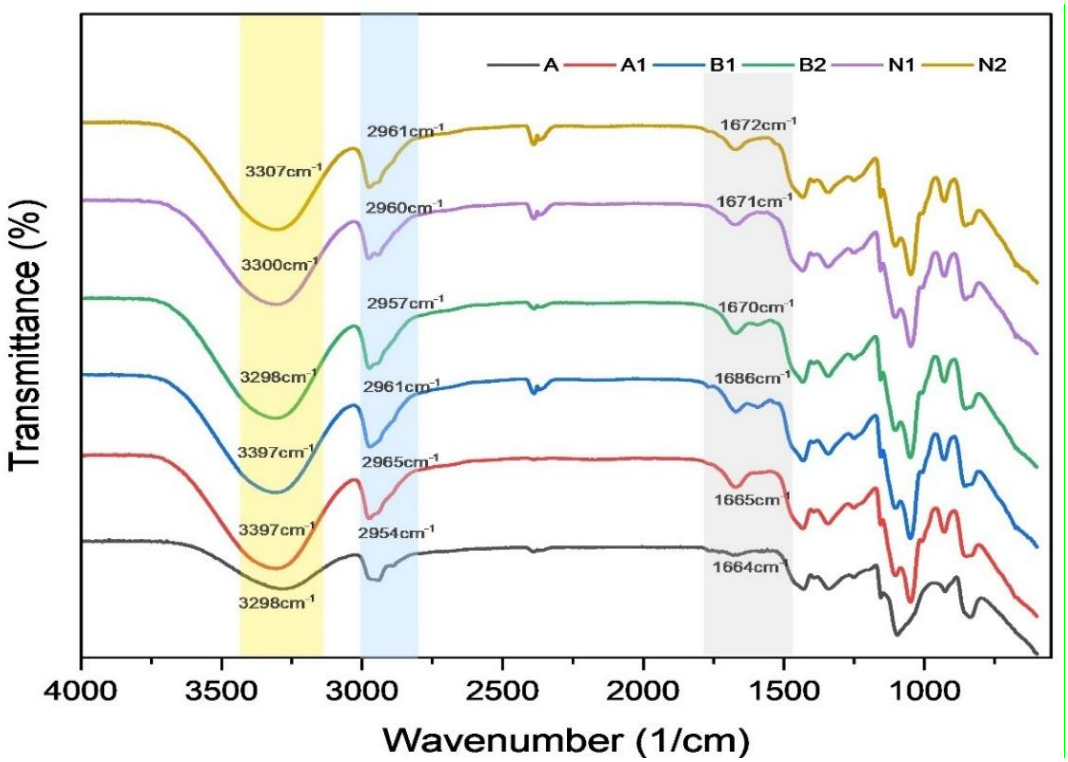

Fig. 2.3 *ATR-FTIR spectra of PVA-based films incorporating chitosan, lignin, and their nano formulations*.

The SEM micrographs reveal distinct morphological characteristics among the six films formulated with various combinations of PVA, glycerol, (nano)chitosan, and (nano)lignin. The neat PVA film (sample A, Fig. 2.4a and Fig. 2.4b) exhibited a smooth and uniform surface, while the cross-sectional view showed a dense, compact structure with no visible pores or layering. The PVA-glycerol film (A1, Fig. 2.4a and Fig. 2.4b) demonstrated a slightly rougher surface due to plasticization, and its cross-section appeared more relaxed and loosely packed, with minor voids emerging between layers. The B1 film (Fig. 2.4a and Fig. 2.4b), incorporating bulk lignin, showed a somewhat uneven surface, while the cross-sectional morphology appeared moderately porous with visible heterogeneity across layers, indicating limited miscibility. Film B2 (Fig. 2.4a and Fig 2.4b), composed of bulk chitosan and lignin, displayed a coarser surface and evident phase separation; the cross-section revealed a layered, less cohesive structure, pointing to poor interfacial bonding between components. On the other hand, the N1 film (Fig. 2.4a and Fig.2.4b), which contained LNPs only, exhibited a relatively smooth surface, and its cross-sectional image showed a well- integrated, compact structure with fewer defects or separation between layers, indicating improved dispersion. The N2 film (Fig. 2.4a and Fig. 2.4b), containing both LNPs and NCH, showed the smoothest and most homogeneous surface morphology among all films. Its cross-section confirmed a tightly packed, continuous internal structure with no noticeable voids or phase separation, reflecting superior compatibility between the components at nanoscale integration. Comparable thickness values were determined for all the films, although they increased with additive inclusion, as seen *e.g.*, for samples B2 (35.24 $\pm$ 0.06 μm) and N2 (35.66 $\pm$ 0.04 μm) compared to pure PVA (sample A) (33.90$\pm$ 0.06 μm) (Table 2.2).

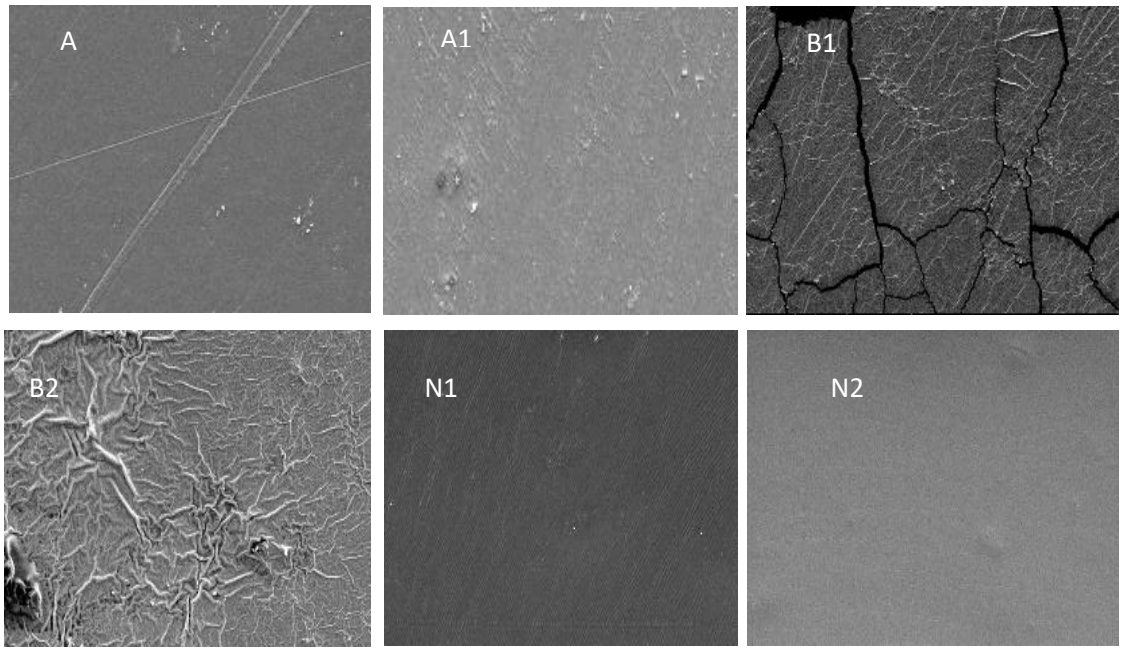

Fig. 2.4a *SEM surface images(200µm) of the PVA-based composite film*

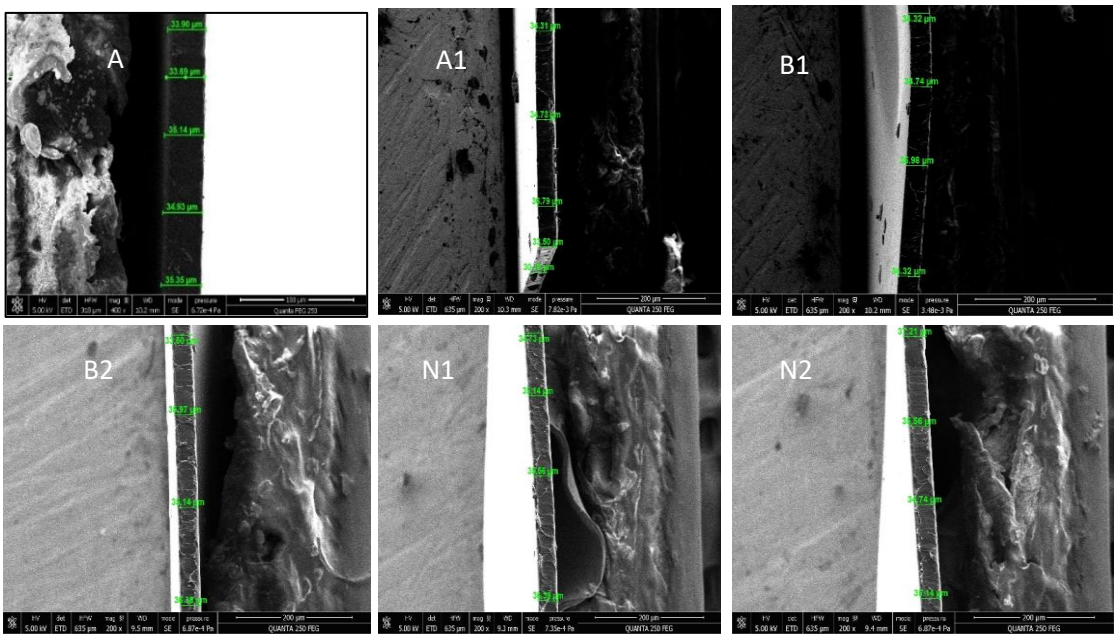

Fig. 2.4b *SEM cross-sectional images(200µm) of the PVA-based composite films*

Transparency is a critical characteristic of food packaging films, enhancing product visibility, consumer trust, and quality assurance. As expected, however, the incorporation of chitosan and especially lignin into the PVA-based composite films significantly influenced their optical properties**,** including opacity and color, providing on the other hand a more efficient UV-Vis blocking efficiency**.** In particular, an increase in opacity from 2.85 ±0.13 mm^{-1} for pure PVA

(sample A) to 5.05 ±0.06 mm^{-1} for N2 was observed (Table 2.2), which was attributed to light blocking by lignin particles and other additives. Colorimetric analysis further supported this trend. The overall color difference (ΔE) compared to a standard white plate increased significantly from 10.80 ± 0.03 in the case of pure PVA (sample A) to 26.23 ± 0.23 in the case of B2, highlighting notable visual changes mainly due to the natural brownish hue of lignin, with a very slight contribution from chitosan (see B1 *vs* B2). Notably, the use of nanoparticles led to significant improvements over bulk additives, since films N1 and N2 exhibited lower ΔE values, indicating less color deviation compared to pure PVA films. In terms of UV-Vis blocking performance, as expected films containing lignin showed a significant decline in transmittance, especially in the range 200-350 nm, due to the UV-absorption properties of phenolic groups in lignin (Zhang *et al*., 2025; Venezia *et al*., 2024) (Fig. 2.5). Indeed, while pure PVA (A) and PVA-glycerol (A1) films allowed >85% visible light transmission with minimal UV shielding, lignin incorporation reduced UV transmittance in the range 200-350 to below 1%. A significant lower UVA (320-400 nm) transmittance was also observed, and visible transmittance was reduced to 40-70%. The film containing both lignin and chitosan in their nanoform (N2) demonstrated superior visible radiation blocking performance-

Table 2.2 *Thickness and optical properties of PVA-based films incorporating chitosan, lignin, and their nanoformulations.* ***Reported are the mean ± SD values from three separate measurements.***

Sample	Thickness (μm)	Opacity (mm^{-1})	ΔE
A	33.90 ± 0.06	2.85 ± 0.13	10.80 ± 0.03
A1	34.60 ± 0.02	2.99 ± 0.06	13.01 ± 0.03
B1	34.84 ± 0.05	3.24 ± 0.06	25.96 ± 0.15
B2	35.24 ± 0.06	3.93 ± 0.08	26.23 ± 0.23
N1	35.45 ± 0.05	3.42 ± 0.07	19.18 ± 0.20
N2	35.66 ± 0.04	5.05 ± 0.06	20.93 ± 0.06

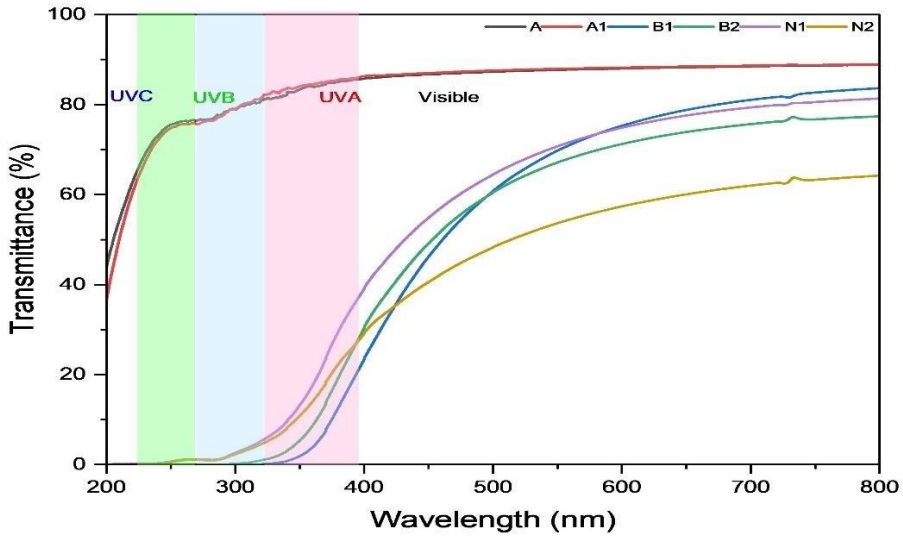

Fig. 2.5 ***UV****-Vis transmittance spectra of PVA-based films incorporating chitosan, lignin, and their nanoformulations.*

When PVA films are placed in a humid or water environment, swelling or even dissolution occurs, which greatly limits its application. Therefore, it is necessary to modify PVA-based films with proper components to improve water resistance to expand their application range (Liu *et al.,* 2022).The observed variations in water content, swelling degree, and solubility across the samples observed in the present study (Fig. 2.6) can be rationally explained by considering the influence of lignin and chitosan and their nanocounterparts on the material properties. While not very significant differences were observed among the samples in terms of moisture content, incorporation of glycerol as plasticizer dramatically reduced swelling degree from 64% in the case of sample A to 25% in the case of sample A1. Moreover, the addition of lignin, a hydrophobic component, reduced also the total soluble matter (as evident in particular for sample B1 and N2). On the other hand, chitosan, which is hydrophilic, slightly increases swelling degree, as observed in samples B2 and N2. Notably, when the nanocounterparts of lignin and chitosan were used (sample N2), total soluble matter decreased to only 4%, likely due to the improved dispersion of hydrophobic LNPs aided by the presence of NCH, resulting in improved film structural integrity.

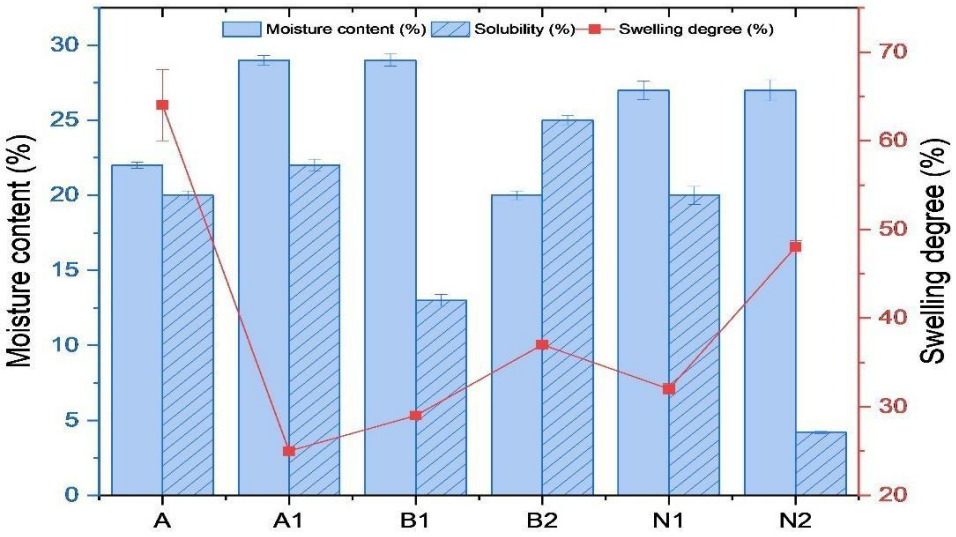

Fig. 2.6 *Moisture content, swelling degree, and total solubility of PVA-based films incorporating chitosan, lignin, and their nanoformulations. Reported are the mean ± SD values from three separate experiments.*

Food packaging films are required to maintain their integrity to withstand the stress that occurs during handling, storage and shipping, so tensile tests were performed according to ASTM D638 to evaluate the effects of LIG/LNPs and CH/NCH on the elastic-plastic response of the PVA-based films. Pure PVA film (sample A) exhibited moderate stiffness (Young's modulus: 22.72 ± 4.68 MPa) (Fig. 2.7) and the highest tensile strength (33.48 ± 3.33 MPa) attributed to its dense hydrogen-bonded crystalline domain, though limited chain mobility restricted its elongation at break (147 ± 18%). Plasticization with glycerol (sample A1) drastically reduced the modulus and tensile strength, as glycerol disrupted crystalline packing, while elongation remained comparable to pure PVA (Fig. 2.7). Incorporation of bulk lignin (sample B1) enhanced stiffness and elongation compared to A1 sample (Fig. 2.7), likely due to lignin rigid aromatic structure and additional hydrogen bonding, which dissipated stress more efficiently. When bulk chitosan was combined with lignin (sample B2), tensile strength and elongation improved slightly compared to sample B1, but modulus decreased (Fig. 2.7), indicating some interfacial incompatibilities between lignin and chitosan in bulk forms that weaken the matrix. Interestingly, no significant mechanical differences were observed between films containing lignin in bulk or nanoform (in the presence or absence of NCH) (sample B1 *vs* N1and N2, Fig.

2.7). Although the nanoforms improved film uniformity and thermal stability, the expected reinforcement effect was offset by possible nanoparticle agglomeration, leading to mechanical properties comparable to bulk formulations. This highlights that, unlike optical and barrier properties, the mechanical response of PVA-based films is less sensitive to additive dispersion scale.

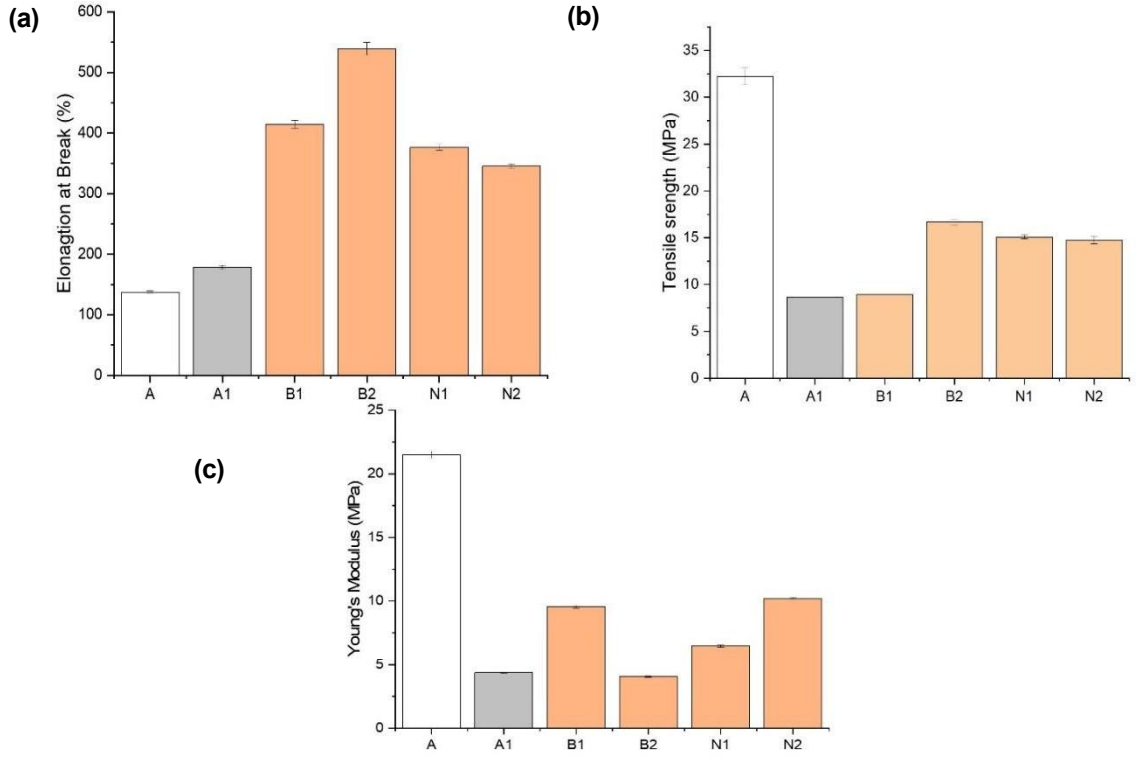

Fig. 2.7 *Mechanical properties of PVA-based films incorporating chitosan, lignin, and their nanoformulations. Reported are the mean ± SD values (n ≥3) for (a) elongation at break (b) tensile strength and (c) Young's modulus.*

DSC revealed distinct thermal degradation profiles for the different films, with onset temperatures and peak morphology directly correlated to additive composition and dispersion scale (Fig. 2.8 and Table 2.3). Pure PVA film (sample A) showed a sharp exothermic degradation onset at 233 °C, consistent with its semicrystalline structure. Plasticization with glycerol (sample A1) slightly increased thermal stability (T_d= 239 °C), whereas addition of lignin and/or chitosan led to a decrease of T_d likely because of increased chain mobility of PVA making its degradation easier. This effect was even more marked when nanolignin, especially

when combined with nanochitosan, was introduced, as a consequence of the more efficient embedding of the additives inside the polymer network. As expected based on these results, a similar trend was observed when the T_m of the different films were compared. Indeed, as the melting process is related to a phenomenon when chains of molecules break out of their orderly arrangements and begin to move freely, the presence of lignin enhanced this process leading to a decrease of the T_m values. Further information could be provided by determination of the glass transition temperature (T_g) of the various films.

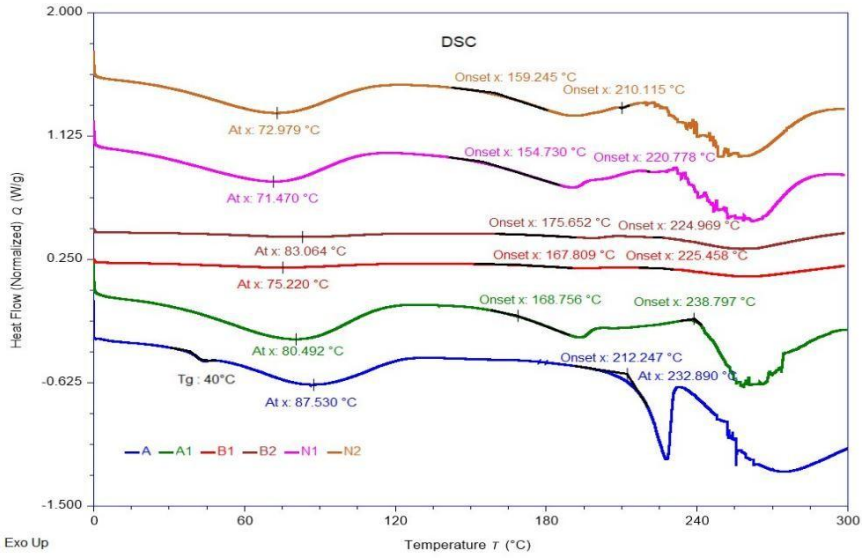

Fig. 2.8 *DSC thermograms of PVA-based films incorporating chitosan, lignin, and their nanoforms.*

Table 2.3 *Temperature of water evaporation (T_e), onset of melting temperature (T_m), and onset for degradation temperature (T_d) of PVA-based films incorporating chitosan, lignin, and their nanoformulations.*

Sample	Key Modifications	T_c (°C)	T_m (°C)	T_d (°C)
A	Neat PVA	87.5	212.2	233
A1	+ Gly	80.5	169	239
B1	+ LIG	75.2	168	225.4
B2	+ CH/LIG	83	176	225
N1	+ LNPs	71.4	155	221
N2	+ NCH, LNPs	73	159.2	210.1

2.1.3.2. Poly (vinyl alcohol) (PVA)-based films antioxidant and antimicrobial properties

Oxidation reactions and microbial spoilage can result in nutrient loss and decline in food quality and consumer acceptance. Therefore, food packaging materials with antioxidant and antimicrobial properties can help extend the shelf life of food. The antioxidant properties of the prepared PVA-based films were evaluated using FRAP (working pH 3.6) and CUPRAC (working pH 7.0) assays (Fig. 2.9). As expected, all the lignin- containing films exhibited stronger reducing properties compared to PVA-glycerol film (sample A1). Quite surprisingly, however, the film containing bulk lignin performed better than the film containing LNPs (see B1 *vs* N1 and B2 *vs* N2). This is apparently in contrast with the results of the FRAP assay performed on lignin and its nanocounterpart, indicating comparable Trolox eqs values (0.12 $\pm$ 0.01 and 0.11 $\pm$ 0.01 mg of Trolox/mg of sample for LIG and LNPs, respectively). On the other hand, in the CUPRAC assay LNPs (0.36 $\pm$ 0.01 Trolox eqs) performed even better than bulk lignin (0.27 $\pm$ 0.01 Trolox eqs).

It can be therefore hypothesized that, in line with what observed by SEM analysis, nanoparticulation allows for a more efficient dispersion and integration of lignin into the PVA matrix, making the phenolic groups less available for interaction with the iron(III) ions in solution. Along the same direction, the presence of chitosan significantly lowered the antioxidant efficacy (sample B2 *vs* sample B1 and sample N2 *vs* sample N1) the case of the FRAP assay, as a consequence of the interactions occurring between chitosan–$NH3^+$ and lignin –OH groups (Ravishankar *et al*., 2019), lowering the availability of these latter to interact with the oxidizing metal ions (Fig. 2.10). This effect was less pronounced in the CUPRAC assay, likely due to the lower amount of protonated chitosan amino groups at the neutral pH adopted in this assay and hence to the weaker interactions with the phenolic lignin groups. In any case, the film containing only bulk lignin (sample B1) was the most promising sample in both assays.

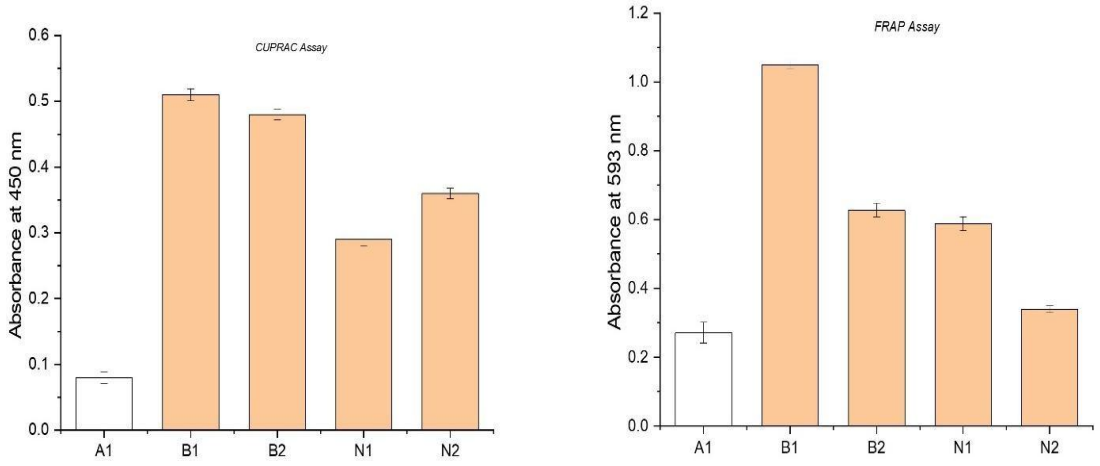

Fig. 2.9 *Antioxidant properties of PVA-based composite films incorporating chitosan, lignin, and their nanoformulations. Shown are the results obtained after 24 h at a film dose of 2.8 mg/mL using the FRAP and CUPRAC assays. Reported are the mean ± SD values from at least three experiments.*

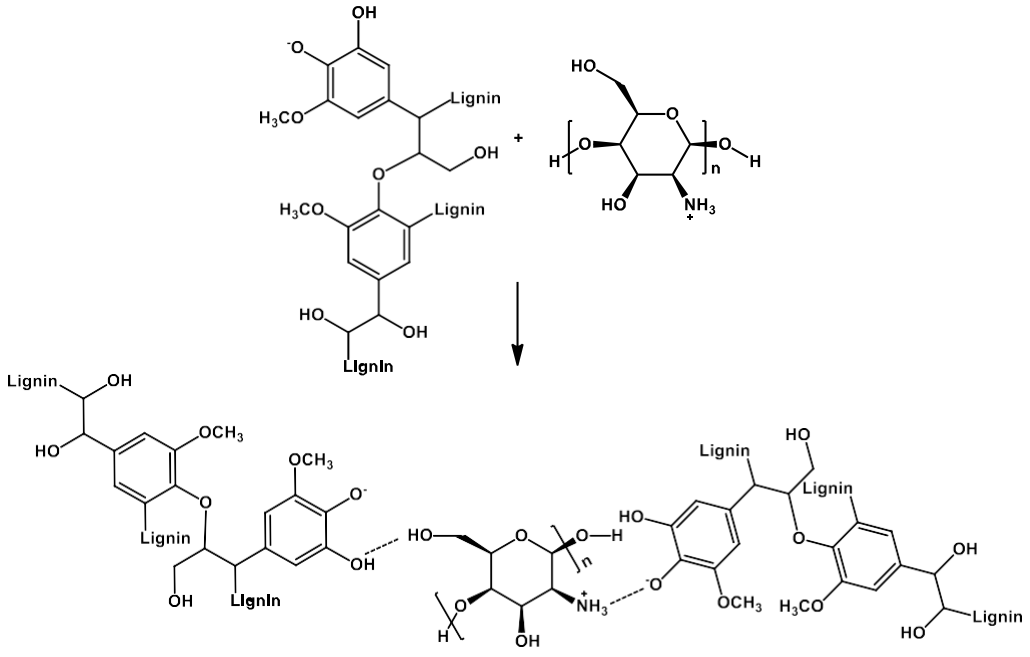

Fig. 2.10 *Schematic representation of the interactions between lignin and chitosan, forming a stable lignin-chitosan complex* (Ravishankar *et al*., 2019).

The antibacterial activity of the PVA-based films was tested against three food-related bacterial strains, that is *Salmonella enterica* serovar Typhimurium ATCC® 14028 (Gram-negative), *Salmonella enterica* serovar Enteritidis 706 RIVM (Gram-negative), and *Enterococcus faecalis*

ATCC® 29212 (Gram-positive). In agreement with the general trend observed in the antioxidant assays, the film containing bulk lignin as the only functional additive (sample B1) was found to be the one exhibiting the most efficient antimicrobial activity, except in the case of *S. enterica* serovar Enteriditis 706 RVM against which the highest activity was exhibited by sam- ple N2 (Fig. 2.11). The detrimental effect of chitosan incorporation was particularly evident against *S. enterica* serovar Typhimurium ATCC® 14028, since sample B2 displayed no de- tectable antimicrobial activity, although the antimicrobial properties of chitosan have been widely reported (Ma *et al*., 2017; Kong *et al*., 2010; Zheng & Zhu, 2003).

Actually, in control experiments PVA-films functionalized with chitosan or nanochitosan only (Fig. 2.12) exhibited comparable or even higher antimicrobial activity compared to the films containing only bulk lignin or LNPs. These data would corroborate the observation that the chemical interactions occurring between lignin and chitosan are unfavorable in terms of active functionality, decreasing the ability of both compounds to express their antioxidant and/or antimicrobial potential. Notably, even in this case, sample B1, containing bulk lignin, exhibited greater or at most comparable efficacy than sample N1, containing lignin in its nanoform.

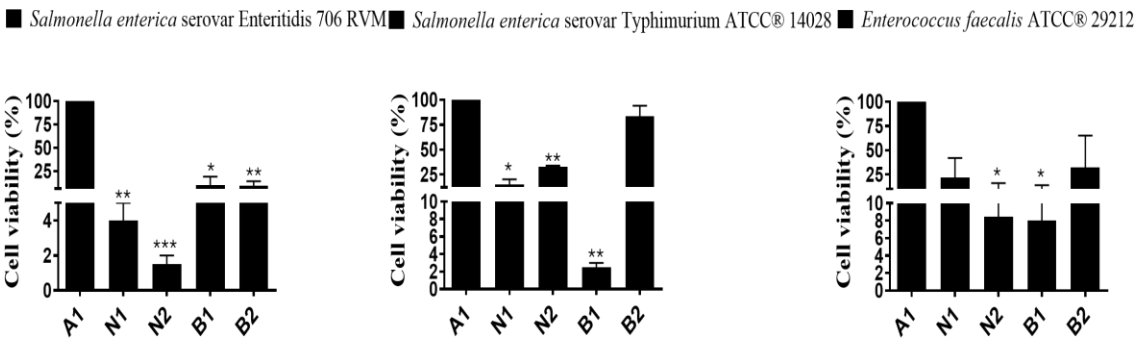

Fig. 2.11 *Antimicrobial activity of PVA-based composite films incorporating chitosan, lignin, and their nano-formulations against S. enterica serovar Typhimurium ATCC® 14028, S. enterica serovar Enteritidis 706 RIVM, and E. faecalis ATCC® 29212. Each graph refers to at least a biological duplicate and statistical analyses were performed by using Student's t-test. Significant differences were indicated as *(P < 0.05), **(P < 0.01) or ***(P < 0.001).*

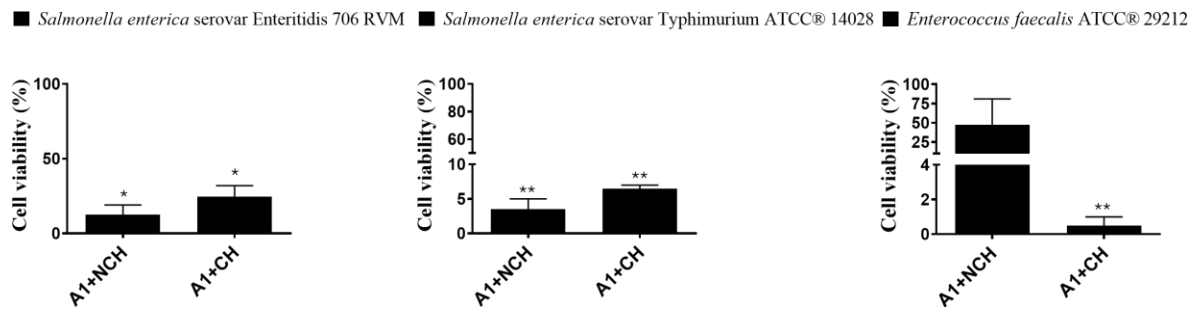

Fig. 2.12 *Antimicrobial activity of PVA-based composite films containing chitosan (CH) or nanochitosan (NCH) against S. enterica serovar Typhimurium ATCC® 14028, S. enterica serovar Enteritidis 706 RIVM, and E. faecalis ATCC® 29212. Each graph refers to at least a biological duplicate and statistical analyses were performed by using Student's t-test. Significant differences were indicated as *(P < 0.05) or **(P < 0.01)*

2.1.4 Conclusions

In conclusion, in this study morphological, optical, mechanical, thermal, antioxidant, and antibacterial properties of PVA-based films incorporating chitosan, lignin or their nanoformula tions were evaluated. Conflicting results were obtained in terms of the effects of the different additives on film performance. Indeed, films containing both nanolignin and nanochitosan exhibited the smoothest and most homogeneous surface (SEM analysis), UV-Vis blocking efficacy, and water resistance, due to improved matrix integrity because of the enhanced compatibility between the different components afforded by the nanoscale. However, mechanical and thermal testing showed reduced performance for nanoparticle containing films. These results are particularly interesting in the light of the rather costly and time-consuming procedures generally required for nanoparticle preparation. Notably, antioxidant and antimicrobial properties were higher for films containing lignin or chitosan alone, while films containing both additives showed reduced activity due to limited active site exposure as a result of the chemical interactions occurring between the two components. A more detailed analysis and critical approach is therefore needed for the understanding of the real effects of functional additives on the performance of films intended for food packaging and guide the selection of proper combinations that may improve film performance. In addition, as the packaging is intended for food applications, the potential release of additives should also be assessed to ensure food safety, in accordance with European

food contact regulations.

2.1.5 References

Irmukhametova, G., Al Azzam, K. M., Mun, G. A., Bekbayeva, L., Dinara, Z., Yermukhambetova, B. B., ... & Samy, M. (2025). Obtaining and Characterization of Biodegradable Polymer Blends Based on Polyvinyl Alcohol, Starch, and Chitosan. *Polymers*, *17*(4), 479.

Haghighi, H., Leugoue, S. K., Pfeifer, F., Siesler, H. W., Licciardello, F., Fava, P., & Pulvirenti, A. (2020). Development of antimicrobial films based on chitosan-polyvinyl alcohol blend enriched with ethyl lauroyl arginate (LAE) for food packaging applications. *Food Hydrocolloids*, *100*, 105419.

Abdullah, Z. W., Dong, Y., Han, N., & Liu, S. (2019). Water and gas barrier properties of polyvinyl alcohol (PVA)/starch (ST)/glycerol (GL)/halloysite nanotube (HNT) bionanocomposite films: Experimental characterisation and modelling approach. *Composites B Engineering, 174*, 107033.

Abraham, A., Soloman, P. A., & Rejini, V. O. (2016). Preparation of chitosan-polyvinyl alcohol blends and studies on thermal and mechanical properties. *Procedia Technology, 24*, 741-748.

Apak, R., Gueclue, K., Oezyuerek, M., & Karademir, S. E. (2004). Novel total antioxidant capacity index for dietary polyphenols and vitamins C and E, using their cupric ion reducing capability in the presence of neocuproine: CUPRAC method. *Journal of Agricultural and Food Chemistry, 52*, 7970-7981.

Apriliyani, M. W., Purwadi, P., Manab, A., Apriliyanti, M. W., & Ikhwan, A. D. (2020). Characteristics of moisture content, swelling, opacity, and transparency with addition of chitosan as edible films/coating base on casein. *Advances in Journal of Food Science and Technology, 18*, 9-14.

Benzie, I. F. F., & Strain, J. J. (1996). The Ferric Reducing Ability of Plasma (FRAP) as ameasure of "antioxidant power": The FRAP assay. *Analytical Biochemistry, 239*, 70-76.

Boarino, A., & Klok, H. A. (2023). Opportunities and challenges for lignin valorization in food packaging, antimicrobial, and agricultural applications. *Biomacromolecules, 24*, 1065-1077.

Chen, Q., Zong, W., Zhou, Q., Zhou, Z., Zhan, Y., Feng, Q., Hu, C., & Jiang, M. (2025). Barrier coating integrated with lignin nanotube and polyvinyl alcohol for variety packaging film. *International Journal of Biological Macromolecules, 314*, 144024.

Choi, I., Choi, M. H., & Han, J. (2024). Exploring the effect of corn starch/pea protein blending on the physicochemical and structural properties of biopolymer films and their aging resistance. *International Journal of Biological Macromolecules, 269*, 132092.

Debeaufort, F., Kurek, M., Fabra, M.-J., Ghasemi, Y., Ščetar, M., Galić, K., & Benbettaieb, N. (2025). Hydrocolloid-based coatings applied on biobased/biodegradable food flexible packaging: A review. Part 1 - Biopolymer to coat and available technologies. *Food Hydrocolloids, 169*, 111624.

Deng, H., Su, J., Zhang, W., Khan, A., Sani, M. A., Goksen, G., Kashyap, P., Ezati, P., & Rhim, J.-W. (2024). A review of starch/polyvinyl alcohol (PVA) blend film: A potential replacement for traditional plastic-based food packaging film. *International Journal of Biological Macromolecules, 273*, 132926.

Fortunati, E., Peltzer, M., Armentano, I., Jiménez, A., & Kenny, J. M. (2013). Combined effects of cellulose nanocrystals and silver nanoparticles on the barrier and migration properties of PLA nano-biocomposites. *Journal of Food Engineering, 118*, 117-124.

Gomes, L. C., Faria, S. I., Valcarcel, J., Vázquez, J. A., Cerqueira, M. A., Pastrana, L., Bourbon, A. I., & Mergulhão, F. J. (2021). The effect of molecular weight on the antimicrobial activity of chitosan from *Loligo opalescens* for food packaging applications. *Marine Drugs, 19*, 384.

Gómez-Cruz, I., Sosa, F., Alfieri, M. L., Esposito, R., Panzella, L., Labidi, J., Goodfellow, B., Castro, E., Silvestre, A. J. D., & Costa Lopes, A. M. (2025). Evaluating the integration of olive tree pruning fractionation with ternary eutectic solvent after aqueous pre-extraction or dilute acid pre-treatment. *Separation and Purification Technology, 372*, 133295.

Grappa, R., Venezia, V., Basta, L., Alfieri, M. L., Panzella, L., Verrillo, M., Silvestri, B., Commodo, M., Luciani, G., Costantini, A. (2024). Green synthesis of stable lignin nanoparticles with reversible swelling behavior and enhanced multifunctional features. *ACS Sustainable Chemistry & Engineering, 12*, 10653-10664.

Green oxidation of corn stover lignin as reinforcing plasticizer and UV-blocking agent for polyvinyl alcohol composites: process optimization and techno-economic analysis. *Bioresource Technology, 439*, 133354.

Haghighi, H., Leugoue, S. K., Pfeifer, F., Siesler, H. W., Licciardello, F., Fava, P., & Pulvirenti,

Hoyos-Merlano, N. T., Borroni, V., Rodriguez-Batiller, M. J., Candal, R. J., & Herrera, M. L. (2022). Nanoreinforcement as a strategy to improve physical properties of biodegradable composite films based on biopolymers. *Food Research International, 162*, 112178.

Irmukhametova, G., Al Azzam, K. M., Mun, G. A., Bekbayeva, L., Dinara, Z., Yermukhambetova, B. B., Nechipurenko, S. V., Efremov, S. A., Negim, E.-S., & Samy, M.

Kadir, M. F. Z., Aspanut, Z., Majid, S. R., & Arof, A. K. (2011). FTIR studies of plasticized poly (vinyl alcohol)–chitosan blend doped with NH4NO3 polymer electrolyte membrane. *Spectrochimica Acta Part A: Molecular and Biomolecular Spectroscopy*, *78*(3), 1068-1074.

Kanimozhi, K., Basha, S. K., & Kumari, V. S. (2016). Processing and characterization of chitosan/PVA and methylcellulose porous scaffolds for tissue engineering. *Materials Science and Engineering C, 61*, 484-491.

Kong, M., Chen, X., Xing, K., & Park, H. J. (2010). Antimicrobial properties of chitosan and mode of action: A state of the art review. *International Journal of Food Microbiology, 144*, 51-63.

Kowalczyk, D., Kordowska-Wiater, M., Nowak, J., & Baraniak, B. (2015). Characterization of films based on chitosan lactate and its blends with oxidized starch and gelatin. *International Journal of Biological Macromolecules, 77*, 350-359.

Kubo, S., & Kadla, J. F. (2003). The formation of strong intermolecular interactions in immiscible blends of poly (vinyl alcohol)(PVA) and lignin. *Biomacromolecules*, *4*(3), 561-567.

Las-Casas, B., Wu, J., Rojas, O. J., & Arantes, V. (2025). Exploring lignin nanoparticle incorporation to develop multifunctional cellulose nanofibril films for active packaging. *International Journal of Biological Macromolecules, 323*, 147013..

Li, Z.-C., Chen, X., Zhang, J.-L., Gao, X.-P., An, Y.-X., Wu, L.-J., Li, M.-Y., Zhao, G.-M., &

Liu, B., Zhang, J., & Guo, H. (2022). Research progress of polyvinyl alcohol water-resistant film materials. *Membranes, 12*, 347.

Ma, Z., Garrido-Maestu, A., & Jeong, K. C. (2017). Application, mode of action, and in vivo activity of chitosan and its micro- and nanoparticles as antimicrobial agents: A review. *Carbohydrate Polymers, 176*, 257-265.

Marcoaldi, C., Acampora, V., Venezia, V., Prieto, C., Grappa, R., Silvestri, B., Luciani, G., & Lagaron, J. M. (2025). Challenges in lignin integration within biopolymer matrices: Toward stable and effective lignin nanoparticles as additives for sustainable food packaging. *Industrial Crops and Products, 224*, 120336.

Mathew, D., Thomas, B., Sudheep, N. M., Muhammed Shamil, K. V., Anjana, R., Krishna, A., Thomas, J. B., & Krishnankutty, R. E. (2025). Development of garlic extract-loaded zinc oxide

nanoparticle/chitosan/polyvinyl alcohol nanocomposite-based active eco-friendly packaging films for extending shelf-life of fish fillets. *International Journal of Biological Macromolecules, 327*, 147273.

Mehrabi Mazidi, M., Arezoumand, S., & Zare, L. (2024). Research progress in fully biorenewable tough blends of polylactide and green plasticizers. *International Journal of Biological Macromolecules, 279*, 135345.

Monteiro, V. A. C., da Silva, K. T., da Silva, L. R. R., Mattos, A. L. A., de Freitas, R. M., Mazzetto, S. E., Lomonaco, D., & Avelino, F. (2021). Selective acid precipitation of Kraft lignin: A tool for tailored biobased additives for enhancing PVA films properties for packaging applications. *Reactive and Functional Polymers, 166*, 104980.

Odili, C. C., Gbenebour, O. P., Olanrewaju, O. A., Badaru, T. O., & Adeosun, S. O. (2025). Physiochemical performance of electrospun PLA-lignin and PVA-lignin. *Journal of Materials Science and Materials Engineering, 20*, 10.

Olunusi, S. O., Ramli, N. H., Adam, F., Hossain, E., & Kim, T. H. (2025). Chitosan as a sustainable alternative for fresh food packaging: Structural insights, modification strategies, and innovations for commercial viability. *International Journal of Biological Macromolecules, 318*, 145065.

Panda, P. K., Sadeghi, K., & Seo, J. (2022). Recent advances in poly (vinyl alcohol)/natural polymer based films for food packaging applications: A review. *Food Packaging and Shelf Life, 33*, 10090.

Panzella, L., Eidenberger, T., Napolitano, A., & d'Ischia, M. (2012). Black sesame pigment: DPPH assay-guided purification, antioxidant/antinitrosating properties, and identification of a degradative structural marker. *Journal of Agricultural and Food Chemistry, 60*, 8895-8901.

Park, H. M., Rhim, J. W., & Ha, C. S. (2013). Bio-nanocomposites for food packaging applications. *Progress in Polymer Science, 38*, 1629-1652.

Pesaranhajiabbas, E., Misra, M., & Mohanty, A. K. (2023). Recent progress on biodegradable polylactic acid-based blends and their biocomposites: A comprehensive review. *International Journal of Biological Macromolecules, 253*, 126231.

Pham, C. D., Truong, T. M., Ly, T. B., & Le, P. K. (2024). Application of lignin from cellulose isolation process in the fabrication of chitosan/lignin film for UV-light blocking and anti-oxidation. *Waste and Biomass Valorization, 15*, 1881–1894.

Pinem, M. P., Wardhono, E. Y., Nadaud, F., Clausse, D., Saleh, K., & Guénin, E. (2020).

Nanofluid to nanocomposite film: Chitosan and cellulose-based edible packaging. *Nanomaterials, 10*, 660.

Prasad, J., Kumar, N., Pratibha, Jaiswal, R., Yadav, A., Sharma, S. P., Fawole, O. A., & Kaushik, N. (2025). Biopolymer based composite packaging: A sustainable approach for fruits and vegetables preservation. *Applied Food Research, 5*, 101211.

Priyadarshi, R., Ghosh, T., Purohit, S. D., Prasannavenkadesan, V., & Rhim, J. (2024). Lignin as a sustainable and functional material for active food packaging applications: A review. *Journal of Cleaner Production, 469*, 143151.

Ravishankar, K., Venkatesan, M., Desingh, R. P., Mahalingam, A., Sadhasivam, B., Subramaniyam, R., & Dhamodharan, R. (2019). Biocompatible hydrogels of chitosan-alkali lignin for potential wound healing applications. *Materials Science and Engineering C, 102*, 447-457.

Rhim, J. W., & Ng, P. K. (2007). Natural biopolymer-based nanocomposite films for packaging applications. *Critical Reviews in Food Science and Nutrition, 47*, 411-433.

Rhim, J. W., Park, H. M., & Ha, C. S. (2013). Bio-nanocomposites for food packaging applications. *Progress in Polymer Science, 38*, 1629-1652.

Riaz, A., Lei, S., Akhtar, H. M. S., Wan, P., Chen, D., Jabbar, S., Abid, M., Hashim, M. M., & Zeng, X. (2018). Preparation and characterization of chitosan-based antimicrobial active food packaging film incorporated with apple peel polyphenols. *International Journal of Biological Macromolecules, 114*, 547-555.

Sobhiga, G., Maria, H. J., Mozetič, M., & Thomas, S. (2024). A review on green materials: Exploring the potential of poly(vinyl alcohol) (PVA) and nanocellulose composites. *International Journal of Biological Macromolecules, 283*, 137176.

Suganthi, S., Vignesh, S., Sundar, J. K., & Raj, V. (2020). Fabrication of PVA polymer films with improved antibacterial activity by fine-tuning via organic acids for food packaging applications. *Applied Water Science, 10*, 1-11.

Tammina, S. K., Priyadarshi, R., Khan, A., Manzoor, A., Rahman, R. S. H. A., & Banat, F. (2025). Recent developments in alginate-based nanocomposite coatings and films for biodegradable food packaging applications. *International Journal of Biological Macromolecules, 295*, 139480.

Vieria, M. G. A., Da Silva, M. A., Dos Santos, L. O., & Beppu, M. M. (2011). Natural-based plasticizers and biopolymer films: A review. *European Polymer Journal, 47*, 254-263.

W. Yang, Fortunati, E., Bertoglio, F., Owczarek, J. S., Bruni, G., Kozanecki, M., Kenny, J. M., Torre, L., & Visai, L. (2018). Polyvinyl alcohol/chitosan hydrogels with enhanced antioxidant and antibacterial properties induced by lignin nanoparticles. *Carbohydrate Polymers, 181*, 275-284.

Wang, H., Qian, J., & Ding, F. (2018). Emerging chitosan-based films for food packaging applications. *Journal of Agricultural and Food Chemistry, 66*, 395-413.

Wang, X.-P. (2024). Unlocking superior preservation: The synergy of lignin and zeolite in chitosan-based composite films for perishable foods. *Food Packaging and Shelf Life, 46*, 101362.

Yaneva, Z., Beev, G., Rusenova, N., Ivanova, D., Tzanova, M., Stoeva, D., & Toneva, M. (2022). Antimicrobial potential of conjugated lignin/morin/chitosan combinations as a function of system complexity. *Antibiotics, 11*, 650.

Yang, W., Fortunati, E., Bertoglio, F., Owczarek, J. S., Bruni, G., Kozanecki, M., Kenny, J. M., Torre, L., & Visai, L. (2018). Polyvinyl alcohol/chitosan hydrogels with enhanced antioxidant and antibacterial properties induced by lignin nanoparticles. *Carbohydrate Polymers, 181*, 275-284.

Yang, W., Fortunati, E., Bertoglio, F., Owczarek, J. S., Bruni, G., Kozanecki, M., Kenny, J. M., Torre, L., & Visai, L. (2018). Polyvinyl alcohol/chitosan hydrogels with enhanced antioxidant and antibacterial properties induced by lignin nanoparticles. *Carbohydrate Polymers, 181*, 275-284.

Yang, W., Owczarek, J. S., Fortunati, E., Kozanecki, M., Mazzaglia, A., Balestra, G. M., Kenny, J. M., Torre, L., & Puglia, D. (2016). Antioxidant and antibacterial lignin nanoparticles in polyvinyl alcohol/chitosan films for active packaging. *Industrial Crops and Products, 94*, 800-811.

Zhang, X., Li, G., Chen, C., Fan, H., Fang, J., Wu, X., Qi, J., & Li, H. (2025). Chitosan/PVA composite film enhanced by ZnO/lignin with high-strength and antibacterial properties for food packaging. *International Journal of Biological Macromolecules, 306*, 141658.

Zhang, Z., Argenziano, R., Konate, A., Shi, X., Salazar, S. A., Cerruti, P., Panzella, L., Terrasson, V., & Guénin, E. (2025). Preparation of chitosan/lignin nanoparticles-based nanocomposite films with high-performance and improved physicochemical properties for food packaging applications. *International Journal of Biological Macromolecules, 293*, 139079.

Zhang, Z., Marin, C. B., Lefebvre, M., Lefebvre, C., Terrasson, V., & Guénin, E. (2022). The preparation of stable spherical alkali lignin nanoparticles with great thermal stability and no cytotoxicity. *International Journal of Biological Macromolecules, 222*, 1830-1839.

Zheng, L.-Y., & Zhu, J.-F. (2003). Study on antimicrobial activity of chitosan with different molecular weights. *Carbohydrate Polymers, 54*, 527-530.

Zhuang, Z., Peng, B., Yu, C., Tang, C., & Jiang, G. (2025). Preparation and application of citric acid crosslinked gelatin-polyvinyl alcohol composite films for active food packaging. *International Journal of Biological Macromolecules, 328*, 1477

2.2 Physicochemical and Functional Characterization of PVA Films Embedded with Duckweed (*Lemna minor)* Leaf Extract and (Nano)chitosan Intended for Active Food Packaging

2.2.1 Introduction

The need for sustainable and functional packaging materials particularly in the food industry has led to a growing interest in biodegradable coatings and films with enhanced thermal, mechanical, and barrier properties (Yuen *et al.,* 2025; Luzi *et al.,* 2023). Biopolymer-based packaging derived from renewable biomass offers an eco-friendly alternative to petrochemical plastics. Materials such as microbial polymers (polyhydroxyalkanoates), wood-derived polymers (cellulose, hemicellulose, starch, lignin), and protein-based materials (gelatin, keratin, soy proteins, whey proteins) are widely employed for food packaging applications due to their biodegradability and functional capabilities (Asgher *et al.,* 2020; Luzi *et al.,* 2023; Miah *et al.,* 2025). The incorporation of biobased reinforcements, including plant extracts, may further enhance oxygen barrier, antibacterial, and antifungal properties of the films (Yuen *et al.,* 2025;). Among these, natural extracts rich in phenolic compounds have gained considerable attention for their antioxidant and antimicrobial effects (Vieira *et al.,* 2022; Luzi *et al.,* 2023). Extracts from rosemary, green tea, lemon balm, clove, cinnamon, anise, and curcumin have shown promising performance when embedded in polymer matrices such as poly(vinyl alcohol) (PVA) or low-density polyethylene (LDPE). For instance, rosemary extract conferred thermal stability and antifungal properties, while green tea extract imparted strong antioxidant activity (Vieira *et al.,* 2022). Curcumin extract also conferred potent antimicrobial and antioxidant effects, whereas lemon balm extract-based films showed significant antibacterial action (Vieira *et al.,* 2022; Özogul *et al*., 2017; Boneza & Niemeyer, 2018). Widely accepted food preservatives like cinnamon and clove extracts also contribute strong antibacterial and antioxidant activities, respectively (Ju *et al.,* 2018; El-Saber Batiha *et al.,* 2020; Ribeiro-Santos

et al., 2017; Luzi *et al.,* 2023). Recent advances include polyphenol-functionalized biopolymers and green nanocomposites, which offer enhanced shelf life and safety by actively inhibiting foodborne pathogens (Periyasamy *et al.,* 2025).

In this context, *Lemna minor* (commonly known as duckweed) is a small, floating aquatic plant that has already found applications in ecological and phytoremediation studies (Artamonova et al., 2020; Panfili, Bartucca, & Del Buono, 2019; Ubuza et al., 2020). Native to various regions across the globe, duckweed is known for its rapid growth rate and remarkable ability to thrive under harsh environmental and climatic conditions (Khellaf & Zerdaoui, 2010; Moradi *et al.,* 2023). Recent studies showed that duckweed is particularly rich in metabolites with antioxidant and other bioactive functions, including notable levels of phenolic acids and flavonoids (Zhang *et al.,* 2023; Panfili *et al.,* 2019). All together, these results highlight duckweed as a promising source of natural antioxidant ingredients for food, feed, and nutraceutical applications.

Starting from this background, and in the frame of a wider project focused on the valorization of duckweed run in collaboration with the Department of Agricultural Sciences of University of Naples Federico II, this study explores the impact of an aqueous extract of *Lemna minor* on the morphological characteristics, optical properties, and antioxidant and antibacterial performance of poly(vinyl alcohol) (PVA)-based films. This latter was selected as a water-soluble polymer able to provide films with good properties for food packaging applications through a simple solvent casting process, hence minimizing the use of high-temperature processes, which could otherwise compromise the stability of natural extracts. To improve the functionality of the packaging system, glycerol was added as a plasticizer. In addition, chitosan in its bulk and nanoforms was also used as additive to improve the physicochemical, mechanical, and functional properties of the films. Indeed, chitosan is a biodegradable polymer with inherent antimicrobial activity, able to strengthen film matrices and enhance barrier

properties (Sanati *et al.,* 2025) and to improve flexibility and mechanical stability of PVA films (Zhang *et al.,* 2023).

2.2.2 Experimental

2.2.2.1. Materials

Duckweed leaf powder was obtained from the Department of Agricultural Sciences of Univer- sity of Naples Federico II. Poly(vinyl alcohol) (PVA; MW 124–146 kg/mol, 99% hydrolyzed), glycerol (≥99%), chitosan (CH) from crab shells (low molecular weight, 75–85% deacetylation), alkali lignin (LIG), sodium acetate (≥99%), 2,4,6-tris(2-pyridyl)-s-triazine (TPTZ, ≥98%), iron(III) chloride hexahydrate ($FeCl_3 \cdot 6H_2O$, ≥97%), copper(II) chloride ($CuCl_2$, ≥97%), neocuproine (≥98%), and hydrogen peroxide solution (30% w/w) were purchased from Sigma-Aldrich (St. Louis, MO, USA). Reagents including hydrochloric acid (HCl, ≥37%), sodium hydroxide (NaOH, ≥98%), sodium metabisulfite ($Na_2S_2O_5$, ≥97%), and dimethyl sulfoxide (DMSO, ≥99.5%) were also obtained from Sigma-Aldrich. Ethylene glycol (≥99%), ethanol (96% v/v), nitric acid (HNO_3, 67–69%), glacial acetic acid (100%), and sodium tripolyphosphate (TPP, ≥98%) were sourced from Thermo Fisher Scientific (Waltham, MA, USA). The buffers for the antioxidant assays were prepared using analytical-grade reagents: the FRAP acetate buffer (0.3 M, pH 3.6) was formulated using sodium acetate trihydrate ($CH_3COONa \cdot 3H_2O$, ≥99.0%) and glacial acetic acid (CH_3COOH, ≥99.5%), while the CUPRAC buffer (1 M, pH 7.0) was prepared with ammonium acetate (NH_4CH_3COO, ≥98.0%). All solutions were prepared using deionized water, and pH adjustments were performed with HCl or NaOH as required. All chemicals were used as received without further purification.

2.2.2.2. Preparation and characterization of plant extract (PE)

10 g of plant material was extracted with 7 × 250 mL of water. Each extraction was performed for 1 h, under stirring at 1300 rpm, at 25 °C. The extracts were collected by filtration, combined and analyzed by UV-Vis spectroscopy and LC-UV-MS. This latter was performed in reverse phase

using an ODS column (150 × 4.60 mm, 5 μm); a gradient elution was performed with 0.1% formic acid (solvent A)/methanol (solvent B): 5% B, 0–10 min; from 5 to 80% B, 10– 47.5 min. The flow rate was 0.4 mL/min, and the detection wavelengths were 254, 280, 320 and 400 nm. MS analysis was performed in both positive and negative ionization mode under the following conditions: capillary voltage 3500 V; drying gas (nitrogen) 10 L/min, 325°C; fragmentor voltage 175 V; nebulizer pressure 35 psig.

2.2.2.3. Preparation of nanochitosan (NCH)

0.6 g of acetic acid were added to 100 mL of water and the mixture was stirred for 10 min at 2000 rpm at room temperature. Then, 0.5 g of CH were added, and the mixture was stirred at 8000 rpm for 5 h, until CH was completely dissolved. Next, 10 mL of a 0.05 g/mL TPP solution in distilled water were added dropwise to the solution, and stirring continued for 30 min. The solution was then ultrasonicated at 20 kHz for 1 h and maintained at 4 °C (Pinem *et al*., 2020). The hydrodynamic diameter and zeta potential of the nanoparticles were characterized by DLS using a Malvern Panalytical Zetasizer Ultra. The morphology of the nanoparticles was characterized by TEM (JEOL, JEM-2100F, Japan) at an acceleration voltage of 200 kV. The samples were dispersed in ultra-pure water and deposited on carbon-coated copper grids for characterization.

2.2.2.4. Preparation of PVA-based films

6 g of PVA were added to 50 mL of distilled water, and the mixture was taken under stirring at 80°C for 6 h until a clear solution was obtained. To remove air bubbles, the solution underwent sonication at 20 kHz for 30 min. For film casting, 3 mL of the solution were poured into a 9 cm Petri dish and dried at 45 °C for 24 h. For blended films, the same process was followed, with the addition of glycerol, PE and/or CH or NCH (Table 2.4), followed by an extra 30 min of stirring. Control films were prepared without the addition of PE and/or (nano)chitosan.

Table 2.4 *Formulation of PVA-based composite films incorporating chitosan (CH), nanochitosan (NCH), and Duckweed leaf extract (PE*).

Sample	Formulation	PVA %w/w	Glycerol %w/w	CH/NCH %w/w	PE %w/w
P1	PVA/Glycerol	98	2	-	-
P2	PVA/Glycerol/PE	92	2	-	6
P3	PVA/ Glycerol/CH/PE	88	2	4	6
N3	PVA/ Glycerol/NCH/PE	88	2	4	6

2.2.2.5. Film characterization

Various characterization techniques were employed to evaluate the properties of the composite films, in line with the methods detailed in Unit 1 of this chapter. The morphology and thickness of the films were analyzed using SEM (JEOL JEM-2100F), with gold coating to enhance conductivity. ATR-FTIR analysis was conducted using a Thermo Scientific Nicolet iS5 FTIR, recording spectra in the range of 600-4000 cm^{-1}. Moisture content, swelling degree, and total soluble matter were determined gravimetrically, as described in Unit 1 of this chapter. The color of the films was measured with a Konica Minolta CR-400 colorimeter, and their transmittance and opacity were assessed using a UV-6300 spectrophotometer. The water vapor transmission rate (WVTR) was evaluated by monitoring desiccant weight change under controlled humidity, as per the adapted method from Phaechamud *et al.* (2016). Mechanical properties, including tensile strength and elongation at break, were tested using a Zwick/Roell universal testing machine, adhering to ASTM D 638 standards. Thermal analysis was conducted using a DSC2500 instrument, and antioxidant and antimicrobial properties were characterized as in Unit 1. A detailed description of the experimental setups and protocols for these methods can be found in Unit 1.

2.2.3 Results and discussion

2.2.3.1. Preparation and characterization of extract from duckweed leaves

Duckweed (*Lemna minor*) leaves were subjected to water extraction, which was repeated seven times to achieve good (36% w/w) extraction yields. Parallel experiments in which ethanol was used instead of water as alternative food grade solvent indicated a lower extraction efficacy.

The UV–Vis spectrum of the water extract (PE) (Fig. 2.13) showed a broad absorbance in the 270–320 nm range, typical of phenolic compounds. For comparison, the spectrum of the ethanol extract is also shown, clearly indicating the presence of chlorophyll (□max= 416 and 660 nm)

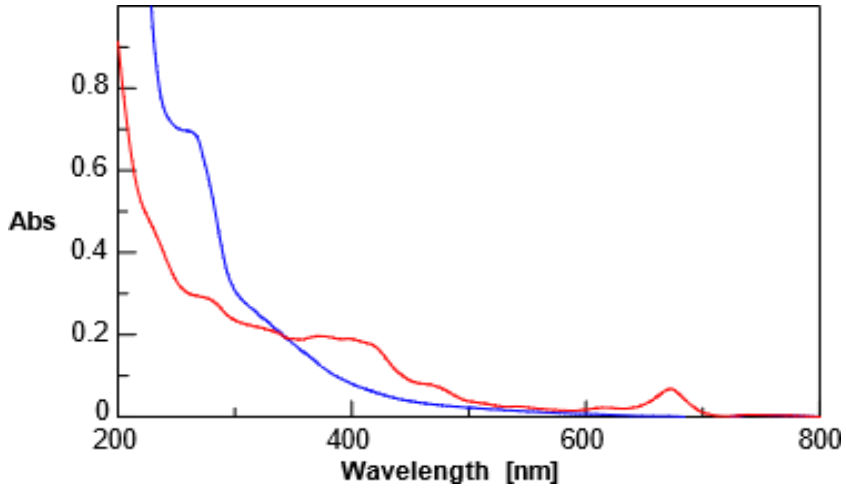

Fig. 2.13 *UV-vis spectra of the water (blu trace) and ethanol (red trace) extract from duckweed leaves.*

With the aim of identifying the main phenolic components present in PE, HPLC analysis with UV and MS detection was performed. In Figure 2.14 the chromatograms recorded at different detection wavelengths are reported, suggesting a flavonoid structure for the compounds eluted at 33-38 min. On the contrary, the main compounds eluted at ca. 8 and 10 min ($[M-H]^-$ at *m/z* 135 and 151, respectively) did not show any significant absorption at 280 nm, as instead expected for phenolic compounds.

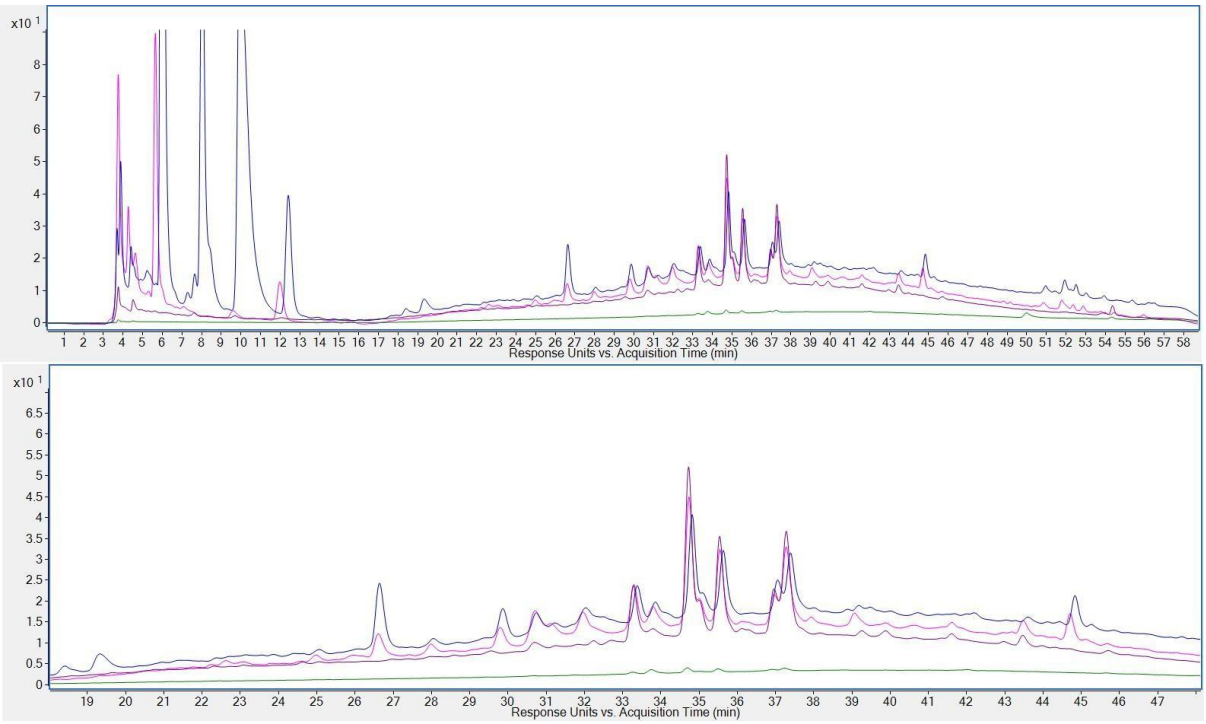

Fig. 2.14 *HPLC profiles of the water extract from duckweed leaves at 254 (blue trace), 280 (pink trace), 320 (purple trace) and 400 (green trace) nm.*

Based on their MS spectra, the compounds eluted at 33-38 min were tentatively identified as reported in Table 2.5.

Table 2.5 *Results from LC-MS analysis of the water extract from Lemna minor leaves.*

Retention time (min)	$[M-H]^-$ (m/z)	Tentative structure
33.5	593	Apigenin 6,8-di-C-glucoside (or its isomer)
34.7	563	Apigenin 7-O-apiosyl-glucoside (or its isomer)
35.6	563	Apigenin 7-O-apiosyl-glucoside (or its isomer)
37.0	431	Apigenin 6-C-glucoside (or its isomer)
37.5	563	Apigenin 7-O-apiosyl-glucoside (or its isomer)

2.2.3.2. ATR-FTIR analysis of the films

ATR-FTIR analysis was conducted to investigate the molecular interactions between chitosan (CS), polyvinyl alcohol (PVA) and the *Lemna minor* natural extract in the films (Fig. 2.15). The FTIR-ATR spectrum of the control film (P1), which consists of pure PVA, exhibited the characteristic spectral profile of the PVA matrix. This included a broad absorption peak at 3275 cm^{-1} corresponding to the stretching frequency of hydroxyl (-OH) groups and peaks at 2925 cm^{-1} and 2840 cm^{-1} associated with the asymmetric and symmetric stretching vibrations of C–H groups, respectively (Rodrigues *et al*., 2007). Upon the incorporation of the *Lemna minor* aqueous extract (P2), the ATR-FTIR spectrum showed characteristic changes in the absorption pattern, including frequency shifts in the lower range. These shifts were attributed to hydrogen bonding interactions between the reactive functional groups of the extract and the polymer matrix (Abdelghany *et al*., 2019; Perdones *et al*., 2016). Specifically, in the range 1250- 857 cm^{-1}, likely resulting from C–C and C–O stretching of the pyranoid ring and C–O–C glycosidic bonds, introduced by the bioactive compounds from the plant extract (Altiok *et al*., 2010). The addition of chitosan (P3) and nanochitosan (N3) further modified the ATR-FTIR spectra, confirming strong interactions within the film polymeric matrices. Key chitosan bands, such as the 1646 cm^{-1} peak for C=O stretching (Amide I) and the 1580 cm^{-1} peak for N–H bending (Amide II), were clearly present, along with the C–N stretching vibration at 1241 cm^{-1} (Anicuta *et al*., 2010; Altiok *et al*., 2010). The overlap of CS (-NH_2 and -OH) and PVA (-OH) bands led to the broadening of the hydroxyl region (Abdelghany *et al*., 2019).

In the case of the nanochitosan film (N3), sharper peak definitions were observed in the fingerprint region compared to the standard chitosan film (P3). This suggests that the nanometric size of nanochitosan facilitates a more ordered molecular arrangement and enhances interfacial bonding within the composite matrix.

.

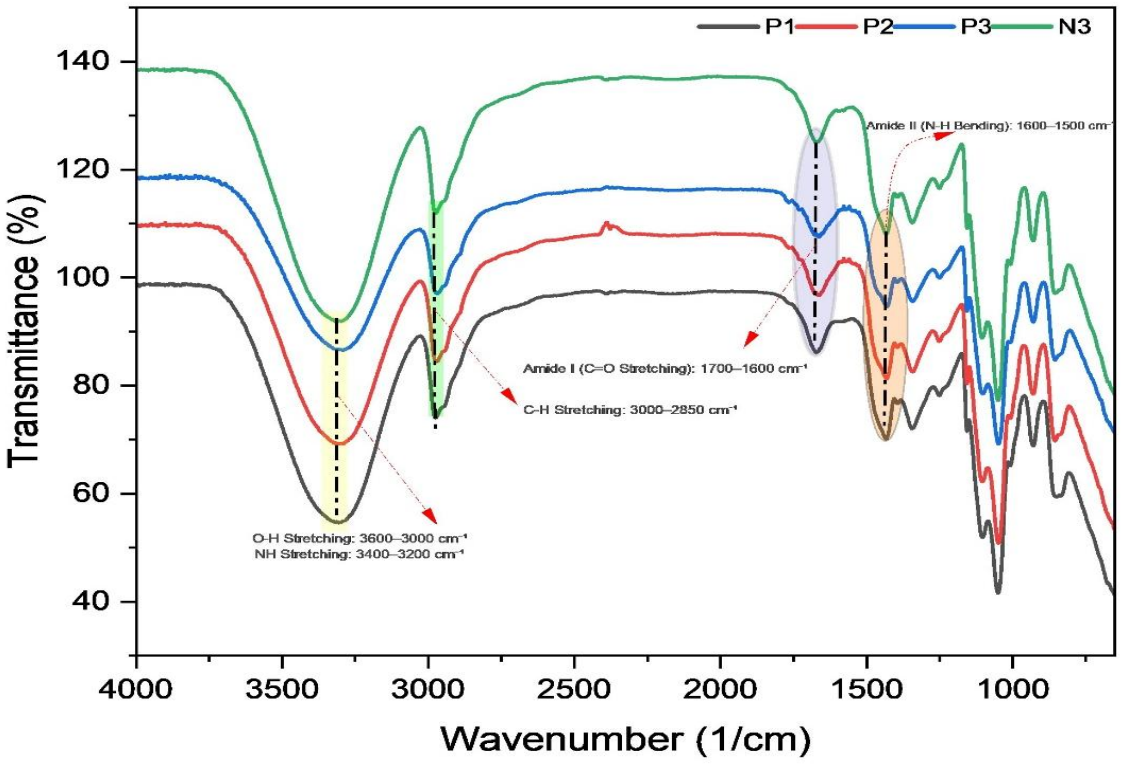

Fig. 2.15 *ATR- FTIR of PVA-based composite films incorporating (nano)chitosan and PE.*

2.2.3.3. Morphology of the films

The surface and internal morphology of the films, as visualized by SEM, revealed substantial differences among the samples influenced by compositional differences (Fig. 2.16). The control film (P1, PVA-Glycerol) displayed a smooth, compact, homogeneous surface with no visible defects or discontinuities. Its cross-section appeared uniform and dense, with a measured thickness of 39.69 ± 0.86 µm, indicating a well-packed polymer matrix, characteristic of pure PVA films. In contrast, P2 (PVA + glycerol + plant extract) showed a rougher surface with distinct microcracks and surface lines, likely arising from phase separation or poor miscibility between PVA and the extract. The cross-sectional image P2 (Fig. 2.16b) showed a thicker (48.51 ± 0.39 µm) and more irregular internal structure suggesting that the addition of plant extract disrupted matrix uniformity, introducing voids and increasing film porosity.

The P3 film (PVA + glycerol + chitosan + plant extract) also exhibited a cracked surface, though the cracks appeared more linear and less severe than those in P2. Its internal morphology revealed a heterogeneous, fibrous structure with embedded particles or agglomerates, likely chitosan-rich regions, and a slightly thinner cross-section **(**Fig. 2.16b) (36.80 ± 0.41 µm). This suggests improved interactions among components compared to P2 although some incompatibility between components still exists. On the other hand, the N3 film (PVA + glycerol + nanochitosan + plant extract) showed a more compact and uniform surface, with fewer visible defects. Its cross-section (36.41 ± 0.04 µm) appeared denser and more integrated compared to P2 and P3, indicating that nanochitosan provided better dispersion and interfacial compatibility **(**Fig. 2.16b**),** contributing to improved film integrity and cohesion. Overall, SEM analysis indicated that plant extract addition disrupted film morphology, leading to increased roughness and porosity. However, the incorporation of nanochitosan mitigated these effects, improving both structural uniformity and mechanical reinforcement, whereas chitosan in P3, though beneficial, showed partial agglomeration and uneven distribution.

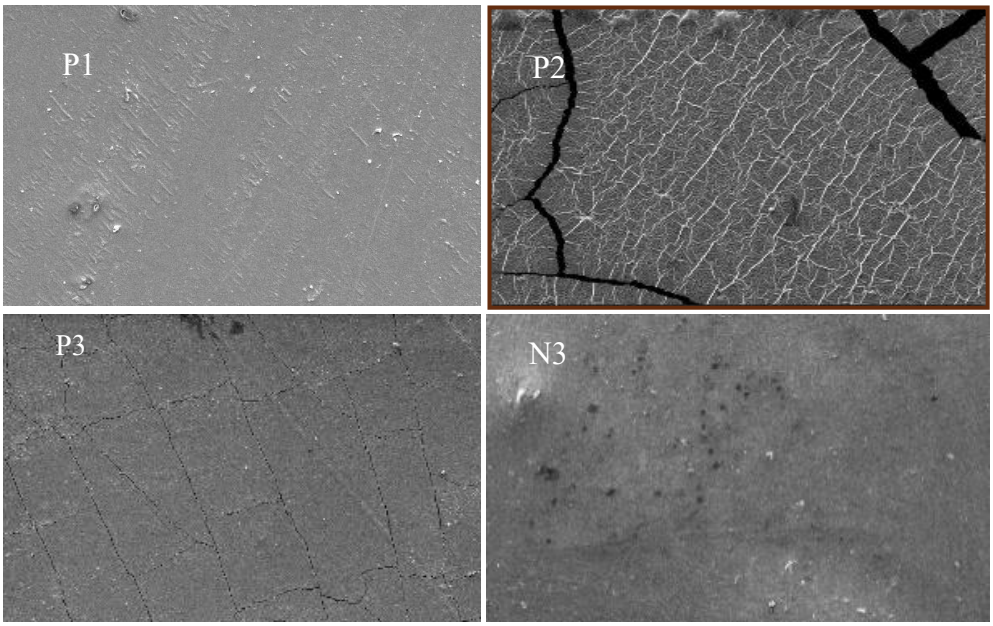

Fig. 2.16a *SEM surface images (200µm) of the PVA-based composi te films incorporating (nano)chitosan and duckweed leaves aqueous extract.*

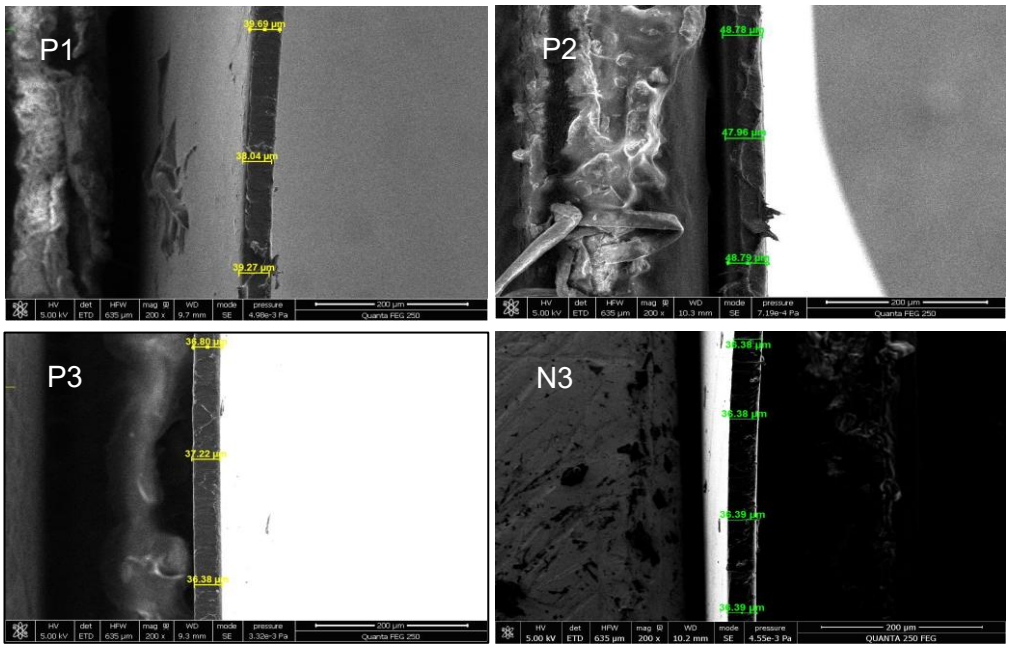

Fig. 2.16b *SEM cross sectional images (200µm) of the PVA-based composite films incorporating (nano) chitosan and duckweed leaves aqueous extract.*

2.2.3.4. Thickness and optical characteristics of PVA-based composite films

The optical characteristics of the developed PVA-based films including colorimetric attributes, opacity, and UV-Vis transmittance are reported in Table 2.6 and Figure 2.17. The control film (P1), composed of neat PVA, exhibited a transparent appearance, as indicated by its low total color difference ($\Delta E = 13.0 \pm 0.1$) compared to the standard plate. This was accompanied by the lowest opacity value (2.99 ± 0.07 mm^{-1}) and the highest transmittance in both UVA and UVB regions. In contrast, the incorporation of plant extract in P2, P3, and N3 films introduced noticeable color changes and enhanced light-blocking performance. P2 showed the highest ΔE indicating a darker film, which was reflected in its highest opacity (4.20 ± 0.16 mm^{-1}) and high UV-blocking capacity. P3, containing both plant extract and chitosan, exhibited a less darkened coloration, although maintaining a relatively high opacity and UV-blocking performance. Notably, the N3 sample, which included nanochitosan, retained a relatively high lightness, as evident from the low ΔE value, which was comparable to that of sample P1, and a low opacity value of 3.31 ± 0.07 mm^{-1}. Its UV transmittance was lower than that of P1, P2, and P3, indicating that N3 provided the most effective UV-shielding among the formulations, while

still maintaining only a moderate increase in visible opacity.

Table 2.6 *Colour and opacity of PVA-based composite films incorporating (nano)chitosan and duckweed leaves aqueous extract.*

Sample Code	ΔE	Opacity (mm^{-1})
P1	13.0 ± 0.1	2.99 ± 0 .07
P2	19.1 ± 0.1	4.20 ± 0 .16
P3	17.2 ±0.1	3.57 ± 0 .03
N3	13.8 ± 0.2	3.31 ± 0 .07

Values are expressed as mean ±standard deviation from three measurements.

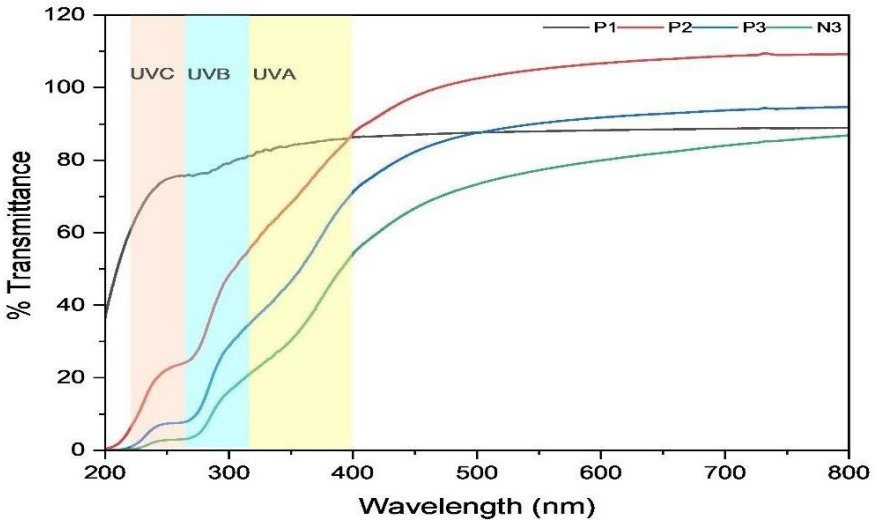

Fig. 2.17 *UV-Vis shielding properties of the PVA-based composite films incorporating (nano)chitosan and duckweed leaf aqueous extract.*

2.2.3.5. Moisture content, swelling degree, total soluble matter and water vapor transmission rate (WVTR)

Compared to the PVA–glycerol film (P1), the incorporation of plant extract (P2) caused a marked decrease in swelling degree (Table 2.7), indicating that the extract contributed to matrix stabilization and limited swelling while still allowing water uptake. This anti-swelling effect was attenuated when chitosan was added together with the extract (P3), although the water vapor transmission rate (WVTR) decreased, consistent with a more compact network formed through additional hydrogen bonding. When nanochitosan replaced chitosan (N3), the moisture content and swellinmg degree of the film remained within the same range as P3, , suggesting

that nanochitosan did not markedly alter the overall water uptake behavior of the films.

Table 2.7 *Moisture content, swelling degree, total soluble matter and water vapor transmission rate of PVA-based films.*

Sample	Moisture content (%)	Swelling degree (%)	Total soluble matter (%)	WVPT (g/m²/day)
P1	29± 3	25± 7	22± 5	64 ± 10
P2	33± 6	6± 2	25± 7	75 ± 18
P3	28± 4	17± 6	19± 4	36 ± 9
N3	34± 7	25± 8	17± 4	35 ± 9

Values are expressed as mean ±standard deviation from three measurements.

2.2.3.6. Mechanical and thermal properties

The mechanical properties of the PVA-based composite films are influenced by the incorporation of duckweed extract and chitosan/nanochitosan (Fig. 2.18). P1, that is the PVA/glycerol film, showed the lowest tensile strength (15.41 ± 0.10 MPa) and elongation (78 ± 7%) likely due to limited intermolecular interactions (Pugar *et al*., 2024). P2, containing the extract, showed a moderate increase in strength (19.12 ± 0.90 MPa) and elongation (119 ± 7%) as PE may act as a plasticizer, enhancing flexibility through hydrogen bonding with PVA (Arıöz, 2024; Dang *et al*., 2024; da Rosa Almeida *et al*., 2022). P3, containing chitosan and extract, showed a significant improvement in both strength (39.12 ± 2.05 MPa) and elongation (217 ± 6) due to the synergistic effect of chitosan reinforcing the matrix and extract maintaining chain mobility (Tan *et al*., 2021; Dang *et al*., 2024; da Rosa Almeida *et al.,* 2022). In contrast, N3, containing nanochitosan instead of chitosan, exhibited lower performance (20.54 ± 1.00 MPa, 112 ± 5% elongation), likely due to increasing dispersion and interfacial bonding issues (Österberg *et al.,* 2023; Soufiani *et al*., 2025).

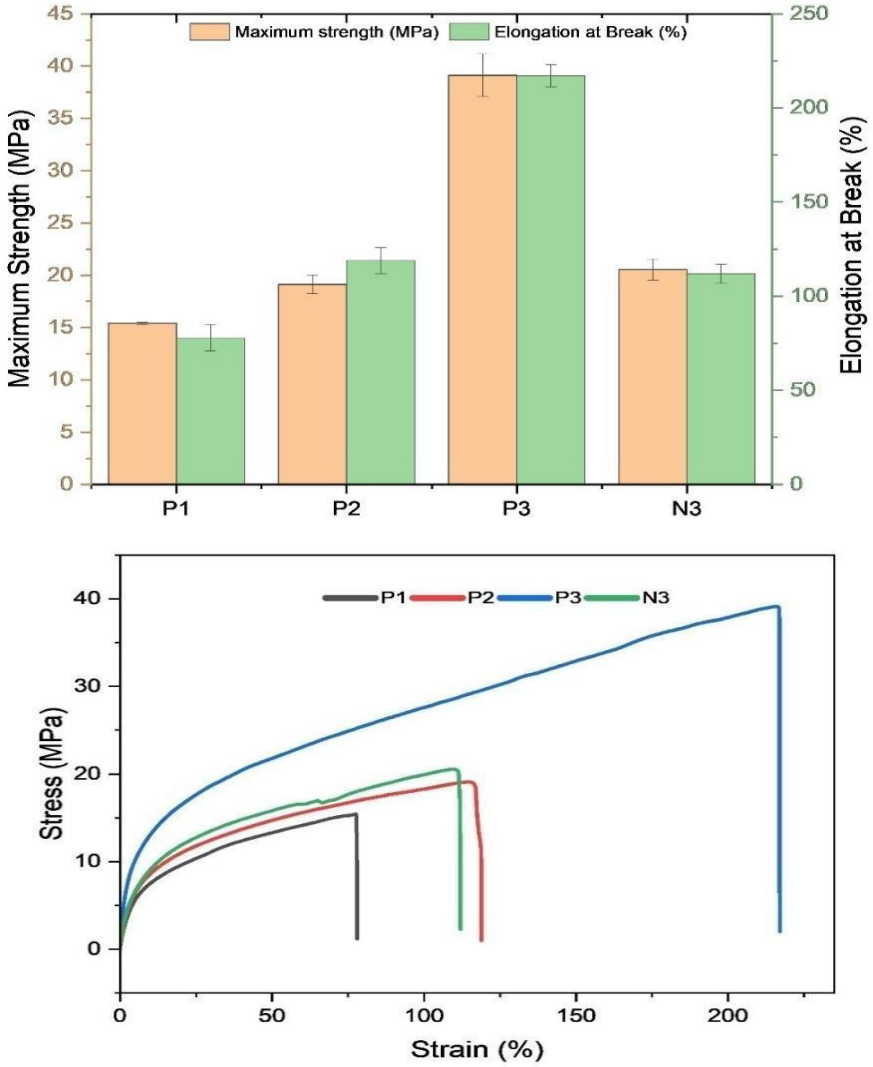

Fig. 2.18 *Mechanical properties of the PVA-based composite films incorporating (nano)chitosan and duckweed leaf aqueous extract.*

DSC analysis (Table 2.8) of the PVA-based composite films revealed notable changes in thermal behavior due to the inclusion of various additives. P1 (PVA-glycerol) exhibited standard DSC transitions, serving as a baseline for comparison. The decomposition temperature (T_d) and melting temperature (T_m) were relatively high, consistent with pure PVA known thermal characteristics. In the case of P2, the inclusion of duckweed extract led to a decrease in T_m, whereas an increase in T_e and T_d was observed, confirming the plasticizing effect of the plant extract. These shifts in thermal transitions are consistent with findings by Phattarateera *et al.* (2023) and Barbălată-Mândru *et al.* (2022) who reported similar reductions in thermal stability when plant extracts were incorporated into PVA-based systems.

No significant variations compared to P2 were observed for P3, expect for a lowering of T_d, likely due to the role of chitosan in altering the crystalline structure of PVA films. As a result of the more efficient embedding in the nanoform, the incorporation of nanochitosan (sample N3) led to an important decrease not only of T_d, but also of T_e and T_m.

Table 2.8 *Onset temperature of water (T_e), melting temperature (T_m) and decomposition temperature (T_d) for PVA-based films incorporating (nano)chitosan and duckweed leaf extract.*

Sample	T_e (°C)	T_m (°C)	T_d (°C)
P1	80	194	240
P2	83	186	254
P3	83	187	239
N3	75	154	226

2.2.3.7. Antioxidant properties

The antioxidant properties of the developed films (Fig. 2.20) varied markedly depending on their composition. The control sample (P1), consisting solely of PVA and glycerol, exhibited the lowest antioxidant efficacy in both CUPRAC and FRAP assays, reflecting the absence of active antioxidant constituents. In contrast, films P2 and P3, which incorporated the plant extract, showed significantly enhanced reducing capacity due to phenolic compounds present in the extract. However, the N3 film exhibited significantly lower antioxidant properties compared to its chitosan-based counterpart (P3). This reduction can be attributed to specific non-covalent interactions between nanochitosan and the extract components, primarily involving extensive hydrogen bonding between the amino ($–NH_2$) and hydroxyl (–OH) groups of nanochitosan and the phenolic hydroxyl groups of the extract (Fig. 2.19). These interactions, together with possible electrostatic attractions, partially shield the active phenolic sites, thereby reducing their accessibility for participation in the redox reactions underlying the CUPRAC and FRAP assays.

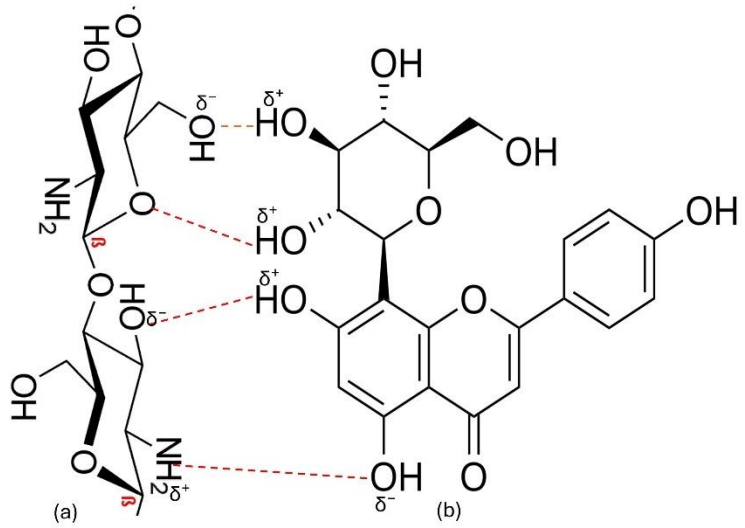

Fig. 2.19 *Possible hydrogen bonding interactions occurring between nanochitosan(a) and a representative apigenin glucoside(b) present in the Lemna minor extract).*

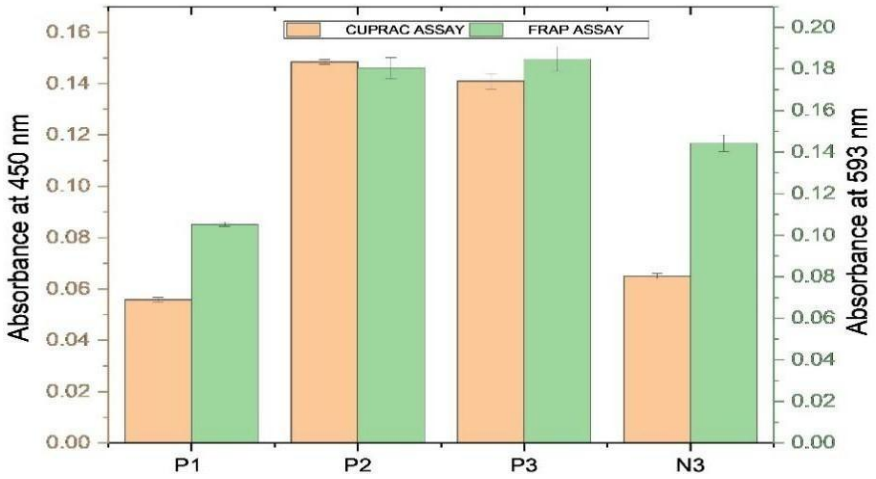

Fig. 2.20 *Antioxidant properties of PVA-based composite films incorporating (nano)chitosan and duckweed leaf extract. Shown are the results obtained after 24 h at a film dose of 2.8 mg/mL using the FRAP and CUPRAC assays. Reported are the mean ± SD values from at least three experiments.*

2.2.3.8. Antibacterial properties

The antibacterial efficacy of the films was tested against *Salmonella* species and *Enterococcus faecalis* (Fig. 2.20*)*. Films composed of PVA and glycerol (P1) exhibited minimal antimicrobial activity, which aligns with literature data indicating that pure PVA films do not possess inherent antibacterial properties. The inclusion of duckweed extract (P2) led to a strong/moderate reduction (depending on the strain) in bacterial viability. An enhancement in antimicrobial activity was generally observed upon integrating chitosan (P3), as evident particularly in the case

of *Salmonella enterica serovar Thyphimurium*, as expected based on the well-documented role of chitosan in disrupting bacterial cell membranes. However, when nanochitosan was used instead of chitosan, a decrease in the antimicrobial efficacy was observed (see N3 *vs* P3), in line with the results of the antioxidant assays, as a consequence of the "too much" efficient interactions between the active sites of chitosan and of the duckweed leaf extract, masking these latter and limiting their contact with microorganisms.

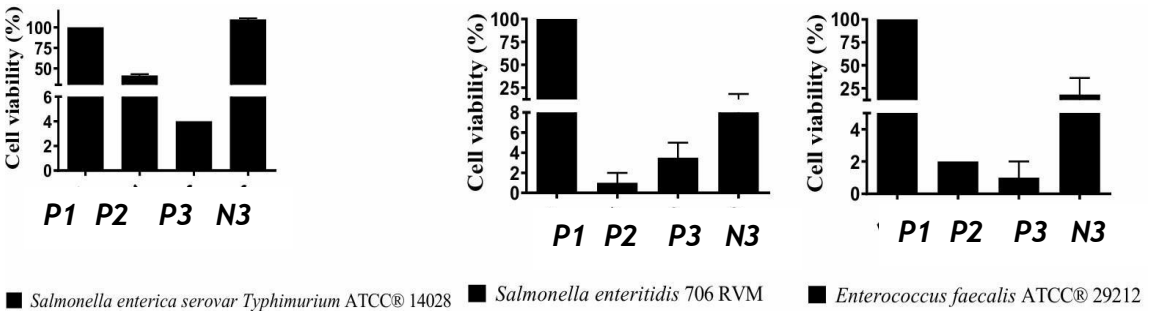

Fig. 2.21. *Antibacterial* activity of PVA-based composite films incorporating (nano)chitosan and duckweed leaf extract.

2.2.4 Conclusions

This study was focused on the characterization of poly (vinyl alcohol) (PVA)-based films incorporating a phenol-rich aqueous extract from duckweed (*Lemna minor*) leaves and chitosan or nanochitosan intended for active food packaging. The results of this study provided a deeper insight into how additives may influence key physicochemical and functional properties of the films. The phenol-rich extract conferred both antioxidant and antimicrobial properties to the PVA-based films. SEM analysis revealed that while the plant extract introduced porosity and roughness, nanochitosan improved dispersion and matrix cohesion, yielding films with fewer defects and more compact cross-sections. Optical analysis demonstrated that films with duckweed extract had increased opacity (up to 4.20 mm^{-1}) and reduced transmittance in the UV region (<400 nm), with nanochitosan modulating this effect by maintaining visual clarity. Water-related properties showed substantial improvement in nanochitosan containing films, which exhibited lower solubility and water vapor transmission rate, and hence enhanced barrier

performance. Future work will focus on biodegradability assessments and migration studies to further establish the applicability and safety of these films in commercial packaging system.

2.2.5 References

Abdelghany, A. M., Menazea, A. A., & Ismail, A. M. (2019). Synthesis, characterization and antimicrobial activity of Chitosan/Polyvinyl Alcohol blend doped with Hibiscus Sabdariffa L. extract. Journal of Molecular Structure, 1197, 603-609.

Ali, M., Mir, S., Atanase, L. I., Abid, O. U. R., & Kazi, M. (2024). Chitosan–PVA–PVP/nano-clay composite: a promising tool for controlled drug delivery. *RSC advances*, *14*(22), 15777-15790.

Altiok, D., Altiok, E., & Tihminlioglu, F. (2010). Physical, antibacterial and antioxidant properties of chitosan films incorporated with thyme oil for potential wound healing applications. Journal of Materials Science: Materials in Medicine, 21(7), 2227-2236.

Arıöz, E., Ay, S. B., & Erkmen, D. (2024). Production and Characterization of Polyvinyl Alcohol (PVA)/Chitosan (CH) Wound Dressings Enriched with Hypericum perforatum ex- tract. *Journal of Engineering and Basic Sciences*, *2*, 1-7.

Artamonova, A. A., Baldov, D. A., Mirzeabasov, O. A., Rasskazova, M. M., Synzynys, B. I., & Shatalova, R. O. (2020, November). Bioassay of radioactive water contamination using duckweed Lemna minor and Spirodella polyrrhiza: experimental justification. In *Journal of Physics: Conference Series* (Vol. 1701, No. 1, p. 012011). IOP Publishing.

Asghar, M. M., Wang, Z., Wang, B., & Zaidi, S. A. H. (2020). Nonrenewable energy—environmental and health effects on human capital: empirical evidence from Pakistan. *Environmental Science and Pollution Research*, *27*(3), 2630-2646.

Barbălată-Mândru, M., Serbezeanu, D., Butnaru, M., Rîmbu, C. M., Enache, A. A., & Aflori, M. (2022). Poly (vinyl alcohol)/plant extracts films: preparation, surface characterization and antibacterial studies against gram positive and gram negative bacteria. *Materials*, *15*(7), 2493.

Boneza, M. M., & Niemeyer, E. D. (2018). Cultivar affects the phenolic composition and antioxidant properties of commercially available lemon balm (Melissa officinalis L.) varieties. *Industrial Crops and Products*, *112*, 783-789.

da Rosa Almeida, A., Maciel, M. V. D. O. B., Machado, M. H., Sganzerla, W. G., Teixeira, G. L., da Rosa, C. G., ... & Barreto, P. L. M. (2022). Production of chitosan and poly (vinyl alco- hol) films functionalized with hop extract (Humulus lupulu L. var. Cascade) for food packaging application. *Food Packaging and Shelf Life*, *32*, 100833.

Dang, T. T., Nguyen, L. A. T., Dau, D. T., Nguyen, Q. S., Le, T. N., & Nguyen, T. Q. N. (2024). Improving properties of chitosan/polyvinyl alcohol films using cashew nut testa ex-tract: potential applications in food packaging. *Royal Society Open Science*, *11*(12), 241236.

Del Buono, D., Bartucca, M. L., Ballerini, E., Senizza, B., Lucini, L., & Trevisan, M. (2022). Physiological and biochemical effects of an aqueous extract of Lemna minor L. as a potential biostimulant for maize. *Journal of Plant Growth Regulation*, *41*(7), 3009-3018.

El-Saber Batiha, G., Magdy Beshbishy, A., G. Wasef, L., Elewa, Y. H., A. Al-Sagan, A., Abd El-Hack, M. E., ... & Prasad Devkota, H. (2020). Chemical constituents and pharmacological activities of garlic (Allium sativum L.): A review. *Nutrients*, *12*(3), 872.

Garavand, Y., Taheri-Garavand, A., Garavand, F., Shahbazi, F., Khodaei, D., & Cacciotti, I. (2022). Starch-polyvinyl alcohol-based films reinforced with chitosan nanoparticles: physical, mechanical, structural, thermal and antimicrobial properties. *Applied Sciences*, *12*(3), 1111.

Ju, J., Yao, W., Sun, S., Guo, Y., Cheng, Y., Qian, H., & Xie, Y. (2018). Assessment of the antibacterial activity and the main bacteriostatic components from bayberry fruit extract. *International Journal of Food Properties*, *21*(1), 1043-1051.

Khan, A. U., Khan, A. N., Waris, A., Ilyas, M., & Zamel, D. (2022). Phytoremediation of pollutants from wastewater: A concise review. *Open Life Sciences*, *17*(1), 488-496.

Khellaf, N., & Zerdaoui, M. (2010). Growth response of the duckweed Lemna gibba L. to copper and nickel phytoaccumulation. *Ecotoxicology*, *19*(8), 1363-1368.

Luzi, F., Del Buono, D., Orfei, B., Moretti, C., Buonaurio, R., Torre, L., & Puglia, D. (2022). Lemna minor aqueous extract as a natural ingredient incorporated in poly (vinyl alcohol)-based films for active food packaging systems. *Food Packaging and Shelf Life*, *32*, 100822.

M. (2022). Poly (vinyl alcohol)/plant extracts films: preparation, surface characterization and antibacterial studies against gram positive and gram-negative bacteria. *Materials*, *15*(7), 2493.

Medrano-Sánchez, E. J., & Sotomayor, C. N. Phytoremediation as a Strategic Alliance between Nature and Mining for a More Sustainable Future: A Literature Review (2019– 2023). *Available at SSRN 5129780*.

Miah, M. R., Wang, J., & Zhu, J. (2025). Introduction: Green Materials and Sustainability in Active Food Packaging. In *Green Materials for Active Food Packaging* (pp. 1-33). Singapore: Springer Nature Singapore.

Nanocrystals (CNCs), Tannic Acid (TA), and Chitosan (CS) for Food Packaging. *Journal of Nanomaterials*, *2021*(1), 4821717.

Osterberg, M., Henn, K. A., Farooq, M., & Valle-Delgado, J. J. (2023). Biobased nanomaterials─ the role of interfacial interactions for advanced materials. *Chemical reviews*, *123*(5), 2200-2241.

Panfili, I., Bartucca, M. L., & Del Buono, D. (2019). The treatment of duckweed with a plant biostimulant or a safener improves the plant capacity to clean water polluted by terbuthylazine. *Science of the Total Environment*, *646*, 832-840.

Periyasamy, Thirukumaran, Shakila Parveen Asrafali, and Jaewoong Lee. "Recent Advances in Functional Biopolymer Films with Antimicrobial and Antioxidant Properties for Enhanced Food Packaging." *Polymers* 17.9 (2025): 1257.

Phattarateera, S., Xin, L., Kaewpheng, K., Kriangburananan, T., & Threepopnatkul, P. (2023). Effects of additives on properties of PVA film for agricultural applications. *ScienceAsia*, *49*, 23.

Pugar, D., Haramina, T., Leskovac, M., & Ćurković, L. (2024). Preparation and characterization of poly (vinyl-alcohol)/chitosan polymer blend films chemically crosslinked with glutaraldehyde: Mechanical and thermal investigations. *Molecules*, *29*(24), 5914.

Ribeiro-Santos, R., Andrade, M., de Melo, N. R., & Sanches-Silva, A. (2017). Use of essential oils in active food packaging: Recent advances and future trends. *Trends in food science & technology*, *61*, 132-140.

Rodrigues, I. R., de Camargo Forte, M. M., Azambuja, D. S., & Castagno, K. R. (2007). Synthesis and characterization of hybrid polymeric networks (HPN) based on polyvinyl alcohol/chitosan. Reactive and Functional Polymers, 67(8), 708-715.

Sadadekar, A. S., Shruthy, R., Preetha, R., Kumar, N., Pande, K. R., & Nagamaniammai, G. (2023). Enhanced antimicrobial and antioxidant properties of Nano chitosan and pectin based biodegradable active packaging films incorporated with fennel (Foeniculum vulgare) essential oil and potato (Solanum tuberosum) peel extracts. *Journal of Food Science and Technology*, *60*(3), 938-946.

Sanati, F., Ashghali Farahani, M., Rostami-Darounkola, M. R., Shokrolahi, F., & Naseri, M. (2025). Assessing the efficacy of polyvinyl alcohol/chitosan nanofibrous mat loaded with myrtle essential oil/gum Arabic in wound healing. *Journal of Biomaterials Science, Polymer Edition*, 1-22.

Soufiani, S. P., Yousefi, S., Honarvar, M., Weisany, W., & Asadi, G. (2025). Polyvinyl alcohol films incorporating cellulose nanocrystals, chitosan, and mesoporous silica nanoparticles for enhanced stability and controlled release of beet extracts. *Carbohydrate Polymer Technologies and Applications*, *10*, 100740.

Tan, R., Li, F., Zhang, Y., Yuan, Z., Feng, X., Zhang, W., ... & Huang, X. (2021). High-Performance Biocomposite Polyvinyl Alcohol (PVA) Films Modified with Cellulose Nanocrystals (CNCs), Tannic Acid (TA), and Chitosan (CS) for Food Packaging. *Journal of Nanomaterials*, *2021*(1), 4821717.

Ubuza, L. J. A., Padero, P. C. S., Nacalaban, C. M. N., Tolentino, J. T., Alcoran, D. C., Tolentino, J. C., ... & Arazo, R. O. (2020). Assessment of the potential of duckweed (Lemna minor L.) in treating lead-contaminated water through phytoremediation in stationary and recirculated set-ups. *Environmental Engineering Research*, *25*(6), 977-982.

Vieira, D. M., Pereira, C., Calhelha, R. C., Barros, L., Petrovic, J., Sokovic, M., ... & Machado, A. V. (2022). Evaluation of plant extracts as an efficient source of additives for active food packaging. *Food Frontiers*, *3*(3), 480-488.

Xu, J., & Shen, G. (2011). Growing duckweed in swine wastewater for nutrient recovery and biomass production. *Bioresource technology*, *102*(2), 848-853.

Yuen, C. B., Chong, H. L., Kwok, M. H., & Ngai, T. (2025). Natural polymer-based food packaging: paving the way to a greener future–a review. *Sustainable Food Technology*, *3*(4), 908-929.

Zhang, L., Rocchetti, G., Zengin, G., Del Buono, D., Trevisan, M., & Lucini, L. (2023). The combination of untargeted metabolomics with response surface methodology to optimize the functional potential of common duckweed (Lemna minor L.). *Antioxidants*, *12*(2), 313.

Chapter 3

Design of Chitosan-Based Bioactive Composite Films Containing Lignin and Lignin-Silver Nanocomposites

3.1 Introduction

Over the past decade, extensive research has focused on developing bio-based active films with antimicrobial properties for biomedical applications or aimed at improving food preservation and reducing the reliance on synthetic chemical preservatives. In this context, chitosan and its derivatives have emerged as promising candidates due to their strong antimicrobial activity and eco-friendly nature, offering sustainable alternatives to conventional plastic packaging (Aider, 2010). Chitosan biodegradability, biocompatibility, and inherent antimicrobial potential make it particularly suitable for food packaging applications. Its amino groups at the C2 position of the sugar moieties provide key functional sites that enable formation of films, gels, beads, and nanoparticles (Dutta *et al.,* 2009), which have been studied for various applications, including food preservation, wound dressings, and medical devices (Jasrotia *et al.,* 2025). The incorporation of bioactive additives such as essential oils, plant extracts, and metal nanoparticles may further enhance the antimicrobial efficacy and functional performance (Cazón & Vázquez, 2022; Julie *et al*., 2025).

Chitosan antimicrobial action primarily stems from its cationic nature, where protonated amino groups interact with negatively charged bacterial cell membranes, causing membrane disrup- tion, leakage of cellular contents, and eventually cell death (Sahariah & Másson, 2017). Chi- tosan may also chelate essential metal ions like calcium and magnesium, limiting microbial growth and biofilm formation, and can penetrate cells to bind DNA and inhibit protein synthe- sis (Yilmaz Atay, 2019; Xia et al., 2020). Despite the strong antimicrobial activity, films made of chitosan alone exhibit limitations in terms of mechanical strength and water resistance. To address these drawbacks, chitosan is often blended with poly (vinyl alcohol) (PVA), a polymer renowned for its tensile strength, flexibility, and excellent film-forming ability (Jasrotia *et al*.,

2025). Chitosan/PVA composite films combine the antimicrobial bioactivity of chitosan with the mechanical durability of PVA, producing materials with enhanced flexibility, tensile strength, and water resistance (Tan & Liu, 2024). Based on this background, in this study chi- tosan/PVA films were prepared by varying the chitosan/PVA ratio from 70:30 to 30:70 w/w, allowing systematic evaluation of how the polymer composition influences the structural, me- chanical, and antimicrobial characteristics of the films. In addition, lignin, a natural phenolic polymer, was also incorporated into the films to enhance antioxidant, UV-Vis radiation block- ing, and antimicrobial properties. A parallel series of films was developed by incorporating hybrid lignin-silver nanocomposites instead of pure lignin. Indeed, the addition of silver nano- particles is known to significantly enhance antimicrobial efficacy and thermal stability while maintaining the film biodegradability (Marsik *et al*., 2024, Slavin *et al*., 2021, Ito *et al*., 2024)

In particular, two different approaches for the preparation of the hybrid nanocomposites were adopted, that is a conventional hydrothermal method and a solvent-free mechanochemical method. Part of this work was performed in collaboration with Prof. Massimo Bonini from the Department of Chemis- try "Ugo Schiff" of the University of Florence and Prof. Angela Arciello from the Department of Chemical Sciences of the University of Naples Federico II.

3.2 Experimental

3.2.1. Materials

Poly(vinyl alcohol) (PVA; MW 124–146 kg/mol, 99% hydrolyzed), glycerol (≥99%), chitosan (CH) from crab shells (low molecular weight, 75–85% deacetylation), alkali lignin (LIG), sodium acetate (≥99%), 2,4,6-tris(2-pyridyl)-s-triazine (TPTZ, ≥98%), iron(III) chloride hexahydrate ($FeCl_3 \cdot 6H_2O$, ≥97%), copper(II) chloride ($CuCl_2$, ≥97%), neocuproine (≥98%), and hydrogen peroxide solution (30% w/w) were purchased from Sigma-Aldrich (St. Louis, MO, USA). Reagents including hydrochloric acid (HCl, ≥37%), sodium hydroxide (NaOH, ≥98%), sodium metabisulfite ($Na_2S_2O_5$, ≥97%), and dimethyl sulfoxide (DMSO, ≥99.5%) were also obtained

from Sigma-Aldrich. The buffers for the antioxidant assays were prepared using analytical-grade reagents: the FRAP acetate buffer (0.3 M, pH 3.6) was formulated using sodium acetate trihydrate ($CH_3COONa \cdot 3H_2O$, ≥99.0%) and glacial acetic acid (CH_3COOH, ≥99.5%), while the CUPRAC buffer (1 M, pH 7.0) was prepared with ammonium acetate (NH_4CH_3COO, ≥98.0%). All solutions were prepared using deionized water, and pH adjustments were performed with HCl or NaOH as required. All chemicals were used as received without further purification.

3.2.2. Synthesis of lignin-silver nanocomposites

3.2.2.1. Hydrothermal method

Silver nanoparticles were synthesized through a hydrothermal method by dissolving 0.17 g of silver nitrate in 10 mL of distilled water, followed by addition of an equal mass (0.17 g) of alkali lignin. The mixture was stirred continuously while being heated at 100°C for 24 h and then cooled in an ice bath. The precipitate was collected by centrifugation, washed with dis- tilled water, dried at 60 °C overnight, and ground in a mortar to obtain a fine powder (Ito *et al.,* 2024).

3.2.2.2. Mechanochemical method

140 mg of lignin was mixed with 25 mg of $AgNO_3$ (15% w/w) and placed into a ball mill (Fritsch Pulverisette 23) operating at 50 osc/s. The mixture was processed for 180 min. After the milling process, the sample was washed three times with 50 mL of water using a centrifuge to remove any unreacted materials. The resulting composite was then lyophilized (Argenziano *et al.,* 2024).

3.2.3. Formulation of chitosan/PVA-based composite

To prepare the chitosan (CH)/PVA films (Table 3.1) with lignin/lignin-silver nanocomposites, the required amount of PVA was added to distilled water to obtain a 2% w/v suspension, which was then stirred and heated at 90 °C for 4 h, until full dissolution. The solution was then left to cool at room temperature. In parallel, a 2% w/w chitosan solution in 1% acetic acid was pre- pared under heating at 40 °C for 3 h For the lignin (LIG)/lignin-silver nanocomposite (LIG-Ag) solution, 20 mg of lignin or lignin-Ag were dissolved in a mixture of 2 mL ethanol and 1 mL acetone or of 1.5 mL

of ethanol and 1.5 mL of water, respectively, under stirring for 30 min at room temperature. Next, the solutions were properly mixed and stirred for 3 h (0.3 mL of glyc- erol were also added). After sonication for 15 min, the final solution was poured into a 8 cm round Petri dish and taken at at 50°C for 48 h to complete the film formation process.

Table. 3.1 *Formulation of chitosan/PVA-based composite films incorporating lignin and lignin-silver nanocomposite. All the amounts are reported as weight percentages.*

Sample Code	Formulation	CH	PVA	Glycerol	LIG/LIG-Ag
CS	CH	98.00	0.00	2.00	0.00
CS-L	CH/LIG	93.45	0.00	2.00	4.55
CP1L	CH/PVA/LIG	46.73	46.73	2.00	4.55
CP2L	CH/PVA/LIG	65.38	28.06	2.00	4.55
CP3L	CH/PVA/LIG	28.06	65.38	2.00	4.55
CP1LAg	CH/PVA/LIG-Ag	46.73	46.73	2.00	4.55
CP2LAg	CH/PVA/LIG-Ag	64.33	29.12	2.00	4.55
CP3LAg	CH/PVA/LIG-Ag	35.00	58.45	2.00	4.55
CP3LAgM	CH/PVA/LIG-Ag (prepared by mechanochemistry)	35.00	58.45	2.00	4.55

3.2.4. Physicochemical characterization of the films

3.2.4.1. Fourier Transform Infrared Spectroscopy (FT-IR)

FT-IR spectra of the films were recorded using a Nexus 870 spectrophotometer equipped with a Golden Gate Attenuated Total Reflectance (ATR) accessory. Measurements were conducted at room temperature over the wavenumber range of 4000–650 cm^{-1}. Each spectrum was ob- tained by averaging 128 scans per sample, with a spectral resolution of 2 cm^{-1}.

3.2.4.2. Thermogravimetric analysis (TGA)

Thermal stability of the films was assessed using a SDT 650 analyzer (TA Instruments, New Castle, DE, USA). Analyses were performed under a nitrogen atmosphere (flow rate: 100 mL/min), with a linear heating rate of 10 °C/min from room temperature up to 1000 °C.

3.2.4.3. Film thickness

Film thickness was determined using a digital micrometer (Mitutoyo, measuring range: 0–25 mm; resolution: 0.001 mm). Measurements were taken at ten random points on each film, and the average value was used for analysis.

3.2.4.4. Tensile testing

Mechanical properties of the films were evaluated through uniaxial tensile tests performed on rectangular specimens (50 mm × 15 mm). Tests were carried out at room temperature using a Universal Testing Machine (UTM-6800, Instron) at a constant crosshead speed of 50 mm/min until fracture. Four specimens were tested for each formulation. Stress–strain data were recorded as stress (MPa) versus percentage elongation (%), calculated according to:

$$Elongation\ (\%) = \frac{l_i - l_0}{l_0} * 100$$

where l_i is the measured gap at the *i*-th point and l_0 is the initial gap at the undeformed state. The initial gap l_0 of each sample was precisely defined as the gap corresponding to the first measured force value exceeding a threshold of 0.1 N.

3.2.4.5. Surface profilometry

Surface topography of the films was analyzed using a 3D surface profiler (VK3000, Keyence) equipped with a 10× lens. Surface roughness was evaluated over 1 mm² areas by determining the root mean square roughness (R_q), defined as:

$$R_q = \sqrt{\frac{1}{N}\sum_{i=1}^{n}\left(z_i - z_{avg}\right)^2}$$

where z_{avg} is the average height value calculated over the *n* pixels and z_i is the height of the *i*-th pixel.

3.2.4.6. Moisture content, swelling degree and total soluble matter determination

Moisture content, swelling degree, and total soluble matter were determined gravimetrically using a three-step method (Apriliyani *et al.,* 2020, Jakubowska *et al*., 2020, Rolińska *et al*., 2024). Briefly, square-shaped film samples (1 cm²) were weighed on an analytical balance with a precision of 0.0001 g to obtain the initial mass (M_1). In the first step, the samples were dried at 105 °C for 24 h to determine the initial dry mass (M_2). In the second step, the oven- dried

samples with a known M_2 value were separately immersed in water (30 mL) and left at room temperature for 24 h, after that any excess water not absorbed by the film specimens was removed using paper wipes, and the samples were weighed again to obtain the wet mass of the film (M_3). In the final third step, the samples were dried once more at 105 °C for 24 h to determine the final dry mass (M_4). All experiments were performed in triplicates. Moisture content, that is the percentage of mass loss due to water evaporation after drying the samples at 105 °C for 24 h, swelling degree, that is the percentage of mass gain resulting from water absorption after immersing the dry samples in water for 24 h, and total soluble matter, defined as the percentage of the film dry matter solubilized after 24 h of immersion in water, were determined according to the following equations:

$$\textit{Moisture content}\ (\%) = (M1 - M2)/M1 * 100$$

$$\textit{Swelling degree}\ (\%) = (M3 - M2)/M2 * 100$$

$$\textit{Total soluble matter}\ (\%) = (M2 - M4)/M2 * 100$$

3.2.4.7. Color properties

The color of the films was determined using a CR-400 colorimeter (Konica Minolta). A white plate was used as the standard (L = 93.25, a = 0.19, b = 3.95), against which the color difference (ΔE) was calculated, where L*, a*, b* represent the tendency towards whiteness, from green to red and from blue to yellow, in that order.

$$\Delta E = \sqrt{(L^*|L)^2 + (a^*|a)^2 + (b^*|b)^2}$$

The transmittance and opacity of the prepared films were determined with a Jasco V-730 spectrophotometer. Film samples were cut into 1 cm × 4 cm dimensions and transmittance was measured. Absorbance values at 600 nm (Abs_{600}) were recorded, and opacity was calculated as follows (Riaz *et al.,* 2018).

$$\textit{Opacity} = Abs_{600}/\textit{film thickness}$$

3.2.4.8. Antioxidant property characterization

A 1 cm² film sample (final dose 2.8 mg/mL) was added to the CUPRAC or DPPH assay solutions, and the absorbance was monitored over time. The CUPRAC solution was prepared by mixing 1 M ammonium acetate buffer (pH 7.0), 10 mM $CuCl_2$, 7.5 mM neocuproine (in ethanol), and distilled water in a 1:1:1:1 v/v ratio, with absorbance measured at 450 nm (Apak *et al.,* 2004). The DPPH solution was prepared in ethanol at a 50 µM concentration, and radical scavenging activity was evaluated by measuring absorbance at 515 nm (Khwaldia, *et al.,* 2023). Control experiments were conducted under the same conditions without the films.

3.2.4.9. Antibacterial activity characterization

3.2.4.9.1. Bacterial strains and culture conditions

Bacterial strains *Staphylococcus aureus* and *Pseudomonas aeruginosa* were cultured in Muller-Hinton Broth (MHB, Becton Dickinson Difco, Franklin Lakes, NJ, USA) and on Luria-Bertani Agar (LBA; tryptone 10 g/L, yeast extract 10 g/L, sodium chloride 5 g/L). For all experiments assessing the antimicrobial activity of air-dried chitosan/PVA-based film, bacterial cells were inoculated into MHB and incubated overnight at 37 °C. The following day, cultures were transferred to fresh MHB and grown to the mid-logarithmic phase.

3.2.4.9.2. Evaluation of bacterial growth inhibition

To assess cell viability, bacterial cells were diluted into 0.5× MHB to approximately 2×10^6 CFU/mL. A 500 µL aliquot of the bacterial culture was placed onto a 1 cm^2 square of each tested film and incubated at 37 °C overnight. The following day, the cultures were diluted in 0.5× MHB medium and plated on LBA to perform the colony counting.

3.3 Results and discussion

3.3.1. Characterization of chitosan/PVA based films

3.3.1.1. FTIR analysis

The ATR-FTIR analysis of chitosan/PVA composite films containing lignin and lignin–silver nanocomposites (Fig. 3.1) reveal that the overall spectral profile remains dominated by the polymeric components, with lignin and lignin–silver nanocomposites acting as inert fillers. The major spectral changes observed were driven by the blending of chitosan and PVA, particularly in the O–H stretching (3600–3000 cm^{-1}) and amide II (around 1650 cm^{-1}) regions. The O–H stretching band, indicated by the green dashed line (Fig. 3.1, left panel), shifts towards lower wavenumbers (~3300 cm^{-1}) with increasing PVA content, indicating hydrogen-bond rearrangement and intermolecular interactions between PVA and chitosan. These shifts are consistent with hydrogen-bond rearrangement and intermolecular associations commonly reported for PVA–chitosan systems (Kadir *et al.,* 2011).

The amide II band, marked by the red dashed line, which is characteristic of chitosan, shows intensity shifts in the composite films, further confirming the influence of PVA on the chitosan matrix (left panel). Additionally, the NH stretching, indicated by the green line, around ~3400 cm^{-1} reflects modifications in chitosan's hydrogen bonding when blended with PVA. Despite these changes, no new diagnostic absorption bands appear in the spectra, indicating that lignin and lignin–silver nanocomposites do not chemically modify the polymer matrix but primarily serve as inert fillers.

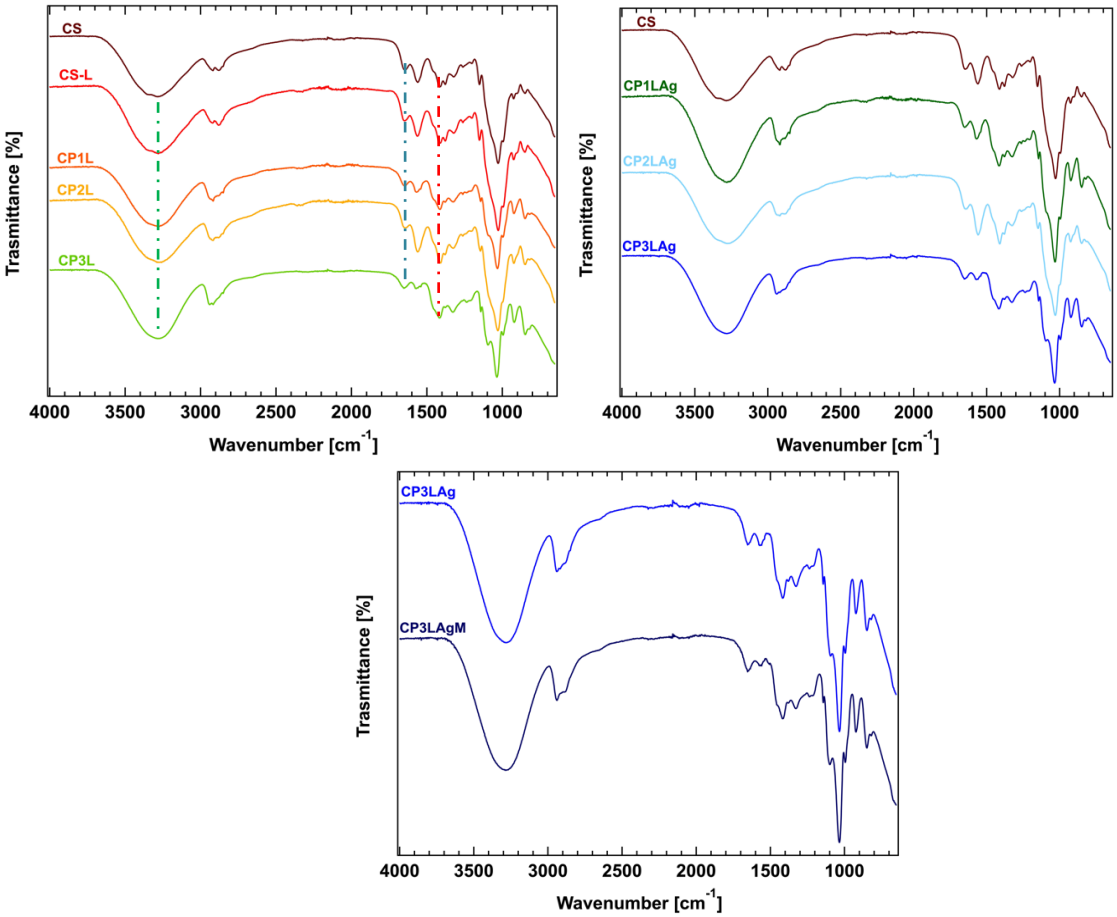

Fig. 3.1 *ATR-FTIR spectra of chitosan/PVA based films as in Table 1.*

3.3.1.2. Surface morphology analysis by profilometry

The profilometer images (Fig.3.2) revealed some differences in the surface morphology and roughness of the films. More in details, the introduction of lignin did not significantly modify surface morphology or roughness value, indicating that it dispersed well within the polymer matrix. Actually, the slightly smoother surface of the CS-L film compared to CS (Rq= 0.256 mm vs 0.469 mm) suggested potential improvements in mechanical proper- ties of the films, making it more suitable for applications where surface finish and ma- terial performance are critical, such as in food packaging. The addition of PVA to the chitosan matrix (samples CP1L-CP3L) did not cause any significant changes in the film morphology or roughness, and no phase separation or aggregation occurred between the two polymer components. On the other hand, the introduction of lignin-silver nanocom- posites into the polymer blend caused an increase in surface roughness

in all samples, regardless of the amount of PVA, likely as a consequence of nanoparticle aggregation or uneven dispersion within the polymer matrix. Notably, however, the nanocomposite pre- pared by mechanochemical synthesis did not impact on surface roughness. This can be attributed to a more uniform dispersion of smaller nanoparticles within the polymer ma- trix, which helps fill gaps and prevent formation of large agglomerates that could increase roughness. This hypothesis could be confirmed when the characterization of the LIG-Ag and LIG-AgM samples, which is currently underway, will be complete.

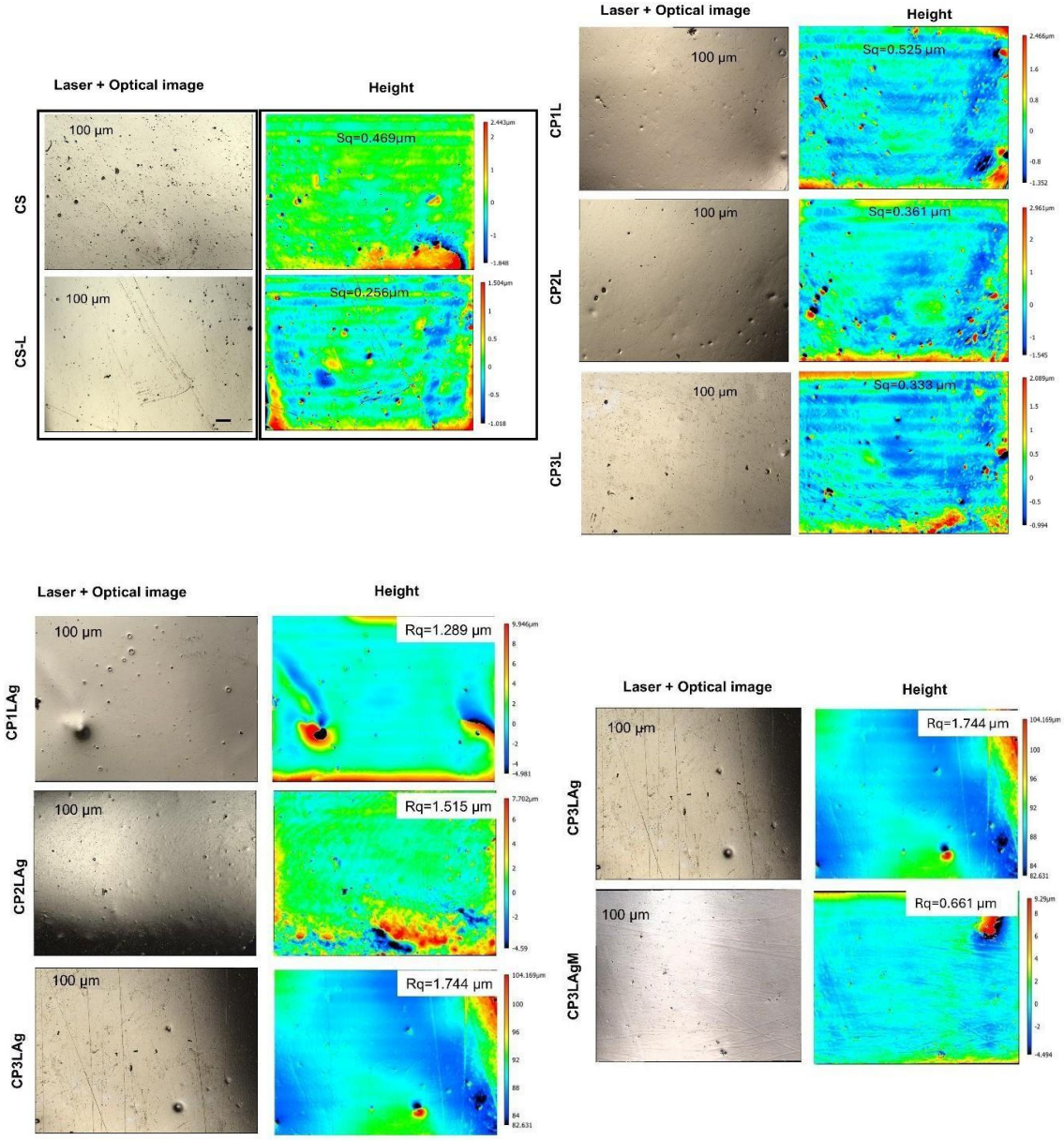

Fig. 3.2 *Profilometry images of chitosan/PVA-based films as in Table 1.*

3.3.1.3. Color, UV-Vis radiation blocking properties and hydrophilic properties

The ΔE value, which represents the total color difference, provides a clear indication of the color shifts in chitosan-based films with different additives (Table. 3.2). All the lignin additivated films exhibited significantly higher DE values (23.7-46.7) compared to pure chitosan films (CS) (ΔE= 6.7 ± 0.1), with differential, at the moment non interpretable, effects due to the presence of PVA

. **Table 3.2.** *Color properties of chitosan/PVA-based films as in Table 1.*

Sample	ΔE
CS	6.7 ± 0.1
CS-L	37.0 ±0.7
CP1L	29.5 ±0.6
CP2L	40.9 ±0.8
CP3L	37.4 ±0.8
CP1LAg	23.7 ±0.5
CP2LAg	39.6 ±0.8
CP3LAg	46.7 ±0.9
CP3LAgM	46.7±0.9

The UV-Vis blocking performance of the films is reported in Fig. 3.3. As expected, films composed of chitosan alone (CS) provided limited protection against UV radiation. In contrast, films containing lignin showed a significant improvement in UV- and visible radiation blocking performance. Indeed, lignin aromatic structures absorb UV radiation effectively, leading to an almost complete reduction in UV transmission. Although some differences were observed, the introduction also of PVA into chitosan films (CP1, CP2, CP3) seems not to significantly affect the UV-Vis blocking properties of the films, or rather, no trend is apparent as a function of the PVA content. A different visible blocking profile was observed when lignin-silver nanocomposite was used in place of lignin, with CP3LAg and CP3LAgM samples exhibiting the best UV-Vis blocking performance.

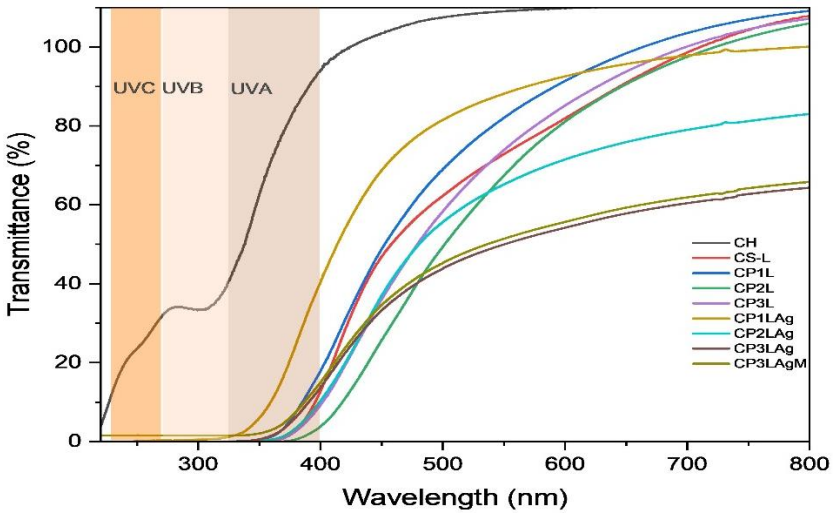

Fig. 3.3 *UV-Vis transmittance spectra of chitosan/PVA-based films as in Table 1.*

The hydrophilicity of the chitosan-based composite films was evaluated based on moisture content, swelling degree, and solubility, which were influenced by the film composition (Fig. 3.4). The moisture content of the films reflects their ability to absorb and retain water, a key indicator of hydrophilicity. The films containing PVA generally showed greater water retention, indicating their higher hydrophilic nature. In contrast, the CS-L sample, which does not contain PVA, exhibited the lower moisture content, even when compared to CS containing chitosan only, in line with the hydrophobic nature of lignin. As to the swelling degree, it is worth of notice that the presence of lignin in CS- L resulted in an exceptionally high swelling degree, possibly due to the porous structure created by lignin that allows high water absorption compared to chitosan alone (CS sample). However, the high swelling did not correspond to a high moisture content, indicating that water was absorbed but not significantly retained. As far as solubility is concerned, a trend similar to moisture content was observed. Indeed, the films with higher PVA content, such as CP3L, CPA3LAg, and CP3LAgM, exhibited the highest solubility, confirming that PVA contributes significantly to the solubility of the films and enhances their hydrophilic properties, overcoming the hydrophobic effect of lignin (see CS-L *vs* CS).

In conclusion, the hydrophilicity of the films was strongly influenced by the ratio of PVA to chitosan and the presence of lignin. These findings suggest that by carefully adjusting the PVA-

to-chitosan ratio and incorporating lignin, it is possible to tailor the hydrophilic properties of the films to suit specific applications. In any case, it is undoubtedly that the water content and swelling properties of all the films are rather high and appear incompatible with packaging applications. However, a better interpretation of these quite unexpected values could be provided following measurement of the storage relative humidity and temperature.

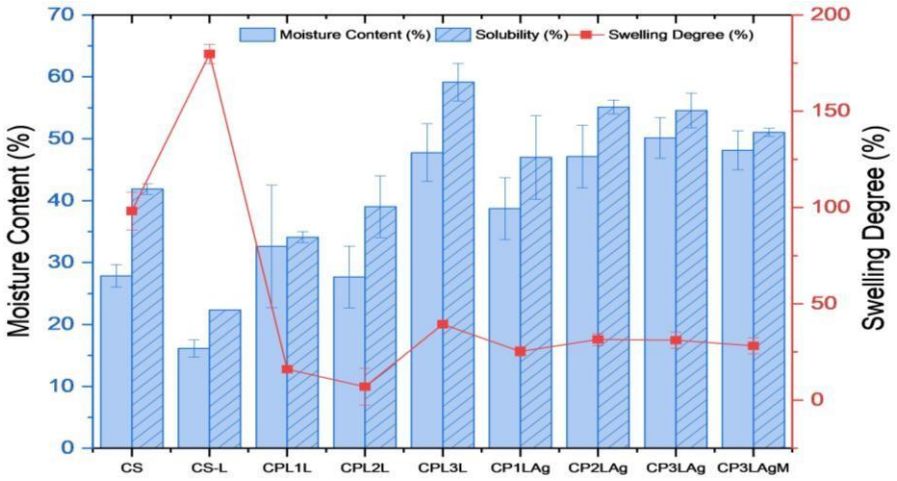

Fig. 3. 4 *Hydrophilicity behavior of chitosan/PVA based films as in Table 1.*

3.3.1.4. Thermal properties

TGA (Fig. 3.5) revealed distinct thermal behaviors across the studied systems. Chitosan powder was used as a reference, showing a primary decomposition around 300 °C following a minor weight loss below 100 °C from moisture evaporation. In film form (CS sample), an additional DTG peak appears near 200 °C likely due to glycerol hygroscopic nature and partial degradation (Zhang *et al*., 2019). The main peak shifts slightly to lower temperatures, indicating reduced thermal stability as glycerol disrupts the chitosan hydrogen-bonding network. Introduction of lignin (CS-L sample) produced no major changes in degradation stages, confirming its role mainly as a filler. In the chitosan–PVA systems, a new peak at~400 °C was observed, due to PVA decomposition (La Mantia *et al*., 2017; Moussout *et al.,* 2016; Muhd Julkapli *et al.,* 2011). The second characteristic peak of PVA around 250/300 °C was superimposed on the second peak of chitosan (and chitosan-lignin) films. Incorporation of lignin-

silver nanoparticles did not noticeably alter the TGA–DTG profile, indicating again a role of filler for the additive, not interfering with the decomposition pattern of the polymer matrix.

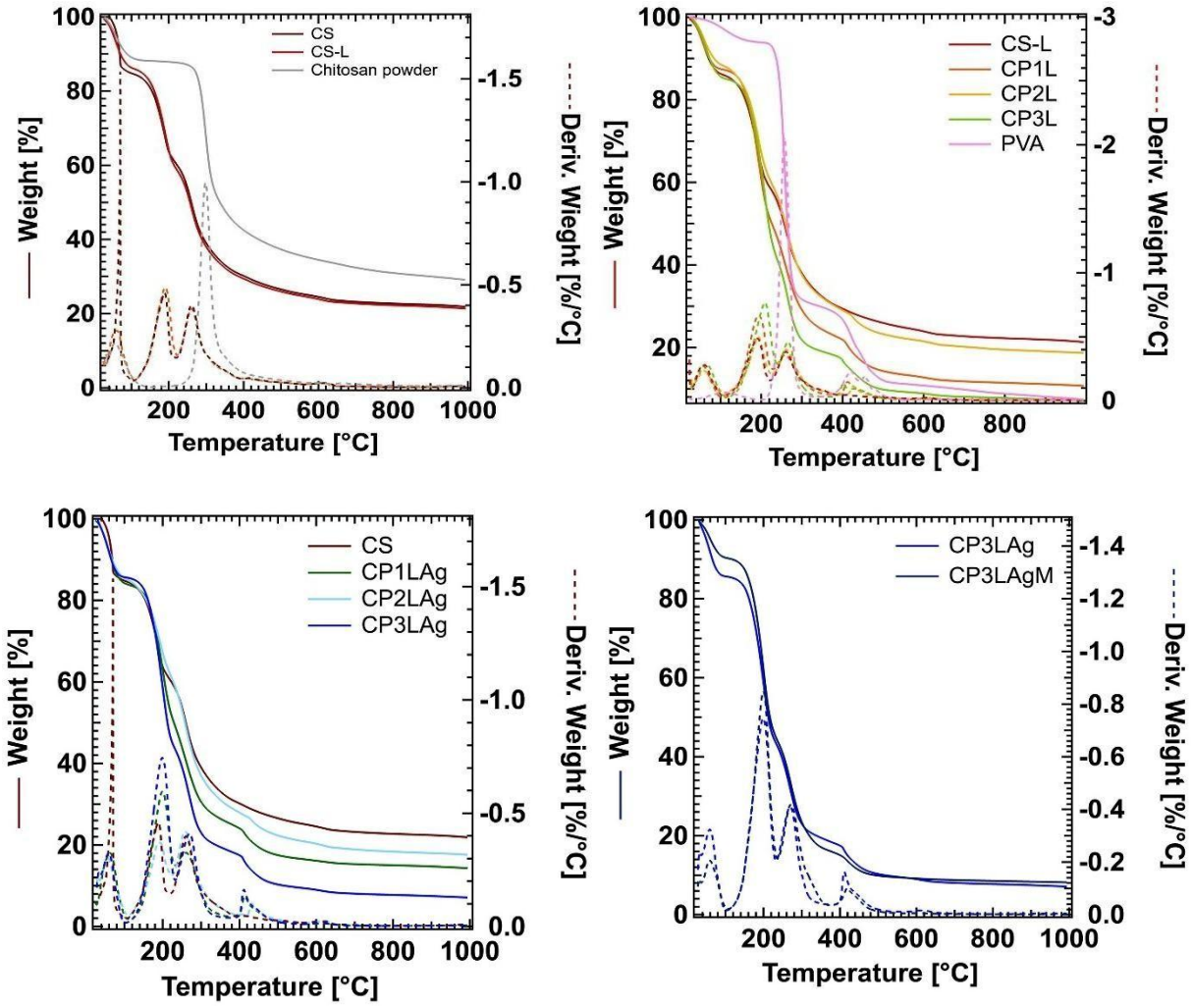

Fig. 3.5 *TGA and DTG thermograms of the chitosan/PVA based films as in Table 1.*

3.3.1.5. Mechanical properties

Mechanical testing showed that adding lignin to chitosan (CS) films reduced elongation and stress at break, making the CS–lignin (CS-L) films more brittle than neat CS(Fig. 3.6a). Lignin acts as a rigid phase that restricts polymer-chain mobility and creates stress-concentrating domains, leading to earlier fracture. However, introducing PVA improved the mechanical properties, particularly for formulations with higher PVA content (CP3L and CP3LAg). PVA's flexibility and ability to form hydrogen bonds with chitosan enhance interchain interactions, allowing more plastic deformation and higher elongation at break(Fig 3.6a and Fig. 3.6b). This

composition–property relationship is confirmed by a linear increase in elongation with higher PVA/CS content, supported by high $R^2 = 0.992$, indicating reproducibility despite experimental scatter. PVA/CS content is a key driver of ductility, improving blend homogeneity and intermolecular interactions(Fig.3.6d). Lignin–silver nanocomposite films benefit from mechanochemical synthesis, which promotes uniform nanoparticle dispersion, better interfacial contact, and stronger physical/chemical interactions, enhancing mechanical performance. In contrast, hydrothermal methods may cause nanoparticle aggregation, weakening the film(Fig.3.6c).. Thus, while lignin alone embrittles CS, PVA addition and well-dispersed lignin–Ag nanophases improve ductility and mechanical robustness by enhancing compatibility, interfacial bonding, and reducing defects.

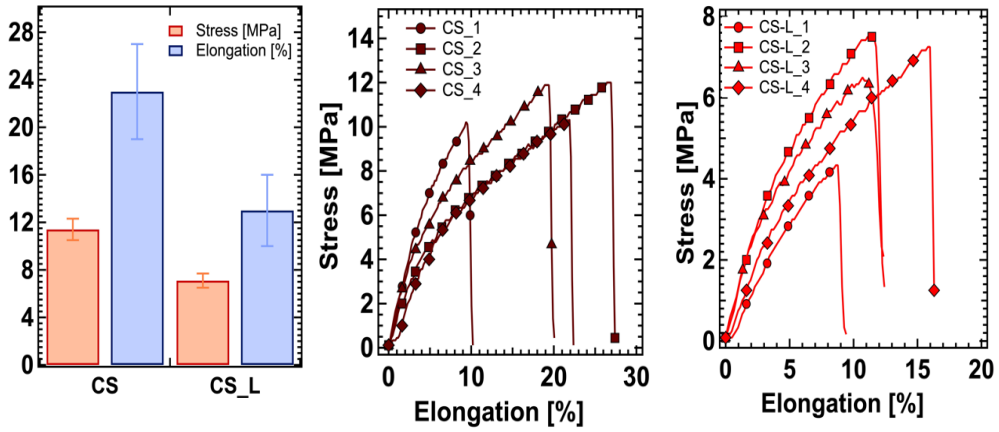

Fig. 3.6a *Mechanical properties (Strength (MPa), Elongation at break (%) and Stress vs strain curves) of chitosan and chitosan-lignin films as in Table 1.*

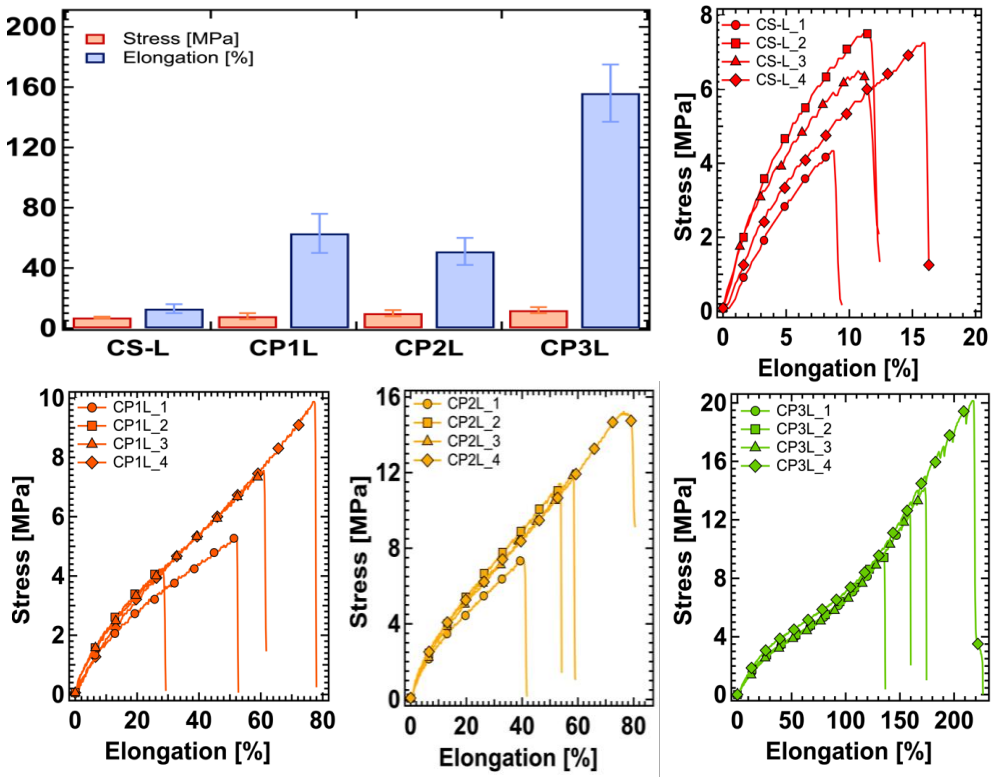

Fig. 3.6b *Mechanical properties (Strength (MPa), Elongation at break (%) and Stress vs strain curves) of chitosan/PVA-lignin films as in Table 1. Reported are the mean ± SD values from three separate experiments.*

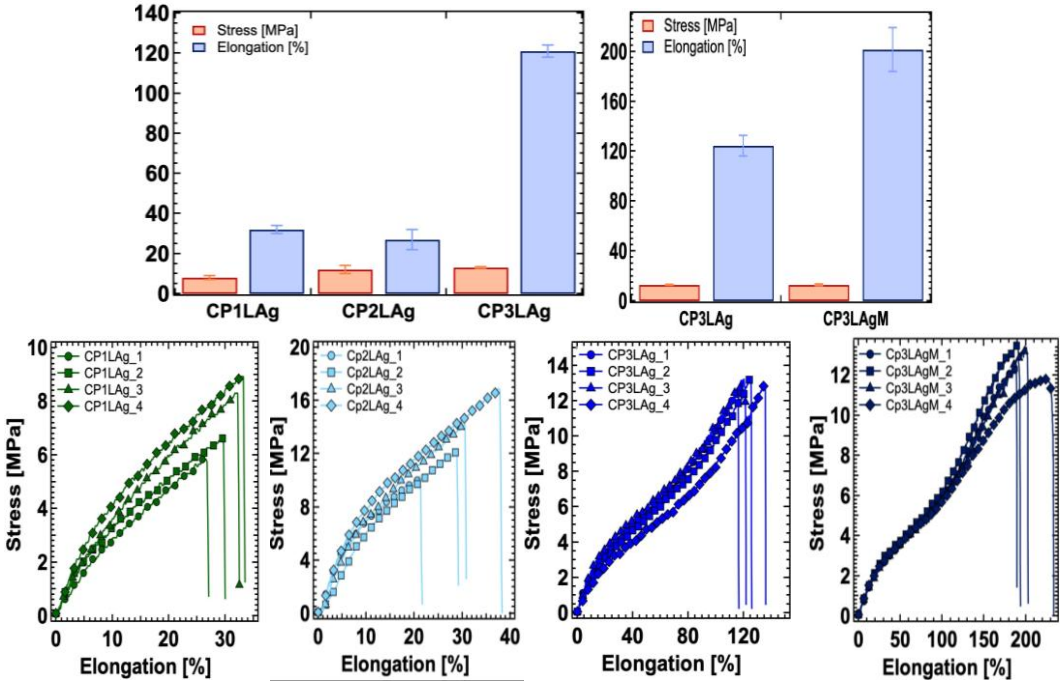

Fig. 3.6c. *Mechanical properties (Strength (MPa), Elongation at break (%), and Stress vs. Strain curves) of chitosan/PVA lignin silver nanocomposite films as shown in Table 1. Reported are the mean ± SD values from three separate experiments.*

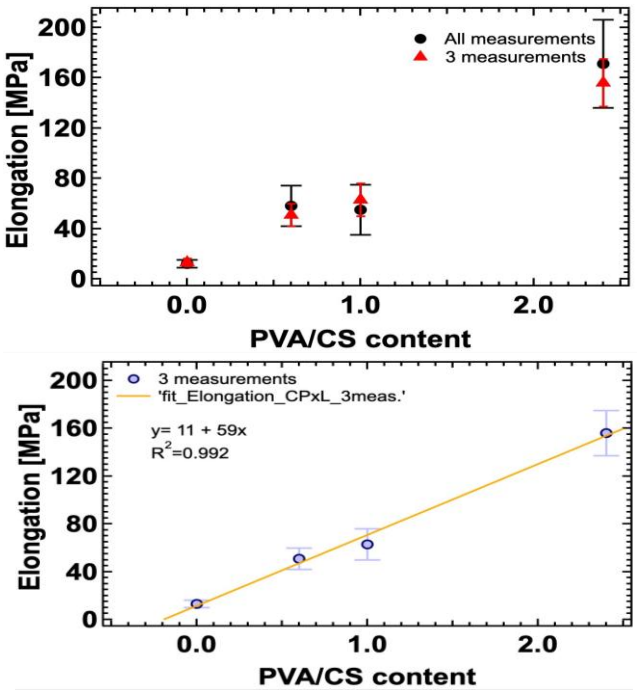

Fig.3.6d. *Effect of PVA/chitosan (PVA/CS) content on elongation at break of the composite films; symbols show mean ± SD for all measurements (black circles) and the subset of three measurements (red triangles), and the lower panel reports the linear fit for the three-measurement dataset* ($y = 11 + 59x$, $R^2 = 0.992$).

3.3.1.6. Antioxidant properties

The antioxidant properties of the films were preliminarily tested using the 2,2-diphenyl-1-picrylhydrazyl (DPPH) and the cupric reducing antioxidant capacity (CUPRAC) assays (Fig.3.7). Notably, PVA markedly enhanced the DPPH reducing properties of the films, with CP3L samples showing the highest radical scavenging activity (RSA), whereas an opposite trend was observed in the case of the CUPRAC assay. These results are in line with the different solvents adopted in the two assays, that is ethanol for the DPPH assay and water in the case of CUPRAC assay. Indeed, the CS-L sample exhibited the highest swelling degree in water among all the films (see Fig. 3.5), whereas the higher affinity toward ethanol of PVA compared to chitosan could be responsible for the highest RSA value determined for the chitosan/PLA films in the DPPH assay. As expected, based on the involvement of the LIG phenolic groups in the silver ion reduction, the films containing LIG-Ag generally exhibited slightly lower antioxidant properties (Argenziano *et al.,* 2024), with the only exception exhibited in the CUPRAC assay by the CP3LAgM film.

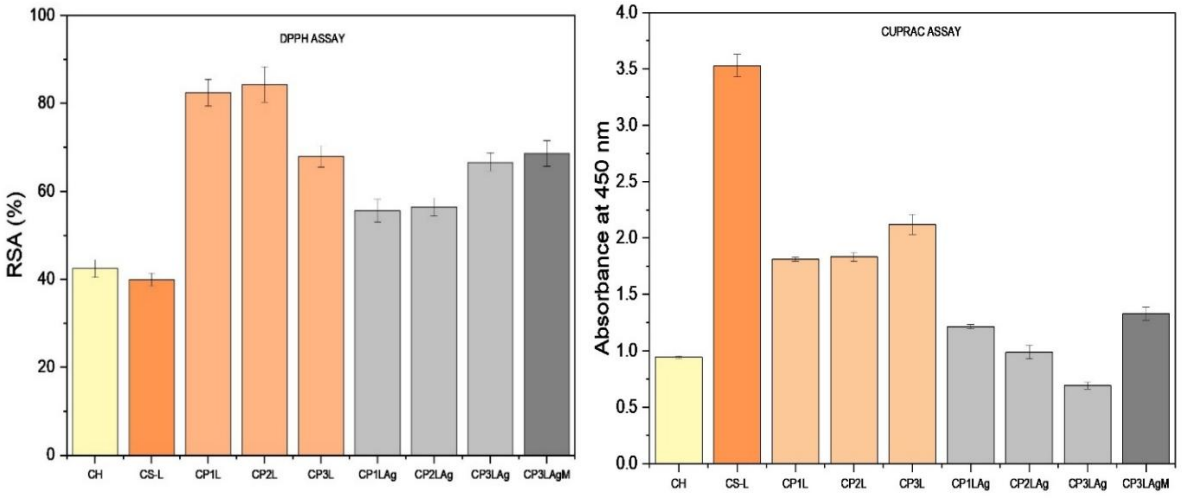

Fig. 3.7 *Results from the DPPH and CUPRAC assays run on chitosan/PVA films as in Table 1. RSA= radical scavenging activity. Reported are the mean + SD values from three separate experiments.*

3.3.1.7. Antimicrobial properties

Antibacterial activity was preliminarily evaluated against the Gram-positive Methicillin-resistant *Staphylococcus aureus (MRSA)* and the Gram-negative *Pseudomonas aeruginosa* **(**Fig. 3.8**).** As expected, chitosan films demonstrated strong antibacterial effects due to protonated amino groups, which may interact with negatively charged bacterial cell walls, increasing membrane permeability and causing leakage of intracellular contents (Jiang *et al*., 2023; Zehra *et al.,* 2022). Notably, in line with what was reported in *Chapter 2*, when chitosan was com- bined with lignin (CS-L sample), the antimicrobial activity was significantly reduced as a consequence of lignin-chitosan interactions, decreasing the availability of chitosan cationic sites (Yaneva *et al*., 2022). The antimicrobial activity was generally recovered when PLA was also present, particularly in the case of MRSA. On the contrary, further experiments are needed to better understand the efficacy of lignin-silver nanocomposites in enhancing the antibacterial performance of the films, since conflicting results were obtained among the different films and bacterial strains.

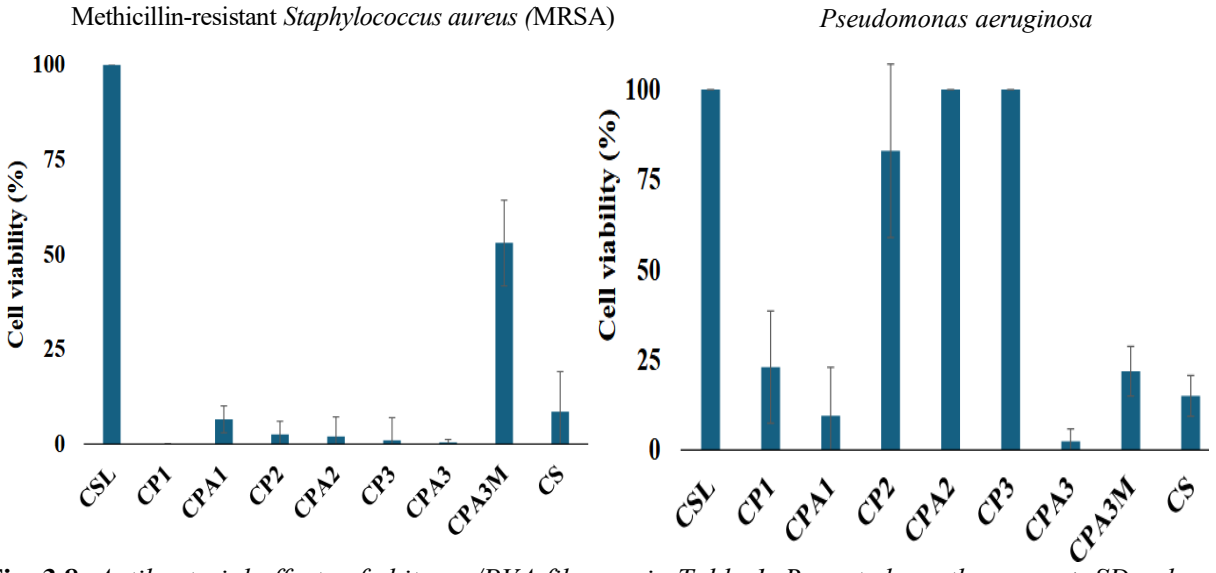

Fig. 3.8 *Antibacterial effects of chitosan/PVA films as in Table 1. Reported are the mean + SD values from three separate experiments.*

3.4 Conclusions

In conclusion, the results presented in this chapter demonstrated that integrating chitosan with PVA, lignin and lignin-silver nanocomposites may significantly enhance the physicochemical and functional performance of films intended for food packaging applications. FTIR analysis revealed that lignin acted primarily as a filler, being physically embedded in the polymer matrix without altering its chemical structure. On the other hand, lignin and particularly the lignin- silver nanocomposite imparted UV-Vis radiation blocking ability to the films. Films with high PVA content exhibited superior flexibility compared to pure chitosan films. Antioxidant assays confirmed potent radical scavenging and reducing properties attributed to the phenolic groups of lignin, with PVA differentially affecting the efficacy of the films depending on the assay medium. Although still preliminary, these results highlight the importance of a more detailed analysis and critical approach to understanding the real effects of the polymer matrix and of the functional additives on the performance of films intended for food packaging and to guide the selection of proper combinations that may improve film efficacy. Future work should focus on investigating not only migration effects, to address food safety issues related to the use of silver nanoparticles, but also the long-term stability and biodegradability of the films under realistic conditions.

3.5 References

Aider, Mohammed. "Chitosan application for active bio-based films production and potential in the food industry." *LWT-food science and technology* 43.6 (2010): 837-842.

Alzagameem, A., Klein, S. E., Bergs, M., Do, X. T., Korte, I., Dohlen, S., ... & Schulze, M. (2019). Antimicrobial activity of lignin and lignin-derived cellulose and chitosan composites against selected pathogenic and spoilage microorganisms. *Polymers*, *11*(4), 670.

Apak, R., Güçlü, K., Özyürek, M., & Karademir, S. E. (2004). Novel total antioxidant capacity index for dietary polyphenols and vitamins C and E, using their cupric ion reducing capability in the presence of neocuproine: CUPRAC method. *Journal of agricultural and food chemis- try*, *52*(26), 7970-7981.

Apriliyani, M. W., Purwadi, P., Manab, A., W Apriliyanti, M., & D Ikhwan, A. (2020). Characteristics of moisture content, swelling, opacity and transparency with addition chitosan as edible films/coating base on casein. *Advance Journal of Food Science and Technology*, *18*(1), 9-14.

Argenziano, R., Viggiano, S., Laezza, A., Scalia, A. C., Aprea, P., Bochicchio, B., ... & Napolitano, A. (2024). Highly cytocompatible polylactic acid based electrospun microfibers loaded with silver nanoparticles generated onto chestnut shell lignin for targeted antibacterial activity and antioxidant action. *ACS applied materials & interfaces*, *16*(22), 28230-28244.

Bonilla, J., Fortunati, E. L. E. N. A., Atarés, L., Chiralt, A., & Kenny, J. M. (2014). Physical, structural and antimicrobial properties of poly vinyl alcohol–chitosan biodegradable films. *Food Hydrocolloids*, *35*, 463-470.

Cazón, P., & Vázquez, M. (2019). Applications of chitosan as food packaging materials. In *Sustainable agriculture reviews 36: chitin and chitosan: applications in food, agriculture, pharmacy, medicine and wastewater treatment* (pp. 81-123). Cham: Springer International Publishing.

Dutta, P. K., Tripathi, S., Mehrotra, G. K., & Dutta, J. (2009). Perspectives for chitosan based antimicrobial films in food applications. *Food chemistry*, *114*(4), 1173-1182.

Ito, N. M., de Andrade Mendes Filho, A., dos Santos, D. J., & dos Santos, L. T. (2024). Synthesis of silver nanoparticles using modified lignin as a reducing agent. *Next Materials*, *2*, 100101.

Jakubowska, E., Gierszewska, M., Nowaczyk, J., & Olewnik-Kruszkowska, E. (2020). Physicochemical and storage properties of chitosan-based films plasticized with deep eutectic solvent. *Food Hydrocolloids*, *108*, 106007.

Jasrotia, S., Gupta, S., Kudipady, M. L., & Puttaiahgowda, Y. M. (2025). Development and Characterization of Chitosan–PVA–Tannic Acid Film for Extended Shelf Life and Safety of Food Products. *ACS omega*, *10*(19), 19361-19378.

Jiang, A., Patel, R., Padhan, B., Palimkar, S., Galgali, P., Adhikari, A., ... & Patel, M. (2023). Chitosan based biodegradable composite for antibacterial food packaging application. *Polymers*, *15*(10), 2235.

Julie, B. A., John, R., & Natalia, M. C. (2025). Microstructural, Bioactive, and Wound-Healing Properties of Chitosan-Based Dressings with Encapsulated Aloe Vera and Curcuma Longa Extracts. *Materials Today Communications*, 113047.

Khwaldia, K., M'Rabet, Y., & Boulila, A. (2023). Active food packaging films from alginate and date palm pit extract: Physicochemical properties, antioxidant capacity, and stability. *Food Science & Nutrition*, *11*(1), 555-568.

La Mantia, F. P., Morreale, M., Botta, L., Mistretta, M. C., Ceraulo, M., & Scaffaro, R. (2017). Degradation of polymer blends: A brief review. *Polymer Degradation and Stability*, *145*, 79-92.

Liu, T., Li, J., Tang, Q., Qiu, P., Gou, D., & Zhao, J. (2022). Chitosan-based materials: An overview of potential applications in food packaging. *Foods*, *11*(10), 1490.

Marsik, D., Danda, M., Otta, J., Thoresen, P. P., Matatkova, O., Rova, U., ... & Masák, J. (2024). Preparation and biological activity of Lignin–Silver hybrid nanoparticles. *ACS omega*, *9*(48), 47765-47787.

Moussout, H., Ahlafi, H., Aazza, M., & Bourakhouadar, M. (2016). Kinetics and mechanism of the thermal degradation of biopolymers chitin and chitosan using thermogravimetric analysis. *Polymer Degradation and Stability*, *130*, 1-9.

Muhd Julkapli, N., Akil, H. M., & Ahmad, Z. (2011). Preparation, properties and applications of chitosan-based biocomposites/blend materials: a review. *Composite Interfaces*, *18*(6), 449-507.

Riaz, A., Lei, S., Akhtar, H. M. S., Wan, P., Chen, D., Jabbar, S., ... & Zeng, X. (2018). Preparation and characterization of chitosan-based antimicrobial active food packaging film incorporated with apple peel polyphenols. *International Journal of Biological Macromolecules*, *114*, 547-555.

Rolińska, K., Jakubowska, E., Żmieńko, M., & Łęczycka-Wilk, K. (2024). Choline chloride-based deep eutectic solvents as plasticizer and active agent in chitosan films. *Food Chemistry*, *444*, 138375.

Sahariah, P., & Másson, M. (2017). Antimicrobial chitosan and chitosan derivatives: A review of the structure–activity relationship. *Biomacromolecules*, *18*(11), 3846-3868

Singh, S., Kumar, S., & Koh, J. (2024). Physicochemical and optical activity of chitosan based ternary nanocomposites for food packaging applications. *Journal of Molecular Structure*, *1311*, 138210.

Slavin, Y. N., Ivanova, K., Hoyo, J., Perelshtein, I., Owen, G., Haegert, A., ... & Bach, H. (2021). Novel lignin-capped silver nanoparticles against multidrug-resistant bacteria. *ACS applied materials & interfaces*, *13*(19), 22098-22109.

Travan, A., Marsich, E., Donati, I., & Paoletti, S. (2010). Silver nanocomposites and their biomedical applications. *Nanocomposites (nanomaterials for life sciences (VCH)). Weinheim: Wiley-VCH*.

Xia, Q., Wang, X., Zeng, Q., Guo, D., Zhu, Z., Chen, H., & Dong, H. (2020). Mechanisms of enhanced antibacterial activity by reduced chitosan-intercalated nontronite. *Environmental Science & Technology*, *54*(8), 5207-5217.

Yaneva, Z., Beev, G., Rusenova, N., Ivanova, D., Tzanova, M., Stoeva, D., & Toneva, M. (2022). Antimicrobial potential of conjugated lignin/morin/chitosan combinations as a function of system complexity. *Antibiotics*, *11*(5), 650.

Yilmaz Atay, H. (2020). Antibacterial activity of chitosan-based systems. In *Functional chitosan: drug delivery and biomedical applications* (pp. 457-489). Singapore: Springer Singapore.

Zehra, A., Wani, S. M., Jan, N., Bhat, T. A., Rather, S. A., Malik, A. R., & Hussain, S. Z. (2022). Development of chitosan-based biodegradable films enriched with thyme essential oil and additives for potential applications in packaging of fresh collard greens. *Scientific Reports*, *12*(1), 16923.

Zhang, X., Liu, J., Qian, C., Kan, J., & Jin, C. (2019). Effect of grafting method on the physical property and antioxidant potential of chitosan film functionalized with gallic acid. *Food hydrocolloids*, *89*, 1-10.

Kadir, M. F. Z., Aspanut, Z., Majid, S. R., & Arof, A. K. (2011). FTIR studies of plasticized poly (vinyl alcohol)–chitosan blend doped with NH4NO3 polymer electrolyte membrane. *Spectrochimica Acta Part A: Molecular and Biomolecular Spectroscopy*, *78*(3), 1068-1074.

Chapter 4

Preliminary Insight into the Effects of Phenol-Rich Extracts Prepared from Agri-Food By-Products by in situ-generated Deep Eutectic Solvents on Chitosan-Based Films

4.1 Introduction

Chitosan has attracted considerable attention as a biodegradable matrix for active food-packaging films because it combines film-forming ability, gas-barrier properties and intrinsic antimicrobial activity, and it is highly compatible with natural plant extracts (Bajić *et al.,* 2019). However, neat chitosan films are usually brittle and sensitive to moisture, so recent work has focused on incorporating active compounds and using alternative plasticization strategies to obtain materials with improved mechanical and functional performance (Bajić *et al*., 2019; Galvis-Sanchez *et al*., 2018).

Deep eutectic solvents (DES) have emerged as promising green media for the extraction of phenols from food plants and agro-industrial by-products because they show low volatility and offer highly tunable solvation properties (Aktaş & Kurek, 2024; González-Laredo *et al.,* 2023). Several reviews and application studies have shown that DES often provide higher extraction yields and antioxidant properties than conventional aqueous or hydroalcoholic solvents, while operating under milder, more sustainable conditions (Saini *et al*., 2022; Li, 2022; Wang *et al.,* 2024). This has been demonstrated for a variety of matrices, including aromatic and medicinal plants, *Michelia alba* flowers and different types of agri-food residues (Aktaş & Kurek, 2024; Wang *et al.,* 2024).

Among agri-food by-products, grape pomace, spent coffee grounds, and pomegranate peels and seeds are particularly rich in phenolic acids, flavonoids and tannins, and have been therefore extensively investigated as sources of high-value antioxidants. Frontini *et al*. (2024) showed that DES can efficiently recover phenolic compounds from different grape pomaces, while García-Roldán *et al.* (2023) reported that DES extracts from spent coffee grounds display

enhanced antioxidant and bioactive properties compared with conventional extracts (Frontini *et al.,* 2024; García-Roldán *et al.,* 2023). These results, together with broader assessments of DES in the valorization of natural products and agri-food residues (González-Laredo *et al.,* 2023; Li, 2022), highlight the potential of DES-based extraction in circular bioeconomy strategies. Qader *et al.,* (2023) further introduced the concept of forming a deep eutectic mixture directly by mechanical mixing of solid components to selectively extract antioxidants from natural sources, suggesting an avenue to integrate DES formulation and extraction in a single step (Qader *et al.,* 2023).

In parallel, DES have been proposed not only as extraction media but also as plasticizers for biopolymer-based films, including chitosan films. Galvis-Sanchez *et al.* (2018) demonstrated that choline-chloride-based DES can act as green plasticizers in chitosan thermoplastics, providing materials with controlled mechanical and barrier properties (Galvis-Sanchez *et al.,* 2018). Recent reviews also emphasize the growing interest in using DES as plasticizers in chitosan-based packaging films and in coupling extraction and film formation in DES-rich systems (González-Laredo *et al.,* 2023; Saini *et al.,* 2022).

Within this literature framework, the work described in this chapter focused on the preparation and preliminary characterization of chitosan-based films functionalized with deep eutectic solvent (DES)-based phenolic extracts from agri-food by-products, building on the concept of mechanically generated deep eutectic mixtures for antioxidant extraction (Qader *et al.,* 2023), with the aim of corroborating the possible exploitation of DES not only as green solvents but also as film plasticizers. Part of the research activity was performed during a four-month stay at Yonsei University in South Korea under the supervision of Prof. Youn Suk Lee.

4.2 Experimental

4.2.1.Materials

Grape pomace was kindly provided by Prof. Naviglio from the Department of Chemical Sciences of University of Naples Federico II. Spent coffee grounds were collected from a local coffee shop and, prior to use, they were oven-dried at 40 °C. Pomegranate peels and seeds were obtained after pomegranate juice preparation by squeezing and lyophilization, followed by mincing with the use of a blender. All other reagents and materials were purchased from Sigma- Aldrich.

4.2.2. Preparation and characterization of extracts from agri-food by-products

4.2.2.1. Extraction by formation of a deep eutectic solvent (DES) through mechanical mixing

Phenolic-rich DES extracts were prepared using the mechanical-mixing approach described by Qader *et al.* (2023). Briefly, 0.5 g of agri-food by-product (spent coffee grounds, pomegranate peels and seeds or grape pomace) were ground in a mortar together with 4.0 g of choline chloride. The resulting mixture was then transferred into a vial and kept at 50 °C under continuous stirring for the first 72 hours, and subsequently at room temperature for 10 days. The mixtures were centrifuged at 7000 rpm for 15 minutes at 4 °C to remove the non-extracted biomass and the supernatant was stored at room temperature until further characterization and incorporation into the chitosan film-forming solutions.

4.2.2.2. Extraction with water

Spent coffee grounds (815 mg), pomegranate-waste powder (575 mg) and grape pomace (3.7 g) were extracted with water at 163 mg/mL, 115 mg/mL or 365 mg/mL solid-to-liquid ratio in that order under stirring (350 rpm) for 1 h at room temperature. The mixtures were then centrifuged (7000 rpm, 4°C) for 15 min and the supernatants were recovered and stored at −25

°C until further use. The solid residues were instead lyophilized to evaluate the extraction yield

by difference (ca. 15 % w/w for spent coffee grounds, 62% w/w for pomegranate peels and seeds and 65% w/w for grape pomace).

4.2.3. Characterization of the extracts

Both DES and water agri-food extracts were characterized by UV-Vis analysis after proper dilution in water. In the case of the water extracts LC-UV-MS analysis was also performed in negative ionization mode (detection wavelength= 254 nm), under the following conditions: drying gas (nitrogen) 5 L/min, 325 °C; fragmentor voltage 175 V; capillary voltage 3500 V; nebulizer pressure 35 psig. An Agilent Eclipse Plus ODS column (150 × 4.6 mm, 5 μm) was used, under the following gradient elution conditions (0.4 mL/min folw rate): 0.1% formic acid (solvent A)/methanol (solvent B), from 0 to 10 min, 5% B 5%; from 10 to 47.5 min, 5-80% B.

4.2.4. Film preparation

To prepare the chitosan-based films, a 2% w/v chitosan (CH) solution was first prepared by dissolving CH in 30 mL of 1% acetic acid. The control film was prepared from this solution without any plant extract, corresponding to 0% extract loading. Films PCH, SCH, and GPH contained 20% w/w aqueous extracts of pomegranate peels and seeds, spent coffee grounds, and grape pomace, respectively. Films PD, SCD, and GPD were prepared using 20% w/w deep eutectic solvent (DES) extracts from the same plant sources. Films PHD, SCHD, and GPHD contained a total of 20% w/w extract as a 1:1 mixture of aqueous and DES extracts. Additionally, PD2, SCD2, and GPD2 films were formulated with 30% w/w DES extract, while PD3, SCD3, and GPD3 contained 50% w/w DES extract (Table 4.1). After the incorporation of the extracts, the casting solutions were poured into 9 cm Petri dishes and dried at 50 °C for 48 hours.

Table 4.1. *Composition of chitosan films containing water and/or DES plant extracts.*

Sample code	Polymer matrix	Plant extract source	Extraction medium	Extract solution content (% w/w)
CH	Chitosan	——	——	0
PCH, SCH, GPH	Chitosan	P, SC, GC	Water	20
PD, SCD, GPD	Chitosan	P, SC, GC	DES	20
PHD, SCHD, GPHD	Chitosan	P, SC, GC	DES/Water (1:1)	20
PD2, SCD2, GPD2	Chitosan	P, SC, GC	DES	30
PD3, SCD3, GPD3	Chitosan	P, SC, GC	DES	50

CH= chitosan; P = pomegranate peels and seeds; SC = spent coffee grounds; GP = grape pomace; DES = deep eutectic solvent (choline chloride-based).

4.2.5. Characterization of film mechanical properties

The tensile strength (TS) and percent elongation (%E) of the prepared chitosan films were analyzed using a universal testing machine (UTM, DaeKyung Tech & Testers Mfg. Co., Ltd., Namdong-ku, Incheon, South Korea) using a 20 kg load cell at a tensile velocity of 500 mm/min. The testing was performed per ASTM D882 (ASTM 1996). All film samples were cut into 10 cm × 2.54 cm dimensions and then the samples were conditioned in an atmosphere- controlled chamber for 48 h at 23°C and 50% relative humidity (RH). Five measurements were performed for each film.

4.3 Results and discussion

4.3.1. Preparation and characterization of extracts from agri-food by products

Spent coffee grounds, grape pomace and pomegranate peels and seeds were selected as the agri-food by-products for the recovery of phenolic compounds based on their large availability and different composition in terms of phenolic components. For the DES-based extraction of phenolic compounds from the selected agri-food by-products, a procedure recently reported in the literature based on the *in situ* generation of a deep eutectic mixture through mechanical

mixing of the sample with choline chloride was exploited (Qader *et al.,* 2023). To demonstrate the possibility of using DES not only as green solvents but also as film plasticizers, for comparison water extracts from the same agri-food by-products pomace were prepared using proper solid-to-liquid ratios able to achieve the same extraction yields obtained with the choline chloride-based DES as determined by UV-Vis analysis. Indeed, this latter allowed to conclude that water and DES were able to extract the same compounds from each starting material, as evident from the almost complete overlapping of the spectra recorded for two different extracts (Figure 1).

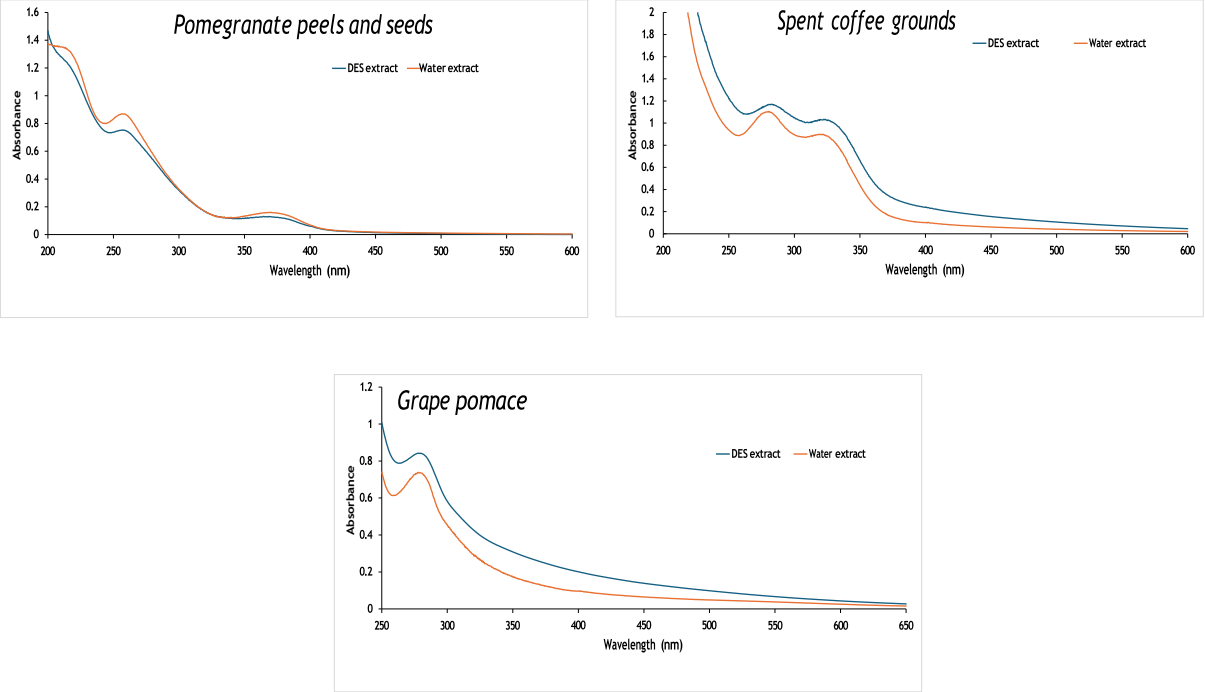

Fig. 4.1 *UV-Vis spectra of DES and water extracts (diluted 1:100 in water) from pomegranate peels and seeds, spent coffee grounds, and grape pomace.*

LC-UV-MS analysis of the water extracts (Figure 2) allowed to identify punicalagins and ellagic acid as the main phenolic compounds in the case of pomegranate peels and seeds, chlorogenic acid and its isomers in the case of spent coffee grounds, and epicatechin and condensed tannins in the case of grape pomace, in line with literature data (Panzella *et al.,* 2020)

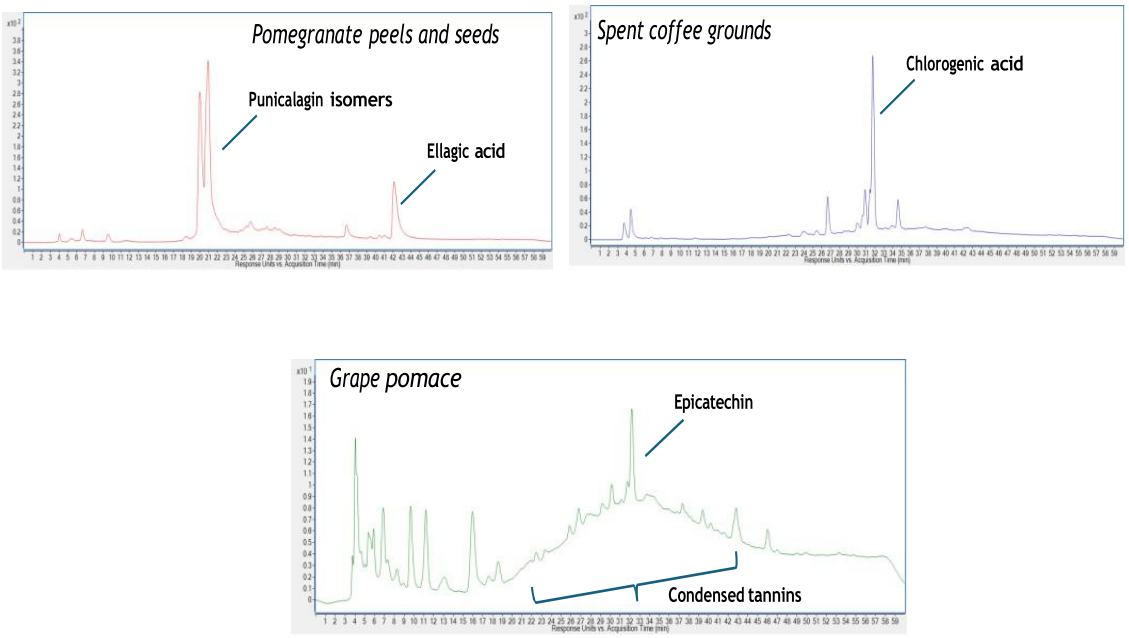

Fig. 4.2 *LC-UV-MS analysis (UV traces) of water extracts from pomegranate peels and seeds, spent coffee grounds, and grape pomace.*

Further structural characterization of both the DES and water extracts by NMR analysis is currently undergoing.

4.3.2 Mechanical properties testing

Although still very preliminary, mechanical testing performed on the different chitosan-based films (see Table 4.1) prepared by solvent casting indicated that incorporation of DES extracts, particularly from pomegranate and coffee by-products, improved elongation at break and hence flexibility of the films (Figure 4.3), highlighting therefore that DES can be easily exploited as both green solvents for the extraction of phenolic compounds from agri-food by-products and as film plasticizers. However, a decrease in tensile strength was observed, especially with higher extract concentrations. These findings align with the several works reported in the literature, which demonstrated that DES-based extracts enhanced the flexibility and mechanical properties of chitosan films, confirming that DES act as effective plasticizers for biopolymers (Wang *et al.,* 2025; Kyriakidou *et al.,* 2021; Velásquez et al., 2021; Liu *et al*., 2024; Rolińska *et al.,* 2025). It is worth of notice, however, that in the present activity

extraction of phenolic compounds was not performed following the usual procedure involving first the preparation of the DES and then the extraction, but a more sustainable and green procedure, based on the *in situ* generation of a DES starting from external choline chloride and hydrogen bond donors present in the starting agri-food by-products.

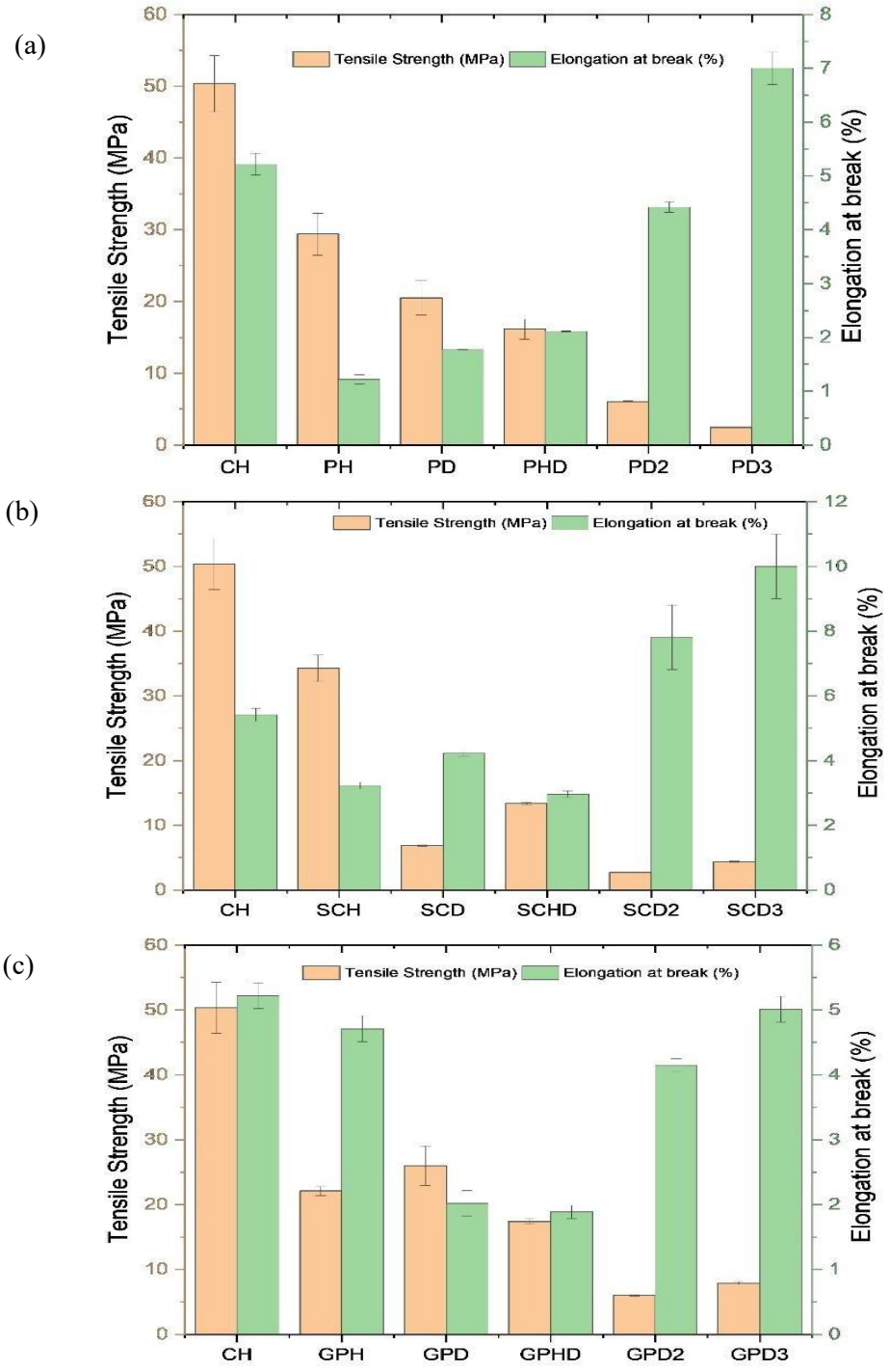

Fig. 4.3 *Mechanical properties of chitosan films incorporating water and deep eutectic solvent extracts from pomegranate peels (a) spent coffee grounds (b) grape pomace (c)*

4.4 Conclusions

In conclusion, this study successfully explored the use of *in situ*-generated deep eutectic solvents (DES) to extract bioactive compounds from agri-food by-products, specifically pomegranate peels and seeds, spent coffee grounds, and grape pomace. UV-Vis and LC-MS analyses in comparison with water extracts confirmed that the choline chloride-based solvents effectively extracted important phenolic compounds such as punicalagins, ellagic acid, chlorogenic acid, epicatechin, and condensed tannins, all well known for their antioxidant properties. Notably, when incorporated into chitosan films, these extracts led to showed significant improvements in flexibility and elongation at break. However, a decrease in tensile strength was observed, especially with higher extract concentrations, suggesting the need for a trade-off between flexibility and strength. Therefore, although several other experiments are needed including for example the complete characterization of the physiochemical and functional properties of the prepared films and a more strict comparison with the films containing the water extracts, the *in situ* generated DES look promising not only as effective solvents but also as biopolymer film plasticizers, lowering strength but increasing elongation and allowing tuning from stiff to ductile behavior for the implementation of functional and flexible films suitable for applications in food packaging.

4.5 References

Aktaş, H., & Kurek, M. A. (2024). Deep eutectic solvents for the extraction of polyphenols from food plants. *Food Chemistry*, *444*, 138629.

Bajić, M., Ročnik, T., Oberlintner, A., Scognamiglio, F., Novak, U., & Likozar, B. (2019). Natural plant extracts as active components in chitosan-based films: A comparative study. *Food packaging and shelf life*, *21*, 100365.

Frontini, A., Luvisi, A., Negro, C., Apollonio, M., Accogli, R., De Pascali, M., & De Bellis, L. (2024). Polyphenols extraction from different grape pomaces using natural deep eutectic solvents. *Separations*, *11*(8), 241.

Galvis-Sanchez, A. C., Castro, M. C. R., Biernacki, K., Goncalves, M. P., & Souza, H. K. (2018). Natural deep eutectic solvents as green plasticizers for chitosan thermoplastic production with controlled/desired mechanical and barrier properties. *Food Hydrocolloids*, *82*, 478-489.

García-Roldán, A., Piriou, L., & Jauregi, P. (2023). Natural deep eutectic solvents as a green extraction of polyphenols from spent coffee ground with enhanced bioactivities. *Frontiers in Plant Science*, *13*, 1072592.

González-Laredo, R. F., Sayago-Monreal, V. I., Moreno-Jiménez, M. R., Rocha-Guzmán, N. E., Gallegos-Infante, J. A., Landeros-Macías, L. F., & Rosales-Castro, M. (2023). Natural deep eutectic solvents (NaDES) as an emerging technology for the valorisation of natural products and agro-food residues: a review. *International Journal of Food Science and Technology*, *58*(12), 6660-6673.

Kyriakidou, A., Makris, D. P., Lazaridou, A., Biliaderis, C. G., & Mourtzinos, I. (2021). Physical properties of chitosan films containing pomegranate peel extracts obtained by deep eutectic solvents. *Foods*, *10*(6), 1262.

Li, D. (2022). Natural deep eutectic solvents in phytonutrient extraction and other applications. *Frontiers in plant science*, *13*, 1004332.

Liu, J. Z., Lu, X. X., Yang, X. T., Jiang, L. J., & Cui, Q. (2024). An efficient approach for the extraction of polyphenols from pomegranate peel using the green solvent and profiling by UPLC-Q-TOF-MS/MS analysis. *Microchemical Journal*, *205*, 111421.

Panzella, L., Moccia, F., Nasti, R., Marzorati, S., Verotta, L., & Napolitano, A. (2020). Bioactive phenolic compounds from agri-food wastes: An update on green and sustainable extraction methodologies. *Frontiers in nutrition*, *7*, 60.

Qader, I. B., Laguerre, M., Lavaud, A., Tenon, M., Prasad, K., & Abbott, A. P. (2023). Selective Extraction of antioxidants by formation of a deep eutectic mixture through mechanical mixing. *ACS Sustainable Chemistry & Engineering*, *11*(10), 4168-4176.

Rolińska, K., Jakubowska, E., Łęczycka-Wilk, K., Żmieńko, M., Mania, S., & Banach-Kopeć, A. (2025). Chitosan-based films embedded with deep eutectic solvent and fruit peel extract for food packaging applications. *Industrial Crops and Products*, *236*, 121895.

Saini, A., Kumar, A., Panesar, P. S., & Thakur, A. (2022). Potential of deep eutectic solvents in the extraction of value-added compounds from agro-industrial by-products. *Applied Food Research*, *2*(2), 100211.

Wang, W., Pan, Y., Zhao, J., Wang, Y., Yao, Q., & Li, S. (2024). Development and optimization of green extraction of polyphenols in Michelia alba using natural deep eutectic solvents (NADES) and evaluation of bioactivity. *Sustainable Chemistry and Pharmacy*, *37*, 101425.

Wang, Z. Q., Chen, H. X., Zhang, Y. C., & Zheng, Y. Z. (2025). Tailoring functional chitosan films using deep eutectic solvents extracts of propolis for active food packaging. *Food Hydrocolloids*, 111822.

Velásquez, P., Bustos, D., Montenegro, G., & Giordano, A. (2021). Ultrasound-assisted extraction of anthocyanins using natural deep eutectic solvents and their incorporation in edible films. *Molecules*, *26*(4), 984.

This PhD thesis was supported by the National Recovery and Resilience Plan (NRRP), Mission 4, Component 2 Investment 1.3 - Call for tender No. 341 of 15 March 2022 of Italian Ministry of University and Research funded by the European Union - NextGenerationEU (Award Number: Project code PE00000003, Concession Decree No. 1550 of 11 October 2022 adopted by the Italian Ministry of University and Research, Project title: “ON Foods - Research and innovation network on food and nutrition Sustainability, Safety and Security – Working ON Foods”).